THE PAIRING STATE OF $YBa_2Cu_3O_{7-\delta}$*

JAMES F. ANNETT,[1,2] NIGEL GOLDENFELD[2,3,4] AND S.R. RENN[2,4]

[1] *Physics Department, The Pennsylvania State University, 104 Davey Laboratory, University Park, Pa. 16802;* [2] *Department of Physics,* [3] *Materials Research Laboratory, and* [4] *Science and Technology Center for Superconductivity, University of Illinois at Urbana-Champaign, 1110 West Green Street, Urbana, Il. 61801, USA.*

* To appear in *Physical Properties of High Temperature Superconductors II*, D.M. Ginsberg, (ed.) (World Scientific, New Jersey, 1990).

ABSTRACT

We review the most reproducible currently available experimental data in order to identify the pairing state of $YBa_2Cu_3O_{7-\delta}$. The data include measurements of: fluctuation specific heat, possible split transitions, Josephson effects, Raman scattering, nuclear magnetic relaxation and Knight shift, infra-red reflectivity, tunneling, low temperature specific heat, and electromagnetic penetration depth. The anisotropy of the Knight shift seems to rule out triplet ('p-wave ') pairing states, leaving two classes of candidate states: an 's-wave' pairing state or 'd-wave' states with line nodes. Each scenario is consistent with all of the experiments only if special assumptions are made either about the excitation spectrum or about the form of the gap function. The temperature dependence of the penetration depth does not appear to be consistent with a pairing state with line nodes, unless certain Fermi liquid effects or scattering processes are present, as in UPt_3, suggesting that the pairing state may be conventional 's-wave'.

CONTENTS

I. INTRODUCTION

The purpose of this chapter is to discuss the experimental constraints on the pairing state of $YBa_2Cu_3O_{7-\delta}$. This analysis may be viewed as premature for two reasons: firstly, the data on certain potentially crucial measurements are not yet of sufficient accuracy or reproducibility that unambiguous conclusions may be drawn. Secondly, certain decisive tests have still not been attempted for a variety of experimental reasons. No single experiment provides unambiguous evidence for 's-wave' pairing. Furthermore, taken at face value, several experiments appear to favour unconventional pairing states. Nevertheless, viewing the data as a whole does suggest that 's-wave' pairing is the most likely scenario, although the reader is cautioned that several important *caveats* apply to this conclusion.

The importance of ascertaining the pairing state cannot be overstated. Both microscopic properties (e.g. excitation spectrum) and macroscopic behaviour (e.g. as described by Ginzburg-Landau theory) depend sensitively on the pairing state. Many physical properties of $YBa_2Cu_3O_{7-\delta}$ indeed show anomalous behaviour which could be attributed to an unconventional pairing state. However, since more prosaic explanations are always possible for each individual experiment, it is not straightforward to conclude that a particular anomaly is a signature of unconventional pairing. Thus, in this chapter we have attempted to find a consistent explanation for the entire data set. A further motivation for studying the pairing state is that its unambiguous determination might help to rule out some of the proposed microscopic mechanisms for superconductivity.

Throughout this chapter, we shall use the term 'unconventional' to mean that the pairing state has lower symmetry than the point group symmetry of the crystal. By contrast, a conventional superconductor has a pairing state with the

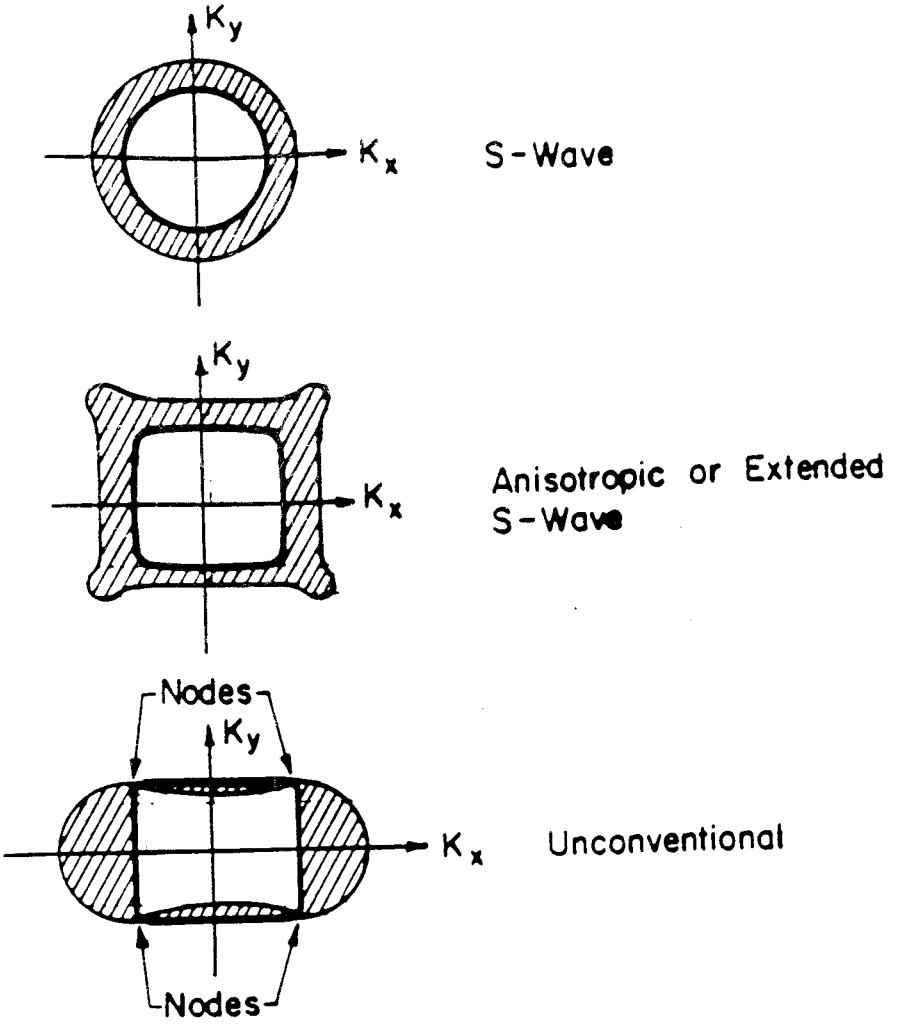

Fig. 1. Gap function $\Delta(k)$ or alternatively the pairing amplitude $< c_\uparrow(k)c_\downarrow(-k) >$ as a function of position on the Fermi surface for a conventional or s-wave superconductor (top), for a spatially anisotropic s-wave superconductor (middle) and for an unconventional superconductor (bottom). The thick line denotes the Fermi surface, and the hatched region is the gap. Note that for the unconventional pairing state the gap has lower symmetry than the crystal.

full point group symmetry of the crystal. This is illustrated in Fig. 1. Some authors (including us, on occasion) use the terms 's-wave', 'anisotropic s-wave' or 'extended s-wave' synonomously with conventional pairing. Strictly speaking, s-wave pairing means that the superconducting gap function is isotropic. Some authors also use the term 'anisotropic' to mean unconventional. Here, however, the term 'anisotropic' is reserved for spatial anisotropy arising from the crystal structure.

Most of the classic superconductors are conventional, but there are well-known examples of unconventional pairing, including ^{3}He, UPt_3 and possibly UBe_{13} and $CeCu_2Si_2$. Although it is still not possible to present unequivocal conclusions about the pairing state in $YBa_2Cu_3O_{7-\delta}$, this article will have served a useful purpose if it alerts the reader to the fact that oft-quoted arguments in favour of conventional pairing employ a variety of hidden assumptions that are questionable.

Our *modus operandi* will be to examine a variety of high quality experiments that could, at least in principle, distinguish among some of the different, group theoretically allowed, pairing states. For each of the experiments discussed, we shall summarize the logically permissible interpretations of the data within the context of a group theoretic classification of pairing states to establish the constraints that the experiments impose on the possible pairing states. We shall concentrate almost exclusively upon $YBa_2Cu_3O_{7-\delta}$, since it is currently the most extensively studied of the cuprate superconductors.

In writing this chapter, we have in mind a reader who may be expert in one sub-field of high temperature superconductivity, but not necessarily familiar with developments in other areas. Thus, we have attempted to be somewhat

pedagogical in our treatment and description of the various experiments.

We have made a number of omissions in this chapter, through lack of space, knowledge or reliable data. We have not discussed the thermoelectric effect,[1-3] the effect of chemical substitutions on T_c (discussed in the chapter by L. Greene and B.G. Bagley in this volume), possible explanations of the curvature of $H_{c2}(T)$ based upon unconventional pairing,[4,5] possible spontaneous strain distortions,[6-8] low temperature thermal conductivity[9,10] and collective mode effects. Any other omissions are inadvertent.

The organisation of this paper is as follows. Firstly, in Section II, we discuss some of the evidence that the superconductivity in $YBa_2Cu_3O_{7-\delta}$ is associated with electron (or hole) pairing. The relevant experiments here include measurements of the flux quantum, observations of the ac Josephson effect, and observations of Andreev reflection. These measurements imply that the flux quantum in $YBa_2Cu_3O_{7-\delta}$ has the standard value, and that the superconducting condensate occupies a zero momentum quantum state. We will assume that these results imply that $YBa_2Cu_3O_{7-\delta}$ is a superconductor formed from Cooper pairs, and we do not consider more exotic possibilities, such as condensation of charge e bosons.

In Section III, we explain how group theory permits a classification of the possible pairing states consistent with the crystallographic symmetry of $YBa_2Cu_3O_{7-\delta}$, and we enumerate these states explicitly. We show, *inter alia*, that there are unconventional pairing states that do not have nodes in the gap: this has the important consequence that experimental findings indicating the absence of nodes do not, on their own, imply that the pairing state is conventional. We also show that the form of the Ginzburg-Landau free energy for some of the

pairing states differs from that appropriate for 's-wave' superconductors. The first part of this Section introduces concepts that are central to the main part of this Chapter. Some readers may wish to omit the more detailed discussion of the symmetry classification of states, which is discussed in the remainder of Section III.

The remainder of this chapter addresses in detail the experimental evidence for or against unconventional pairing in $YBa_2Cu_3O_{7-\delta}$. We have separated the experiments and potential experiments into two categories: those that directly reflect the structure of the order parameter, and those that probe the excitation spectrum. The experiments that are sensitive to the order parameter structure either count the number of components of the order parameter or reveal its symmetry properties. The data that we shall mention here are: fluctuation specific heat near T_c, fluctuation diamagnetism near T_c, Josephson effects between classic superconductors and $YBa_2Cu_3O_{7-\delta}$, anisotropy of H_{c2} in the basal plane, and peak splitting effects due to strain. All of these experiments are reviewed in Section IV. We shall conclude that, at present, experimental data in this category do not rule out any of the candidate pairing states. In particular, we mention that the observation of Josephson effects in a non-planar junction between $YBa_2Cu_3O_{7-\delta}$ and a classic superconductor does not rule out unconventional pairing states, as is sometimes claimed.

Next, in Section V, we discuss the second class of measurements. These reveal the existence of low-energy excitations below T_c for which one explanation might be the presence of nodes in the gap. We discuss Raman scattering, infrared reflectivity data, quasiparticle tunneling, nuclear magnetic resonance experiments, and low temperature specific heat.

These data do not, at first sight, give a consistent picture of the excitation spectrum. On the one hand, observations of Raman scattering, of nuclear magnetic relaxation rate and of quasi-particle tunneling in planar junctions show strong evidence that low-lying excitations exist in the superconducting state. On the other hand, point-contact tunneling experiments seem to show evidence for a well-defined gap, although reproducibility is difficult in these measurements. The interpretation of the infra-red reflectivity is a matter of controversy, but in our opinion, the data do not provide evidence for a gap. The apparent existence of low-lying excitations is, however, neither necessary nor sufficient to establish unconventional pairing in $YBa_2Cu_3O_{7-\delta}$. First, the low-lying excitations may have causes other than nodes in the gap. Second, there are various triplet states that are nodeless. Perhaps the strongest constraint comes from the measurements of the Cu(2) Knight shift: the measured anisotropies seem to exclude triplet pairing.

In a separate Section (Section VI) we discuss the temperature dependence of the electromagnetic penetration depth, which is sometimes considered to be the strongest evidence in favour of 's-wave' pairing. Such a conclusion is overstated. In fact, most of the data are not in the asymptotic low temperature regime, and therefore are determined principally by strong-coupling effects, inelastic scattering and the precise form of the gap function, all of which may conceal the presence of nodes in the gap. The data are not consistent with weak-coupling 's-wave' pairing, but appear consistent with strong-coupling 's-wave' pairing. The data have not yet been systematically compared to predictions from unconventional pairing states, taking into account strong-coupling corrections and realistic forms of the gap function. It is probable, however, that the nodeless triplet states would also fit the data if strong-coupling corrections were taken into account. The strongest

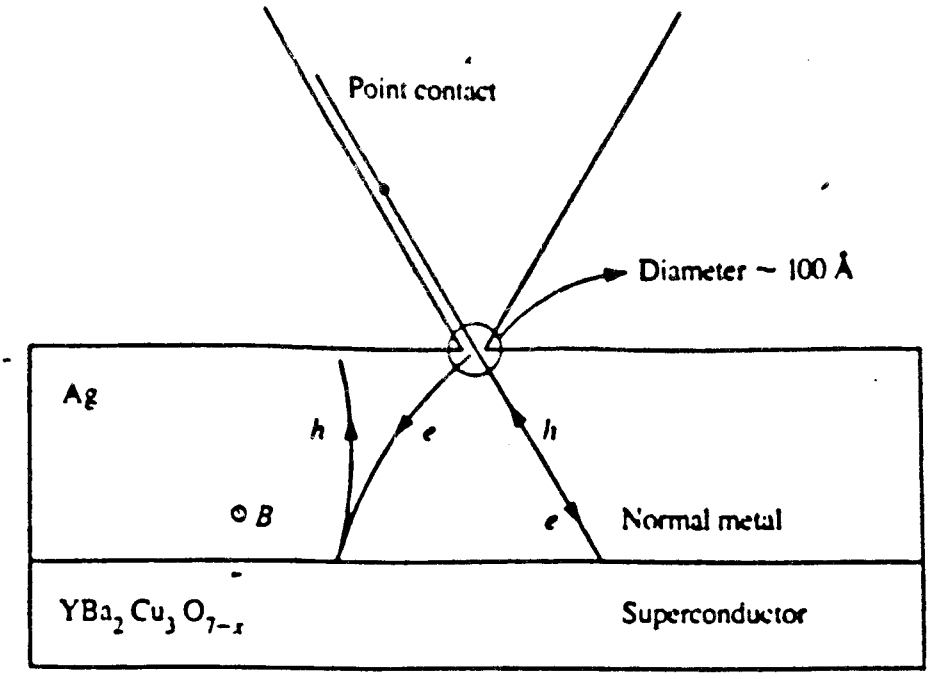

Fig. 2. Typical Andreev reflection experimental arrangement.[20] The electrons are injected into the normal film with known energy with a point contact.

Further evidence for pairing is seen in the Shapiro steps which occur in the I-V characteristics of Josephson tunnel junctions with an applied ac voltage of angular frequency ω.[15–17] The steps are found to have a spacing of $\hbar\omega/2e$.[17]

Lastly, we mention the observation of Andreev scattering.[18–20] In this technique, the sample to be studied is coated with a thin film of a non-superconducting metal, and a current of electrons is injected into the film via a point contact, as illustrated in Fig. 2. In the process of Andreev scattering, an electron incident on the metal-superconducting boundary combines with another electron in the normal metal and is absorbed into the condensate, leaving behind a hole in the normal metal. Provided that the condensate consists of pairs of electrons with opposite momentum and spin, the result of this process is the creation of a hole with momentum and spin exactly opposite to that of the incident electron. In principle (i.e. with a high quality interface and negligible scattering in the metallic film) the hole should return to the point contact, increasing the observed current there, and, hence, decreasing the contact resistance relative to the normal state. In a superconductor with a gap Δ, for a bias voltage slightly less than Δ, all incident electrons produce a hole and the observed resistance drops to one half of the normal state value. However if the bias voltage is well above Δ, then the incident electrons are converted to quasiparticles which propagate through the sample without the production of holes at the metal-superconductor boundary. In this case, the junction resistance is that of the normal state. The observation of Andreev reflection in accord with theoretical predictions would imply that the condensate is formed from pairs of electrons with zero net momentum.

Andreev scattering in $YBa_2Cu_3O_{7-\delta}$ has been observed by Hoevers *et al.*[21]

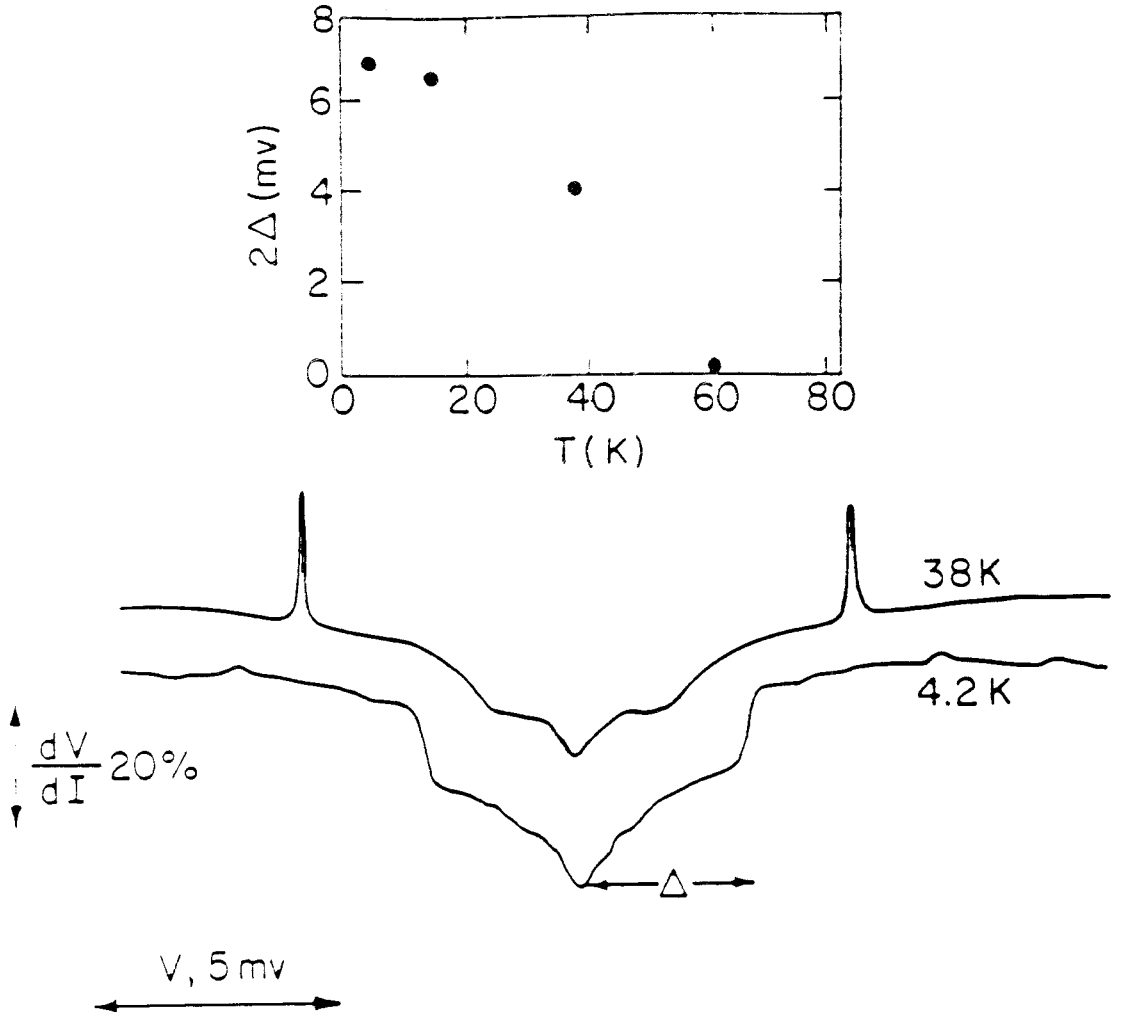

Fig. 3. Plot of dV/dI of a low-resistance Au-I-$YBa_2Cu_3O_{7-\delta}$ crystal junction vs. bias V at two temperatures. The figure inset shows the dependence of the 'gap'. (After Ref. 22.)

who used nonoriented $YBa_2Cu_3O_{7-\delta}$ films. Their sample was coated with a 0.25 μm Ag film. When the sample was superconducting the resistance sharply dropped below the normal state value when the bias voltage was decreased below about 12.5 mV. The zero bias resistance was only 1% less than the normal state resistance. Nevertheless, since the magnetic field dependence of the point contact resistance was in good agreement with theory, it was concluded that Andreev scattering was indeed being observed.

Recently Ong *et al.*[22] observed Andreev reflection from a single crystal on whose chemically etched surface they had sputtered a gold film. In the superconducting state, below 10 K, they observed an abrupt decrease in the point contact resistance at 7mV. The zero bias resistance was less than 30% of the normal state value (see Fig. 3). Ong *et al.* were also able to track the gap-like feature as the temperature was increased (see inset). It is interesting to note that the gap vanished at 60K, even though the bulk T_c of the sample was 90K, so presumably the experiment was probing a surface phase of the oxygen depleted $T_c = 60$K material.

Having established that the normal state carriers are indeed paired in the superconducting state, we now turn to the question of which pairing states are consistent with the point group symmetry of $YBa_2Cu_3O_{7-\delta}$.

III. THE POSSIBLE SYMMETRIES OF THE PAIRING STATE

A. Symmetry and the Superconducting State

In this Section we show how to enumerate all the possible superconducting states by using group theory. Our discussion is based upon the work of many authors.[23-25]

All superconducting states may be classified according to their symmetry properties.[25] Close to T_c, this classification can be formulated entirely in terms of the macroscopic Ginzburg-Landau order parameter, and requires no knowledge of the microscopic details of the superconductivity. Away from T_c, for orthorhombic and tetragonal crystals, the classification scheme is not changed, unless there is a distinct phase transition to another superconducting state.[25]

The central symmetry argument that we shall use is that the order parameter must transform according to an irreducible representation of the symmetry group of the crystal. To see why this is so, it is sufficient to look at the first term in a Ginzburg-Landau expansion of the free energy density, $f[\Delta_{\alpha\beta}(k)]$. The first terms in the Ginzburg-Landau free energy are:

$$f[\Delta_i] = \alpha_{ij}\Delta_i^*\Delta_j + \ldots O(\Delta_i^4) + \ldots O((\nabla\Delta_i)^2), \tag{3.1}$$

where for brevity we denote $(\alpha\beta;k)$ by the symbol i, and use the Einstein summation convention. At high temperatures the superconducting state is unstable, i.e. the matrix α_{ij} is positive definite. On lowering the temperature, the superconducting transition occurs when the matrix α_{ij} ceases to be positive definite, i.e. when an eigenvalue first becomes negative. Let that eigenvalue be denoted by $\alpha'(T - T_c)$ and the corresponding eigenvectors be $\vec{x}^{(a)}$, $a = 1, 2, \ldots D$. Then

group theory tells us that, neglecting accidental degeneracies, these eigenvectors transform into one another according to an irreducible representation of the symmetry group. The degeneracy of the eigenvalue, D, is the dimensionality of the irreducible representation. Close to T_c, where Ginzburg-Landau theory is valid, the gap matrix can be written as a linear combination of the unstable eigenvectors $\vec{x}^{(a)}$:

$$\Delta_i = \sum_{a=1}^{D} \eta_a x_i^{(a)}. \tag{3.2}$$

The set of D quantities $\vec{\eta} = (\eta_1, \eta_2, \ldots, \eta_D)$ is called the order parameter. Thus, a $D > 1$ dimensional irreducible representation will give rise to a multi-component order parameter. Physically distinct superconducting order parameters therefore correspond to different irreducible representations of the symmetry group. For each possible order parameter, there is a Ginzburg-Landau free energy density, the minima of which are the possible superconducting ground states.

To clarify the above discussion we now give some concrete examples of unconventional pairing states and their gap functions. First, it is helpful to rewrite the gap matrix $\Delta_{\alpha\beta}(k)$ in the standard form:

$$\Delta_{\alpha\beta}(k) = i[\Delta(k) + \vec{\sigma} \cdot \vec{d}\,(k)]\sigma_y \tag{3.3}$$

where $\vec{\sigma} = (\sigma_x, \sigma_y, \sigma_z)$ and $\sigma_x, \sigma_y, \sigma_z$ are the Pauli matrices. Fermi statistics implies that the scalar function $\Delta(k)$ is even, $\Delta(k) = \Delta(-k)$, and that the spin-space vector $\vec{d}\,(k)$ is odd, $\vec{d}\,(k) = -\vec{d}\,(-k)$. For lattices with inversion symmetry, the irreducible representations can be classified according to their parity. The above results show that for an even parity representation, only the scalar function $\Delta(k)$ is non-zero, while for the odd parity representations only

$\vec{d}\ (k)$ is non-zero. These are said to be singlet or triplet states respectively, since $\Delta(k)$ and $\vec{d}\ (k)$ transform according to the $S = 0$ and $S = 1$ representations respectively under rotations in spin space. As examples, in an isotropic system, conventional singlet 's-wave' pairing corresponds to a gap function $\Delta(k) = \Delta_0$; one possible singlet 'd-wave' state would have a gap function $\Delta(k) = \Delta_0 \times (k_x k_y)$. We also mention three triplet states which are important in superfluid ^{3}He. The first is the Balian-Werthamer (BW) state $\vec{d}\ (k) = \Delta_0 \times (k_x, k_y, k_z)$. The second is the axial, or Anderson-Brinkman-Morel, state $\vec{d}\ (k) = (\hat{e}_1 + i\hat{e}_2) \cdot \vec{k}\,\vec{d}_0$, where $\hat{e}_1$ and $\hat{e}_2$ are orthogonal unit vectors and $\vec{d}_0$ is an arbitrary vector in spin-space. The third is the polar state $\vec{d}\ (k) = \hat{\ell} \cdot \vec{k}\,\vec{d}_0$, where $\hat{\ell}$ is a unit vector. Of these, the BW state has an energy gap which is non-zero everywhere on the Fermi surface, the axial state has point nodes of the gap on the anisotropy axis $\hat{\ell} = \hat{e}_1 \times \hat{e}_2$, and the polar state has an equator of nodes in the plane perpendicular to $\hat{\ell}$.

We are now ready to enumerate all the possible irreducible representations which may correspond to the superconductivity in $YBa_2Cu_3O_{7-\delta}$. The only difficulty is to determine the symmetry group of the normal state, since some knowledge of the microscopic details is required. In particular one needs to know whether the spin-orbit coupling is important or not in the Ginzburg-Landau free energy density, and whether the appropriate crystal point group is orthorhombic or tetragonal.

This last point deserves further comment. Superconducting $YBa_2Cu_3O_{7-\delta}$ is known to possess orthorhombic symmetry: why then should we even contemplate expanding the order parameter in a tetragonal basis set? The answer lies in the fact that we normally perform the group theoretic analysis assuming that there are no accidental degeneracies present. However, in $YBa_2Cu_3O_{7-\delta}$, only

a relatively small distortion would be required to make the crystal symmetry tetragonal, suggesting that the eigenvectors $\vec{x}^{(a)}$ could be nearly degenerate. In such a situation, it would be appropriate to describe the system as tetragonal, with an orthorhombic perturbation. On the other hand, if $YBa_2Cu_3O_{7-\delta}$ were quite markedly orthorhombic, then no vestige of the degeneracy of the tetragonal representation would remain. The tetragonal symmetry may be important if the superconductivity is primarily associated with the nearly square CuO_2 planes, while the orthorhombic symmetry group may be relevant if the pair condensation energy on the CuO chains is comparable to that on the CuO_2 planes. In light of these uncertainties, we shall consider the four possible combinations of orthorhombic or tetragonal symmetry with weak or strong spin-orbit coupling. For brevity we shall give the full details only for the simpler orthorhombic case, and simply summarise the results for the tetragonal case.

B. Orthorhombic Symmetry

If the point group is the orthorhombic (D_{2h}) group and the spin orbit coupling is unimportant, then the possible superconducting states are derived from the irreducible representations of the group $SU(2) \times D_{2h}$. The representations of the relevant spin rotation group are singlet or triplet, which are to be combined with one of the eight irreducible representations (IRs) of D_{2h}: $A_{1g}, B_{1g}, B_{2g}, B_{3g}, A_{1u}, B_{1u}, B_{2u}, B_{3u}$ (in the notation of Tinkham[26]). As we mentioned earlier, with singlet states only the even parity IRs can occur, while for triplet states, only the odd IRs occur. We thus have a total of eight possible irreducible representations for the superconductivity in $YBa_2Cu_3O_{7-\delta}$, which we can denote as: ${}^1A_{1g}, {}^1B_{1g}, {}^1B_{2g}, {}^1B_{3g}, {}^3A_{1u}, {}^3B_{1u}, {}^3B_{2u}, {}^3B_{3u}$, using the notation

state	g.s. order parameter	residual group	gap function $\Delta(\underline{k})$	nodes: sphere	nodes: cylinder	name
$^1A_{1g}$	1	$SO(3)\times D_{2h}\times T$	1	-	-	s-wave
$^1B_{1g}$	1	$SO(3)\times D_2(C_2^z)\times i\times T$	XY	line	line	
$^1B_{2g}$	1	$SO(3)\times D_2(C_2^y)\times i\times T$	XZ	line	line	
$^1B_{3g}$	1	$SO(3)\times D_2(C_2^x)\times i\times T$	YZ	line	line	

Table 1: The singlet superconducting phases in an orthorhombic crystal. The columns indicate the nomenclature,[24,25] the ground state order parameter, the residual symmetry group, an example gap function, the gap nodes occuring on a spherical or cylindrical fermi surface, and the usual name. In the example gap function, the notation X, Y, and Z denote $\sin(k_x a)$, $\sin(k_y b)$, and $\sin(k_z c)$ where a, b, and c are the orthorhombic lattice constants. The first point group given refers to spin rotations, the second to spatial point group rotations.

$^{2s+1}\Gamma$, where Γ is the representation. Each of the singlet representations is one dimensional, while the triplet representations are three dimensional.

We can now derive the possible gap matrices for each of these representations. For each of the four singlet IRs the gap function can be written down immediately (see Table 1). Here X,Y, and Z denote $\sin(k_x a)$, $\sin(k_y b)$, and $\sin(k_z c)$ with a, b and c being the orthorhombic lattice constants. For example from Table 1, we find that the $^1B_{1g}$ phase has $\Delta(k) = \eta_0 XY$,[27] where η_0 is a temperature dependent number which vanishes as $\sqrt{T - T_c}$ near T_c. The value η_0 is equal to $|\eta|$, which is determined by minimising the free energy density

$$f[\eta] = \alpha'(T - T_c)|\eta|^2 + \beta|\eta|^4 + \frac{\hbar^2}{2m_{ij}} \nabla_i \eta^* \nabla_j \eta. \tag{3.4}$$

Of the four singlet states given in Table 1, the first corresponds to the usual singlet 's-wave' pairing, while the others are 'd-wave' states. It should be noted that for all of these pairing states the Ginzburg-Landau free energy density (Eq. (3.4)) has the form familiar from the theory of conventional (i.e. 's-wave') superconductors.

Now we consider the possibility of nodes in the gap. The existence of nodes depends upon two factors: the topology of the Fermi surface and the symmetry of the state. This is a very important point, because even if the symmetry of the superconducting state requires the existence of zeros in the *gap function*, this will only give rise to a vanishing *energy gap* if the gap function happens to vanish *on the Fermi surface*. We will shortly encounter examples of triplet states that are nodeless precisely because the gap function vanishes at points in k-space which do not lie on the Fermi surface. For definiteness, we shall assume here

state	g.s.order parameter	residual group	gap function $\underline{d}(\underline{k})$	nodes: sphere	nodes: cylinder	name
$^3A_{1u}(a)$	(0,0,1)	$D_\infty(C_\infty)\times D_2\times i(E)\times T$	(0,0,1)XYZ	line	line	
$^3A_{1u}(b)$	(1,i,0)	$D_\infty(E)\times D_2\times i(E)$	(1,i,0)XYZ	surface	surface	
$^3B_{1u}(a)$	(0,0,1)	$D_\infty(C_\infty)\times D_2(C_2^z)\times i(E)\times T$	(0,0,1)Z	line	line	
$^3B_{1u}(b)$	(1,i,0)	$D_\infty(E)\times D_2(C_2^z)\times i(E)$	(1,i,0)Z	surface	surface	
$^3B_{2u}(a)$	(0,0,1)	$D_\infty(C_\infty)\times D_2(C_2^y)\times i(E)\times T$	(0,0,1)Y	line	line	
$^3B_{2u}(b)$	(1,i,0)	$D_\infty(E)\times D_2(C_2^y)\times i(E)$	(1,i,0)Y	surface	surface	
$^3B_{3u}(a)$	(0,0,1)	$D_\infty(C_\infty)\times D_2(C_2^x)\times i(E)\times T$	(0,0,1)X	line	line	
$^3B_{3u}(b)$	(1,i,0)	$D_\infty(E)\times D_2(C_2^x)\times i(E)$	(1,i,0)X	surface	surface	

Table 2: The triplet superconducting phases in an orthorhombic crystal, assuming weak spin-orbit coupling. Notation as in Table 1.

that the Fermi surface has a shape similar to that calculated by band theory,[28] i.e. essentially cylindrical with the axis along k_z.[29] In this case the ${}^1A_{1g}$ state (s-wave) is the only singlet state with a gap that is non-zero everywhere on the Fermi surface. The other three singlet states have line nodes in the gap.

We now classify the possible triplet states in exactly the same way. The only complication is that the triplet Ginzburg-Landau order parameter is a spin-space vector $\vec{\eta} = (\eta_1, \eta_2, \eta_3)$. The Ginzburg-Landau free energy density is slightly more complicated than before:

$$f[\eta_\mu] = \alpha'(T - T_c)\eta_\mu^*\eta_\mu + \beta_1(\eta_\mu^*\eta_\mu)^2 + \beta_2|\eta_\mu\eta_\mu|^2 + \frac{\hbar^2}{2m_{ij}} \nabla_i \eta_\mu^* \nabla_j \eta_\mu. \qquad (3.5)$$

The equilibrium states are obtained by finding the spatially uniform minima of Eq. (3.5). The minima depend upon the sign of β_2/β_1. If $\beta_2/\beta_1 < 0$, then $\eta_\mu \propto (0,0,1)$, and if $\beta_2/\beta_1 > 0$, then $\eta_\mu \propto (1,i,0)$. Both of these vectors are unique up to arbitrary rotations in spin-space. Either of these minima could occur for each of the four triplet irreducible representations, so there are a total of eight possible states of distinct symmetry (see Table 2). The quasiparticle excitation gap is zero for a triplet state whenever

$$|d(k)|^2 = |\vec{d}^* \times \vec{d}| \qquad (3.6)$$

so in Table 2 all the (a) type states discussed above have line nodes of the gap, while the (b) type states have a gap that vanishes on all of the Fermi surface. This completes the classification of all twelve possible symmetry-distinct superconducting states that may occur in an orthorhombic crystal in which the spin-orbit coupling is weak.

state	order parameter	residual group	gap function $\underline{d}(\underline{k})$	nodes: sphere	nodes: cylinder	name
A_{1u}	1	$D_2 \times i(E) \times T$	(AX,BY,CZ)	-	-	BW
B_{1u}	1	$D_2(C_2^z) \times i(E) \times T$	(AY,BX,CXYZ)	point	-	
B_{2u}	1	$D_2(C_2^y) \times i(E) \times T$	(AZ,BXYZ,CX)	point	point	
B_{3u}	1	$D_2(C_2^x) \times i(E) \times T$	(AXYZ,BZ,CY)	point	point	

Table 3: The triplet phases in an orthorhombic crystal, assuming strong spin-orbit coupling. The complex numbers A,B, and C must be obtained by solving an appropriate gap equation. The point group given refers to combined rotations in spin and orbit space, otherwise the notation is the same as in Table 1.

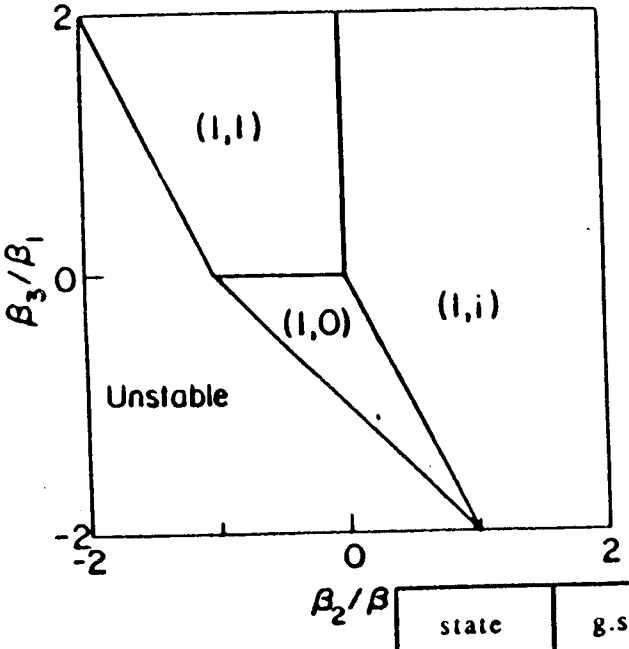

Fig. 4. Phase diagram for the two-dimensional representation E_{1g} of the tetragonal group.

Table 4: The singlet states in a tetragonal crystal. Notation as in Table 1.

state	g.s.order parameter	residual group	gap function $\Delta(\underline{k})$	nodes: sphere	nodes: cylinder	name
$^1A_{1g}$	1	$SO(3)\times D_{4h}\times T$	1	-	-	s-wave
$^1A_{2g}$	1	$SO(3)\times D_4(C_4)\times i\times T$	$XY(X^2-Y^2)$	line	line	
$^1B_{1g}$	1	$SO(3)\times D_4(D_2)\times i\times T$	(X^2-Y^2)	line	line	
$^1B_{2g}$	1	$SO(3)\times D_4(D_2')\times i\times T$	XY	line	line	
$^1E_g(a)$	(1,0)	$SO(3)\times D_2(C_2')\times i\times T$	XZ	line	line	
$^1E_g(b)$	(1,1)	$SO(3)\times D_2(C_2'')\times i\times T$	(X+Y)Z	line	line	
$^1E_g(c)$	(1,i)	$SO(3)\times D_4(E)\times i$	(X+iY)Z	line	line	

The classification of states is slightly different for the triplets if the spin-orbit coupling is significant, since it breaks the three-fold degeneracy of these states. In the strong spin-orbit coupling case the states are made up of irreducible representations of the point group D_{2h} alone, and are given in Table 3. These states correspond to one dimensional representations, so the Ginzburg-Landau free energy is the conventional one of Eq. (3.4). Observe that on the $YBa_2Cu_3O_{7-\delta}$ Fermi surface the A_{1u} and B_{1u} states have a quasiparticle excitation gap that is non-zero everywhere, while the other two states have point nodes on the Fermi surface. This example illustrates the important point that *experimental observation of a gap that is non-zero everywhere would not be sufficient to establish 's-wave' pairing.*

In conclusion, there are a wide variety of possible states for the case of orthorhombic symmetry, including unconventional states with no gap nodes, point, or line nodes, and even states with surfaces of nodes.

C. TETRAGONAL SYMMETRY

The classification of superconducting states in a tetragonal crystal proceeds in much the same way as in the orthorhombic case. There is little point in discussing all the tetragonal states here, but for completeness we list them in Tables 4, 5, 6, 7, and 8. In fact the number of symmetry distinct states is considerably greater for tetragonal crystals than for othorhombic. This is because the tetragonal point group has both one and two dimensional irreducible representations.

Here we shall just give one example for the tetragonal group, which illustrates the additional complexity arising from having a two-dimensional irreducible representation of the point group. The cases with one dimensional representations

state	g.s.order parameter	residual group	gap function $\underline{d}(\underline{k})$	nodes: sphere	nodes: cylinder	name
$^3A_{1u}$(a)	(0,0,1)	$D_\infty(C_\infty)\times D_4\times i(E)\times T$	(0,0,1)XYZ(X^2-Y^2)	line	line	
$^3A_{1u}$(b)	(1,i,0)	$D_\infty(E)\times D_4\times i(E)$	(1,i,0)XYZ(X^2-Y^2)	surface	surface	
$^3A_{2u}$(a)	(0,0,1)	$D_\infty(C_\infty)\times D_4(C_4)\times i(E)\times T$	(0,0,1)Z	line	line	
$^3A_{2u}$(b)	(1,i,0)	$D_\infty(E)\times D_4(C_4)\times i(E)$	(1,i,0)Z	surface	surface	
$^3B_{1u}$(a)	(0,0,1)	$D_\infty(C_\infty)\times D_4(D_2)\times i(E)\times T$	(0,0,1)XYZ	line	line	
$^3B_{1u}$(b)	(1,i,0)	$D_\infty(E)\times D_4(D_2)\times i(E)$	(1,i,0)XYZ	surface	surface	
$^3B_{2u}$(a)	(0,0,1)	$D_\infty(C_\infty)\times D_4(D_2')\times i(E)\times T$	(0,0,1)Z(X^2-Y^2)	line	line	
$^3B_{2u}$(b)	(1,i,0)	$D_\infty(E)\times D_4(D_2')\times i(E)$	(1,i,0)Z(X^2-Y^2)	surface	surface	

Table 5: The triplet superconducting phases in a tetragonal crystal, assuming weak spin-orbit coupling, and a one dimensional representation of the tetragonal point group D_{4h}.

state	g.s.order parameter	residual group	gap function d(k)	nodes: sphere	nodes: cylinder	name
$^3E_u(a)$	$\begin{pmatrix} 0 & 0 & 1 \\ 0 & 0 & 0 \end{pmatrix}$	$D_{\infty}(C_{\infty})\times D_2(C_2')\times i(E)\times T$	(0,0,1)X	line	line	polar
$^3E_u(b)$	$\begin{pmatrix} 1 & i & 0 \\ 0 & 0 & 0 \end{pmatrix}$	$D_{\infty}(E)\times D_2(C_2')\times i(E)$	(1,i,0)X	surface	surface	
$^3E_u(c)$	$\begin{pmatrix} 0 & 0 & 1 \\ 0 & 0 & 1 \end{pmatrix}$	$D_{\infty}(C_{\infty})\times D_2(C_2'')\times i(E)\times T$	(0,0,1)(X+Y)	line	line	polar
$^3E_u(d)$	$\begin{pmatrix} 1 & i & 0 \\ 1 & i & 0 \end{pmatrix}$	$D_{\infty}(E)\times D_2(C_2'')\times i(E)$	(1,i,0)(X+Y)	surface	surface	
$^3E_u(e)$	$\begin{pmatrix} 0 & 0 & 1 \\ 0 & 0 & i \end{pmatrix}$	$D_{\infty}(C_{\infty})\times D_4(E)\times i(E)$	(0,0,1)(X+iY)	point	-	axial
$^3E_u(f)$	$\begin{pmatrix} 1 & i & 0 \\ i & -1 & 0 \end{pmatrix}$	$D_{\infty}(E)\times D_4(E)\times i(E)$	(1,i,0)(X+iY)	surface	surface	γ
$^3E_u(g)$	$\begin{pmatrix} 1 & 0 & 0 \\ 0 & 1 & 0 \end{pmatrix}$	$D_4\times i(E)\times T$	(X,Y,0)	point	-	planar
$^3E_u(h)$	$\begin{pmatrix} 0 & -1 & 0 \\ 1 & 0 & 0 \end{pmatrix}$	$D_4(C_4)\times i(E)\times T$	(Y,-X,0)	point	-	
$^3E_u(i)$	$\begin{pmatrix} 1 & 0 & 0 \\ 0 & -1 & 0 \end{pmatrix}$	$D_4(D_2)\times i(E)\times T$	(X,-Y,0)	point	-	
$^3E_u(j)$	$\begin{pmatrix} 0 & 1 & 0 \\ 1 & 0 & 0 \end{pmatrix}$	$D_4(D_2')\times i(E)\times T$	(Y,X,0)	point	-	
$^3E_u(k)$	$\begin{pmatrix} 1 & 0 & 0 \\ 0 & i & 0 \end{pmatrix}$	$D_4^*(D_2)\times i(E)$	(X,iY,0)	point	-	bipolar
$^3E_u(l)$	$\begin{pmatrix} 1 & i & 0 \\ i & 1 & 0 \end{pmatrix}$	$D_4^*(D_2')\times i(E)$	(X+iY,iX+Y,0)	point	-	bipolar

Table 6: The inert triplet phases in a tetragonal crystal, assuming weak spin-orbit coupling, and the two dimensional E representation. Where only one point group is given it refers to combined rotations in spin and orbit space.

may be worked out in precisely the same way as for the orthorhombic states listed above. We shall consider a singlet state which belongs to the E_g representation of the tetragonal (D_{4h}) point group. This representation is two dimensional and thus the order parameter of the superconducting phase is a pair of complex numbers, (η_x, η_y). The Ginzburg-Landau free energy density[30] for this situation is quite complicated:

$$f[\eta_i] = \alpha'(T - T_c)\eta_i^*\eta_i + \beta_1(\eta_i^*\eta_i)^2 + \beta_2|\eta_i\eta_i|^2 + \beta_3(|\eta_1|^4 + |\eta_2|^4)$$

$$+\frac{\hbar^2}{2m_1}\nabla_i\,\eta_j^*\,\nabla_i\,\eta_j + \frac{\hbar^2}{4m_2}(\nabla_i\eta_i^*\,\nabla_j\,\eta_j + \nabla_i\eta_j^*\,\nabla_j\,\eta_i)$$

$$+\frac{\hbar^2}{2m_3}|\,\nabla_i\,\eta_i|^2 + \frac{\hbar^2}{2m_4}|\,\nabla_z\,\eta_i|^2 \qquad (3.7)$$

There are three distinct types of minima to this free energy; the order parameter (η_1, η_2) may be either a vector like $(1,0)$, $(1,1)$ or $(1,i)$, depending upon the relative sizes of the parameters β_2/β_1 and β_3/β_1. (See Fig. 4.) The basis functions for the E_g representation are the pair of functions XZ and YZ (X, Y and Z as defined above). See entries ${}^1E_g(a)$, ${}^1E_g(b)$, and ${}^1E_g(c)$ in Table 4. All of these phases have line nodes on the $YBa_2Cu_3O_{7-\delta}$ Fermi surface.

state	g.s.order parameter	residual group	gap function $\underline{d}(\underline{k})$	nodes: sphere	nodes: cylinder	name
$^3E_u(m)$	$\begin{pmatrix} 0 & 0 & A \\ 0 & 0 & B \end{pmatrix}$	$D_{-}(C_{-})\times C_2(E)\times i(E)$	(0,0,1)(AX+BY)	point	-	
$^3E_u(n)$	$\begin{pmatrix} A & iA & 0 \\ B & iB & 0 \end{pmatrix}$	$D_{-}(E)\times C_2(E)\times i(E)$	(1,i,0)(AX+BY)	surface	surface	
$^3E_u(o)$	$\begin{pmatrix} A & 0 & 0 \\ 0 & B & 0 \end{pmatrix}$	$D_2\times i(E)$	(AX,BY,0)	point	-	
$^3E_u(p)$	$\begin{pmatrix} A & B & 0 \\ -B & A & 0 \end{pmatrix}$	$D_{-}(E)\times C_4\times i(E)$	(AX-BY,BX+AY,0)	point	-	
$^3E_u(q)$	$\begin{pmatrix} A & B & 0 \\ B & A & 0 \end{pmatrix}$	$D_2'\times i(E)$	(AX+BY,BX+AY,0)	point	-	
$^3E_u(r)$	$\begin{pmatrix} 0 & A & 0 \\ B & 0 & 0 \end{pmatrix}$	$D_2(C_2)\times i(E)$	(BY,AX,0)	point	-	
$^3E_u(s)$	$\begin{pmatrix} A & B & 0 \\ -B & -A & 0 \end{pmatrix}$	$D_2'(C_2)\times i(E)$	(AX+BY,-BX-AY,0)	point	-	
$^3E_u(t)$	$\begin{pmatrix} A & B & 0 \\ B & -A & 0 \end{pmatrix}$	$C_4(C_2)\times i(E)$	(AX+BY,BX-AY,0)	point	-	
$^3E_u(u)$	$\begin{pmatrix} A & B & 0 \\ C & D & 0 \end{pmatrix}$	$C_2\times i(E)$	(AX+CY,BX+DY,0)	point		

Table 7: The non-inert triplet superconducting states in a tetragonal crystal, assuming weak spin-orbit coupling, and the two dimensional point group E representation. Where only one point group is given it refers to combined rotations in spin and orbit space.

state	g.s.order parameter	residual group	gap function d(k)	nodes: sphere	nodes: cylinder	name
A_{1u}	1	$D_4 \times i(E) \times T$	(AX,AY,BZ)	-	-	BW
A_{2u}	1	$D_4(C_4) \times i(E) \times T$	$(AY,-AX,BXYZ(X^2-Y^2))$	point	-	
B_{1u}	1	$D_4(D_2) \times i(E) \times T$	(AX,-AY,BXYZ)	point	-	
B_{2u}	1	$D_4(D_2') \times i(E) \times T$	$(AY,AX,BZ(X^2-Y^2))$	point	-	
E_u (a)	(1,0)	$D_2(C_2') \times i(E) \times T$	(A,0,BX)	-	-	
E_u (b)	(1,1)	$D_2(C_2'') \times i(E) \times T$	(A,A,B(X+Y))	-	-	
E_u (c)	(1,i)	$D_4(E) \times i(E)$	(A,iA,B(X+iY))	point	-	

Table 8: The triplet superconducting states in a tetragonal crystal, assuming strong spin-orbit coupling. The point group given refers to the combined rotations in spin and orbit space.

IV. ORDER PARAMETER STRUCTURE

This Section is concerned with experimental probes that directly reflect the structure of the order parameter. The first subsection discusses the use of fluctuation effects to count the number of components of the order parameter. The second subsection describes the phenomenon of a split transition, which is observed in some samples. The third subsection discusses Josephson effects between $YBa_2Cu_3O_{7-\delta}$ and conventional superconductors. The fourth subsection describes a proposal of Gorkov to search for exotic angular dependence of the in-plane upper critical field. In most of these experiments, positive observation of the phenomenon would be unambiguous evidence for an unconventional pairing state. However, the failure to observe any one of these phenomena would eliminate only some of the non-conventional pairing states. The exception to this state of affairs is the potential suppression of the Josephson effect in planar junctions.

A. Counting The Number of Components of The Order Parameter

One measure of the structure of the order parameter is the number of independent components. An attempt was made to ascertain this number from detailed measurements of the shape of the specific heat curve near the superconducting transition,[31,32] where the contribution to the specific heat from Gaussian fluctuations was observed for the first time. Measurements have also been reported of fluctuation contributions to the conductivity,[33–39] the magnetic susceptibility,[40–42] and the thermopower.[43] In these cases too, the temperature dependence of the data is consistent with the interpretation that Gaussian fluctuations – the lowest order fluctuations about mean field theory – are responsible

for the observations. Note that there is no *a priori* reason for there to be a wide temperature range over which Gaussian fluctuations are observable; however, for $YBa_2Cu_3O_{7-\delta}$ this does seem to be the case empirically. Fluctuation effects in the specific heat have also been observed by Fossheim *et al.*[44] The magnitude of the specific heat peak in their data is, however, only about one half that observed by Inderhees *et al.*[31]

The basic procedure by which the Gaussian contribution to the specific heat is obtained has been described previously.[45] In that analysis it was possible to identify the fluctuation contribution to the specific heat of the form

$$C_{\rm fluct} = C_{\pm} \left| \frac{T - T_c}{T_c} \right|^{-1/2}, \tag{4.1}$$

where the plus sign applies above T_c and the minus sign below. For states with a single complex order parameter, the ratio of the amplitudes C_+ and C_- is

$$C_+/C_- = \frac{1}{\sqrt{2}} \tag{4.2}$$

which is independent of the spatial anisotropy as well as the other Ginzburg-Landau parameters. A larger amplitude ratio implies that the superconductivity is described by a multicomponent, and therefore unconventional, order parameter. The observation of an amplitude ratio with the value $1/\sqrt{2}$ implies that either the pairing is 's-wave' or it is an unconventional state with a single component order parameter.

The measurements of Ref. 31 did indeed show a significantly larger amplitude ratio ($3.5 < C_+/C_- < 6.4$) than could be explained by a conventional Ginburg-Landau theory ($C_+/C_- = 0.7$), apparently ruling out a conventional pairing

state. In order to identify those pairing states consistent with the data, the ratio C_+/C_- must be calculated using the Ginzburg-Landau free energy densities appropriate for the various unconventional pairing states, as discussed in Section III. The result of this analysis[46] is that all of the triplet states with weak spin-orbit coupling as well as the 'd-wave' states ^1E_g a-c (see Table 4) are consistent with the fluctuation data.

Several studies have searched for an alternative explanation of the anomalously large fluctuation specific heat amplitude ratio. In one study, it was shown that electromagnetic interactions, neglected in the Ginzburg-Landau model, cannot account for the enhanced amplitude ratio.[47] The effect of sample inhomogeneities has also been investigated,[48] and it was found that the data could be fit by using conventional s-wave Ginzburg-Landau theory, provided that a distribution of T_c's occured in the sample.

A subsequent measurement of the specific heat of an untwinned region of a single crystal found an amplitude ratio which is smaller than that inferred previously, and which may be consistent with that of a conventional Ginzburg-Landau theory.[49] If confirmed, this result would still be inconclusive in the sense that both conventional and unconventional pairing states could be consistent with the new data.

The principal problem with the analysis of the fluctuation specific heat is that the background subtraction is delicate. In order to extract the fluctuation contribution, it is necessary to remove both the phonon background and the mean-field electronic specific heat. If the fluctuations are observed over a sufficiently small temperature interval, these background subtractions above and below T_c can be approximated by linear functions of temperature. However, if

the fluctuation specific heat is fit over too wide a temperature interval, deviations of the background from linearity are difficult to ascertain, and contaminate the inferred fluctuation contribution. Indeed, in Ref. 44, the authors fit the background to a quadratic form, but neglect to include the mean-field electronic specific heat below T_c. Whilst it is quite clear that the fluctuation effects are present in this data, it was not possible to make a convincing fit to Gaussian or critical fluctuations even if one takes into account the electronic mean-field specific heat.[50]

Measurements of the fluctuation diamagnetism above T_c also effectively count the number of components of the order parameter. Detailed data have been reported in Ref. 41, and have been fit by assuming conventional pairing. So far no attempt has been made to use these data to test the hypothesis that the pairing is conventional, but this certainly should be done.

In summary, early measurements of the Gaussian specific heat amplitude ratio implied that the pairing state is unconventional. One recent measurement on an untwinned sample gives a value of the ratio which is consistent with both conventional and certain unconventional pairing states. More work is required in this area before firm conclusions can be drawn.

B. Splitting Of The Transition

We turn now to an effect that exists only when the order parameter has two or more complex components. As shown in Section III above, states with more than a single complex order parameter are associated with irreducible representations of the symmetry group with dimension, D, greater than one. In this case external perturbations that lower the symmetry, such as a strain or magnetic

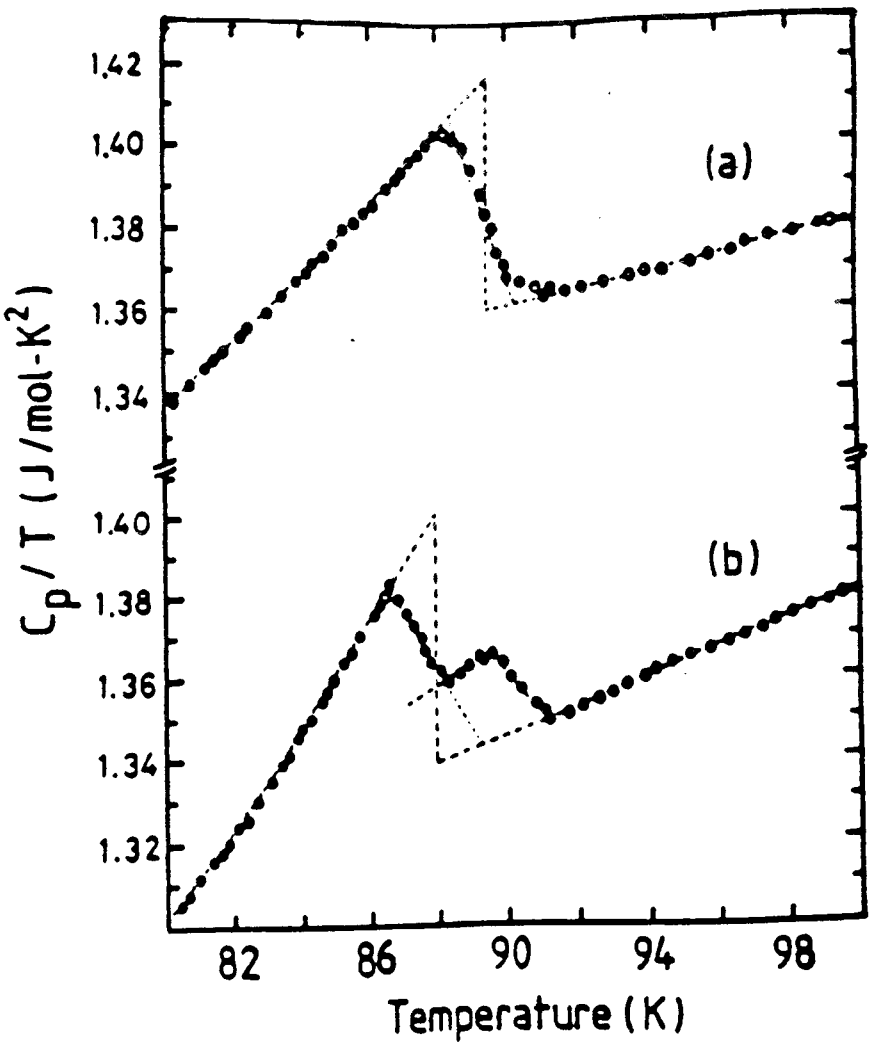

Fig. 5. Specific heat curves C_p/T vs T around T_c for different samples (a) This sample shows a single sharp transition whereas (b) the other sample shows a split superconducting transition. (After Ref. 57.)

field, can split the multi-dimensional representation into several representations of lower dimensionality. This splitting of the degeneracy implies that the different components of the order parameter no longer become non-zero at the same T_c. There are, therefore, slightly different T_c's associated with the different components. In a measurement of, for example, the heat capacity close to T_c, this effect could then lead to two separate peaks.[51–53] Such a splitting was recently seen[54,55] in the heavy fermion compound UPt_3, confirming earlier suspicions that its superconductivity is unconventional.

This effect could also occur in $YBa_2Cu_3O_{7-\delta}$ if, for example, it is a singlet superconductor with a two component order parameter, (η_x, η_y), transforming according to the tetragonal E_g representation. The degenerate basis functions for this representation may be chosen to be XZ and YZ [where as in Section III X=sin($k_x a$) etc.] and the gap function is $\Delta(k) = \eta_x XZ + \eta_y YZ$. Then the slight orthorhombic distortion of the crystalline lattice may split this two-dimensional representation into two one-dimensional representations. The functions XZ and YZ are no longer degenerate, since the x and y axes are not equivalent; this gives rise to distinct T_c's for each component, say T_c^x and T_c^y. At the higher of these transitions, say T_c^x, there is a phase transition from the normal state to superconductivity with $(\eta_x, \eta_y) \propto (1, 0)$. Below that temperature there may or may not be a second phase transition at T_c^y. There would be a second transition if, in the absence of the orthorhombic distortion, the stable ground state is $(\eta_x, \eta_y) \propto (1, 1)$ or $(\eta_x, \eta_y) \propto (1, i)$. There would not be a second transition if the tetragonal ground state were $(\eta_x, \eta_y) \propto (1, 0)$. This example illustrates that, while positive observation of a split phase transition is decisive evidence for a multi-component order parameter, and hence unconventional pairing, the absence of a splitting is

not conclusive, and may be consistent with either a single or multi-component order parameter.

There are two examples in the literature[56,57] of observations of split superconducting transitions in $YBa_2Cu_3O_{7-\delta}$. However, they are not consistent with each other in either the magnitude of the splitting or in the peak shapes. In the study of Ref. 57, a second superconducting phase in addition to the ordinary 90 K orthorhombic phase was sought by high resolution X-ray diffraction, but was not found. The data of Ishikawa *et al.* are reproduced in Fig. 5, and are reported to be reproducible.[58] An early observation[31] of a possible split transition did not appear to be reproducible in subsequent measurements on other samples.[49]

There is a crucial difference between the possible peak splitting observed in $YBa_2Cu_3O_{7-\delta}$ and that more convincingly seen in UPt_3. In UPt_3, the splitting is observed in the best samples, and its magnitude is not sample dependent. On the other hand, for $YBa_2Cu_3O_{7-\delta}$, the splitting seems very sample dependent, being absent in some of the samples with the sharpest phase transitions. This may indicate that the split transition in $YBa_2Cu_3O_{7-\delta}$ is due to local inhomogeneities rather than being a transition between superconducting phases.

There is a clear way to rule out sample inhomogeneity as a cause of a split transition. If the split transition is caused by a near degeneracy between two order parameter components, then the temperature interval between the two transitions should change when a magnetic field is applied.[59] This effect has indeed been observed[55] in UPt_3. Unfortunately it is not clear whether this technique would work in $YBa_2Cu_3O_{7-\delta}$ since the effect of an external magnetic field of even 1.5T causes a large broadening of the critical region.[32] This broadening may be so severe as to make it difficult to observe the field dependence of the splitting.

C. Josephson Effects

The Josephson effect between a conventional superconductor (such as Nb or Pb) and $YBa_2Cu_3O_{7-\delta}$ may be used as a probe of the pairing state. The Josephson effect has been observed in superconductor-insulator-superconductor(SIS) junctions where one of the superconductors is $YBa_2Cu_3O_{7-\delta}$ and the other is a conventional one such as In.[60,61] Flux quantization and persistent currents have also been observed in superconducting rings consisting of part niobium and part $YBa_2Cu_3O_{7-\delta}$ in series,[62,63] which also indicates that a non-zero Josephson coupling exists between Nb and $YBa_2Cu_3O_{7-\delta}$. It is sometimes stated that the Josephson effect cannot occur between a singlet and a triplet superconductor,[64] because the singlet and triplet superconductor order parameters transform differently under spin-space rotations. The observations might be taken as evidence that $YBa_2Cu_3O_{7-\delta}$ is a singlet superconductor. Unfortunately the evidence is by no means conclusive: there are two effects which can cause the Josephson coupling to be non-zero, even for triplet-singlet junctions. These are spin-orbit coupling, on either side of or inside the junction, and paramagnetic impurities in the junction.[65] Therefore, these experiments do not rule out the possibility of triplet pairing.

Can the above experiments rule out 'd-wave' pairing? Again, the answer is no. In general there is no selection rule forbidding the Josephson coupling between s- and d-wave superconductors.[66,67]

The only selection rule for Josephson effects between conventional and unconventional superconductors requires planar junctions that preserve some crystallographic symmetry (such as a two-fold axis or mirror plane) of the $YBa_2Cu_3O_{7-\delta}$ crystal. In this case, for many of the unconventional superconducting states that

could occur in $YBa_2Cu_3O_{7-\delta}$, the Josephson effect is forbidden whether or not spin-orbit coupling is present.[68] As an example, suppose that $YBa_2Cu_3O_{7-\delta}$ is a 'd-wave' superconductor with a gap function of the form $\Delta(k) \propto (X^2 - Y^2)$ where, as before, $X = \sin(k_x a)$ etc. Imagine that a planar Josephson junction is fabricated perpendicular to the crystal c-axis and that the interface is free from defects. Under 90° rotations about the c-axis, the $YBa_2Cu_3O_{7-\delta}$ gap function changes sign. If the other superconductor is 's-wave' then its gap function would be invariant under this rotation. This difference implies that there can be no Josephson coupling between the two superconductors in this planar junction, and hence no observed Josephson effect.[25] Similar symmetry arguments are possible for a variety of planar junction orientations and unconventional pairing states; a summary of the various selection rules has been given by Gorkov.[24]

Such a planar junction has been fabricated by Greene *et al.*,[69] who made a $YBa_2Cu_3O_{7-\delta}$-Au-Pb junction perpendicular to the $YBa_2Cu_3O_{7-\delta}$ c-axis. The junction did show some signs of Shapiro steps in a microwave field, suggesting that the ac-Josephson effect was indeed occuring. If confirmed, this observation would eliminate a large number of the possible pairing states; in particular, it would rule out all singlet pairing states other than 's-wave'. Such a crucial experiment needs to be checked, especially to see whether the Josephson effect becomes stronger or weaker as the junction quality is improved. The poorly developed Shapiro step structure in Ref. 69 may indicate that in an ideally planar junction, the Shapiro steps would be absent. It is important to check this, since even small deviations from a perfectly planar junction invalidate the selection rules.

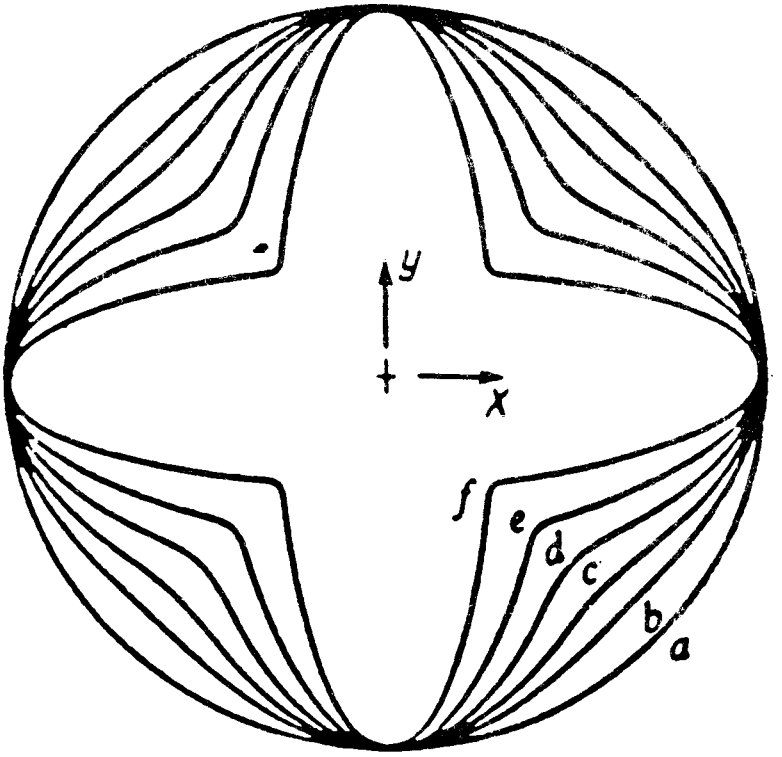

Fig. 6. Angular dependence of H_{c2} in the basal plane of a tetragonal crystal. The different curves are compufed for the following values of the anisotropic gradient terms in Eq. (3.7): $P_1 : P_2 : P_3$ = (a) 1 : 1 : 0; (b) 1 : 1 : 0.5; (c) 1 : 1 : 1; (d) 1 : 1 : 2; (e) 1 : 1 : 4; (f) 1 : 1 : 10.0. (After Ref. 71.)

D. Angular Dependence of H_{c2}

The final probe of order parameter structure that we mention is the angular dependence of the upper critical field H_{c2} in the basal plane. The reason why this is potentially a powerful probe of the superconducting pairing state is that H_{c2} and its angular dependence are determined entirely by the Ginzburg-Landau equations describing the superconductor. As we have emphasised above, many unconventional superconducting states give rise to Ginzburg-Landau theories which are considerably more complicated than the usual one. For the conventional Ginzburg-Landau free energy density, the angular dependence of H_{c2} arises only from the effective mass tensor m_{ij} in Eq. (3.4). The angular dependence of $H_{c2}(\phi)$, where ϕ is the angle in the basal plane, is therefore given by an ellipse, whose principal axes are determined by m_{ij}. However, for some unconventional order parameters, such as those corresponding to the tetragonal E representation, there are many gradient terms in the free energy, as shown in Eq. (3.7). Consequently, for fields in the symmetry plane, $H_{c2}(\phi)$ can be a complicated function[70] of the angle ϕ between the external field and the in-plane crystal axis. For example, in the case of the singlet E-representation tetragonal states, Burlachkov[71] has shown that

$$H_{c2} = \frac{\alpha c}{2e}(P_4^{1/2}[P_1 + \frac{P_2 + P_3}{2} - \frac{1}{2}(P_2^2 + (2P_2P_3 + P_3^2)\cos^2 2\phi)^{1/2}]^{1/2})^{-1} \quad (4.3)$$

where $P_i = 1/2m_i$, $i = 1 \ldots 4$, as defined in eqn. (3.7). When plotted as a function of ϕ, this gives the characteristic rosette shape shown in Fig. 6.

There have, as yet, been no experimental measurements of the angular dependence of H_{c2} in the basal plane, as far as we are aware. There are two

experimental difficulties which must be overcome. First, this measurement must be performed on an untwinned crystal so that any rosette structure is not mistaken for the superposition of two ellipses. Second, many measurements of H_{c2} in $YBa_2Cu_3O_{7-\delta}$ are complicated by irreversible effects.[72]

What would one anticipate seeing in $YBa_2Cu_3O_{7-\delta}$, which, after all, has an orthorhombic structure? If there are no accidental near degeneracies, then the only possible outcome is an elliptical angular dependence. On the other hand, if, as seems likely, there are accidental near degeneracies corresponding to orthorhombic perturbations of the tetragonal pairing states, then it is possible that one would obtain a tetragonal rosette structure with a weak orthorhombic distortion superimposed. If such a result were to be obtained, this would be clear evidence for unconventional superconductivity.

V. LOW-ENERGY EXCITATIONS

A. Overview

One of the most well-known predictions of BCS theory is the existence of the energy gap for quasi-particle excitations. The quasi-particle energies in a singlet superconducting state are given by

$$E_k^2 = \epsilon_k^2 + |\Delta(k)|^2, \tag{5.1}$$

where ϵ_k is the normal state quasi-particle energy measured relative to the chemical potential, and $\Delta(k)$ is the gap function. The original BCS theory[73] treated an isotropic system, and the gap function was a single temperature dependent constant. In a real system, with crystalline anisotropy, the gap function depends

on the momentum k. The threshold energy required to break Cooper pairs is the minimum value of $2|\Delta(k)|$ on the Fermi surface, $2\Delta_{\rm min}$. Both spectroscopic measurements and low temperature properties depend sensitively on $\Delta_{\rm min}$. Note the important distinction between the *gap function*, $\Delta(k)$, and the *energy gap for quasi-particle excitations*, $\Delta_{\rm min}$.

The quasi-particle energies in a triplet superconducting state are given by

$$E_k^2 = \epsilon_k^2 + |\vec{d}(k)|^2 \pm |\vec{d}(k)^* \times \vec{d}(k)|^2. \tag{5.2}$$

where the different signs are associated with the different quasi-particle spin polarizations. Again, one can define

$$\Delta_{\rm min} = \min\left\{\sqrt{|\vec{d}(k)|^2 \pm |\vec{d}(k)^* \times \vec{d}(k)|^2}\right\}. \tag{5.3}$$

The symmetries of unconventional states often require that $\Delta_{\rm min}$ vanishes. For example, consider a superconducting state that is unconventional because the gap function changes sign under reflection through a mirror plane of the crystal. Then $\Delta(k)$ must vanish on the mirror plane, so $\Delta_{\rm min} = 0$. For a conventional superconductor, there are no symmetry reasons for $\Delta_{\rm min}$ to be zero. However, for a dirty superconductor with paramagnetic impurities, the excitation gap may be zero.[74,75]

When $\Delta_{\rm min} = 0$, there is no energy gap for quasi-particle excitations, and the low temperature behaviour of the system is very different from that of a conventional superconductor, for which $\Delta_{\rm min} \neq 0$. In this Section, we review various experimental probes of the excitation gap of $YBa_2Cu_3O_{7-\delta}$ in the hope of determining whether $\Delta_{\rm min}$ is zero.

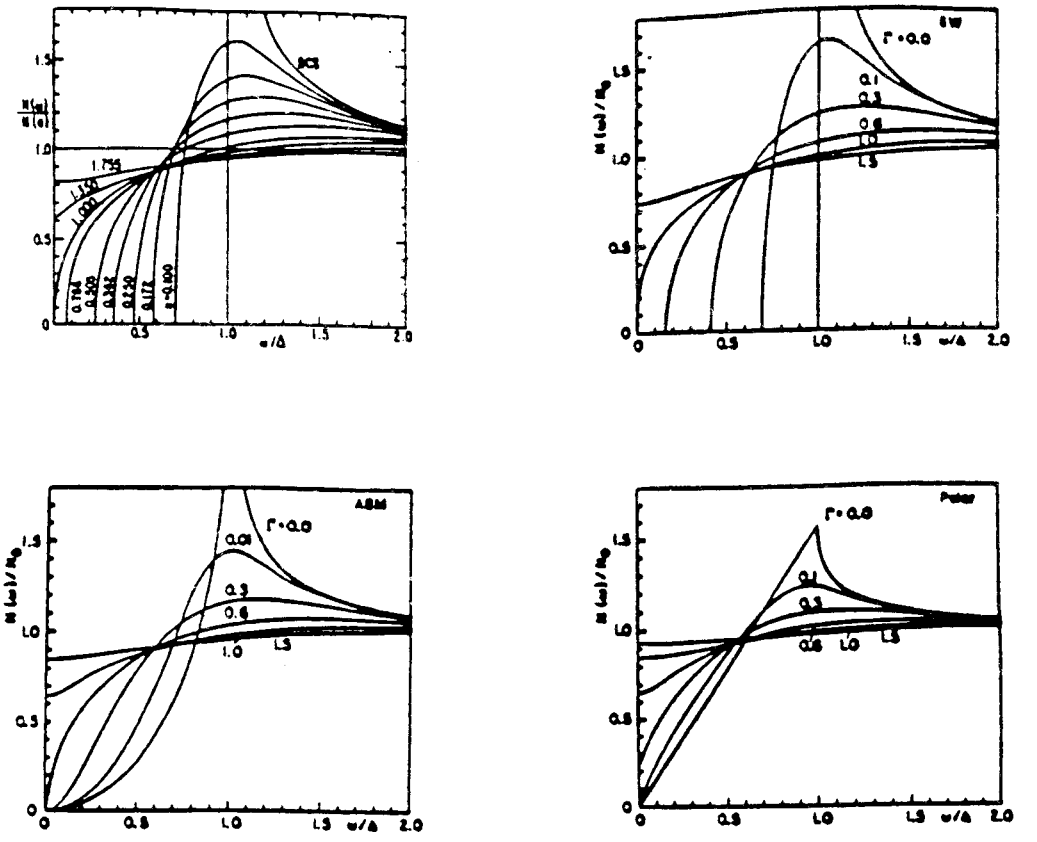

Fig. 7. The zero temperature density of quasi-particle states for several types of superconductors. In each figure, the evolution of the density of states in going from the clean to the dirty limit is shown. Starting from the upper left hand corner and proceeding clockwise these are: (a) a conventional superconductor (after A. Griffin and V. Ambegaokar, in *Proc. Int. Low Temp. Phys. Ohio* (1964), J.G. Daunt *et al.* (eds.), p.524.) (b) a nodeless Balian-Werthamer state (c) an axial triplet state with point nodes and (d) a polar triplet state with line nodes. (The plots for the three triplet states are from K. Ueda and T.M. Rice, in *Theory of Heavy Fermions and Valence Fluctuations*, T. Kasuya and T. Saso (eds.), (Springer-Verlag, Berlin, 1985), p.263). Notice that in all cases the density of states has a peak in the clean limit, although in the ABM and polar cases there is no minimum gap.

Although many of these probes reveal the presence of low energy excitations, as we will see, much care must be exercised in their interpretation. Indeed, to infer the existence of nodes, one must be able to argue that the low energy excitations arise from the carriers, not from local moments, phonons, impurity phases, or dead surfaces. At low temperatures it is unlikely that the low energy excitations are due to gapless 's-wave' superconductivity, since the Drude scattering rate $1/\tau$ is small[76] compared to typical values of the zero temperature gap function,[77] that are observed in some experiments.

Many experiments have not found a clear minimum excitation energy that could be identified with $\Delta_{\rm min}$. Neverthless it is common for authors to report excitation gap values, based upon the observation of a peak in the density of states. This might correspond to the excitation gap if $YBa_2Cu_3O_{7-\delta}$ is a conventional superconductor. However even if the superconductivity in $YBa_2Cu_3O_{7-\delta}$ is unconventional, such a feature might still occur, and could correspond to the gap maximum $\Delta_{\rm max}$. This is illustrated in Fig. 7. Furthermore if one wishes to identify a particular feature in the density of states as originating from a superconducting gap function, it is important to show that the feature vanishes as $T \to T_c$ and is absent above T_c.

B. Raman Scattering

We now turn to our discussion of the various classes of experiments, which appear to indicate the presence of low energy excitations, beginning with a discussion of the results of Raman scattering from $YBa_2Cu_3O_{7-\delta}$.[78–91] These experiments show evidence for low-lying excitations, both from direct observations of an electronic background, and from measurements of temperature dependent

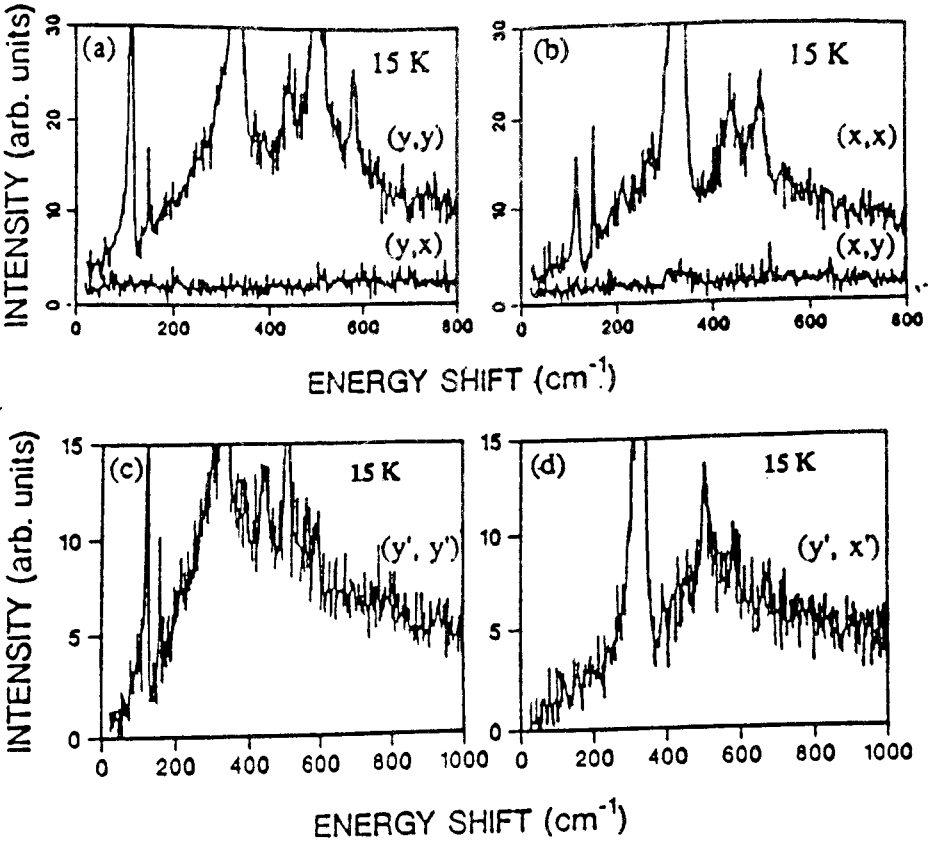

Fig. 8. Low temperature spectra in a single-crystal $YBa_2Cu_3O_{7-\delta}$, including (a) polarized (y,y) (=A_{1g}-along the Cu-O chain) and depolarized (y,x) spectra at 15K; (b) polarized (x,x) (=A_g-perpendicular to the Cu-O chain) and depolarized (x,y) spectrum at 15K; (c) polarized (y',y') (A_{1g} -tetragonal) spectrum at 15K; d) depolarized (y',x') (=B_{1g}-tetragonal) spectrum at 15K. Here x and y refer to the orthorhombic a and b axis directions. (After Ref. 90.)

phonon linewidths.

5.1.1 Electronic continuum

The most striking feature of the Raman scattering intensity plotted as a function of energy shift is a background that is present for polarizations (y',y') (A_{1g}) and (y',x') (B_{1g}) at all temperatures studied, both above and below T_c. Fig. 8 shows the data below T_c. The data show the presence of Fano anti-resonances in the A_{1g} phonon peaks at 115cm^{-1} and in the B_{1g} phonon at 330cm^{-1}, which have been interpreted as suggesting that the background is an intrinsic bulk electronic effect, not associated with the surface. The presence of a sharp unsplit peak at 500cm^{-1} from the A_g bridging oxygen mode indicates that the surface layer is not oxygen depleted.[92,93] Furthermore, for temperatures $T \ll T_c$, the continuum background is depleted at small ω, again indicating that the continuum is associated with a superconducting region of the sample. The Raman background continuum has also been observed in $Bi_{2.2}Sr_{1.8}CaCu_2O_{8+\delta}$[94] with features at $\omega = 250\text{cm}^{-1}$ (xx) and 550cm^{-1} (xy), in $Tl_2Ca_2Ba_2Cu_3O_{10}$ (2223),[95] in $(La_{1-x}Sr_x)_2CuO_4$,[96] and in $Ba_{0.6}K_{0.4}BiO_3$.[97,98] This universality also suggests that this background is an intrinsic feature.

In a superconductor with a non-zero excitation gap Δ_{min}, there should be no Raman scattering intensity below $\omega = 2\Delta_{min}$. The data shown in Fig. 8 do not show any minimum gap Δ_{min}, although they do show the appearance of a depleted region at low frequencies well below T_c. Furthermore, in a superconductor with an excitation gap, the Raman intensity should show a sharp peak at a characteristic excitation energy 2Δ. Indeed there are broad maxima at 350cm^{-1} (A_{1g}) and 550cm^{-1} (B_{1g}). One possible interpretation of the depletion is that it arises from an unconventional pairing state with nodes. In this case

there would be no minimum excitation gap, a depleted region, and the broad features at 350cm^{-1} and 550cm^{-1} would then be identified with the appropriate Fermi surface averages of this presumed anisotropic gap function. Unfortunately such an explanation seems unlikely, since the 550cm^{-1} feature does not move to significantly lower frequencies[82] in the oxygen depleted superconductor $YBa_2Cu_3O_{6.8}$, for which the transition temperature (T_c=50K) is smaller than that of $YBa_2Cu_3O_{7-\delta}$. The 550cm^{-1} feature also does not vanish as $T \rightarrow T_c$, and therefore cannot be a gap feature.[99] Furthermore, it is difficult to imagine how the Fermi surface variation of the gap function associated with either nodal structures or other gap anisotropies could lead to linear behavior in the B_{1g} spectrum for frequencies as large as 2Δ.[100] Evidently, the feature at 550cm^{-1} is not a superconducting gap, but instead is intrinsic to the normal state. The significance of the 350cm^{-1} feature it is not yet clear; however, the 350cm^{-1} feature ($2\Delta/k_BT_c$ =5.5) occurs at about the same energy relative to T_c as the gap like feature at 20meV ($2\Delta/k_BT_c = 6.0 \pm 0.1$) often observed in tunnelling conductance data (see Section C).

The normal state Raman scattering spectra cannot be straightforwardly ascribed to intra-band particle-hole excitations because the scattering intensity would be non-zero only up to a frequency qv_f, which is estimated to be of order 20cm^{-1}, and not 500cm^{-1} as observed. Here q is the inverse of the optical penetration depth and v_f is the Fermi velocity. The estimated frequency range of intra-band excitations neglects elastic and inelastic scattering; however, the measured scattering rates[76] are too small to account for the spectrum.

An alternative explanation of this continuum has been given by Monien and Zawadowski (MZ).[100] On the basis of band structure calculations,[103] they argue

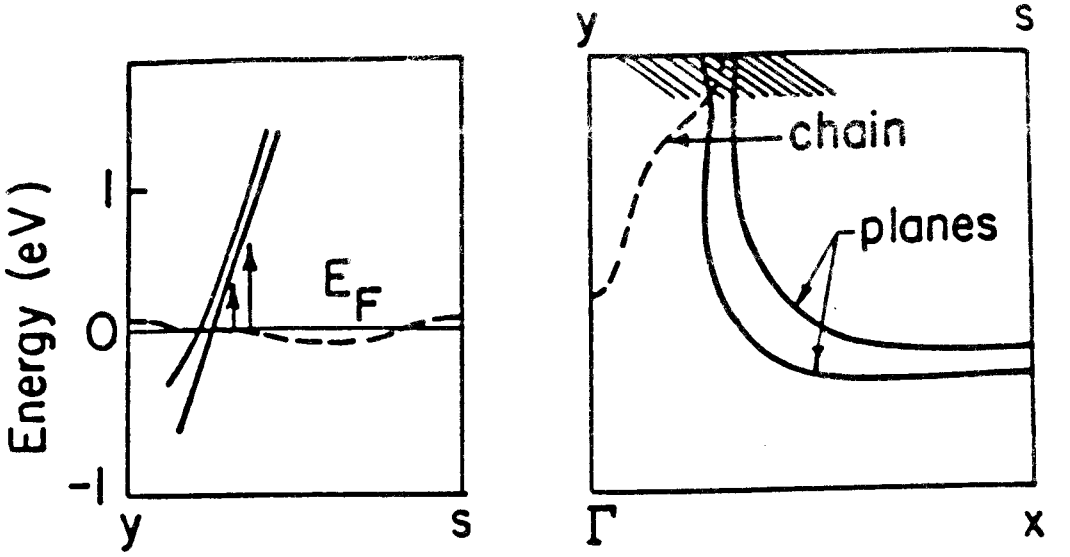

Fig. 9. Left: the energy vs. k as obtained in Ref. 103 is sketched along the YS line in the Brillouin zone. The solid lines are the bands associated with planes, and the dashed line with the bridging oxygen. The arrows indicate the interband transition. The Fermi energy is the light line. Right: the Fermi surface is shown in the k_x-k_y plane of the Brillouin zone. (After Ref. 100.)

that the B_{1g} Raman scattering component is due to interband excitations between the CuO_2 plane bands and the O(4) bridging oxygen band. If the crossing between these two bands occurs sufficiently close to the Fermi surface, as shown in Fig. 9, then a B_{1g} background with characteristic linear behavior occurs. MZ explain the absence of an excitation gap, Δ_{min}, below T_c in the B_{1g} spectrum by supposing that the gap function has a line of nodes on the YS boundary line of the Brillouin zone where the band crossing occurs. The possible pairing states with such a line of nodes are the d-wave states transforming according to ${}^1B_{2g}$ ($k_x k_y$), ${}^1E_g$ ($k_z k_z$ and $k_y k_z$), and the p-wave state (without spin orbit coupling) ${}^3E_u(a)$ which transforms like k_y.

5.1.2 Phonon Linewidth

We conclude our discussion of Raman scattering experiments with measurements of phonon linewidths. These provide further evidence[88,89,90] suggesting that there are low energy excitations in superconducting $YBa_2Cu_3O_{7-\delta}$. We assume that the lifetimes of the Raman active phonons are determined by the coupling to an electron-hole continuum. In a single band model, the phonon linewidth is proportional to the single particle density of states. By determining the phonon linewidth at different wavenumbers and temperatures, it is, therefore, possible to get a crude indication of the behaviour of the density of states. In a conventional system with a clean gap, Δ_{min}, the linewidth of any phonon whose frequency is smaller than Δ_{min} should first increase as T becomes smaller than T_c, reaching a maximum when the peak in the single particle density of states crosses the optical phonon frequency. As the temperature is reduced further, the linewidth should dramatically fall to a value below that in the normal state because of the gap in the single particle density of states.

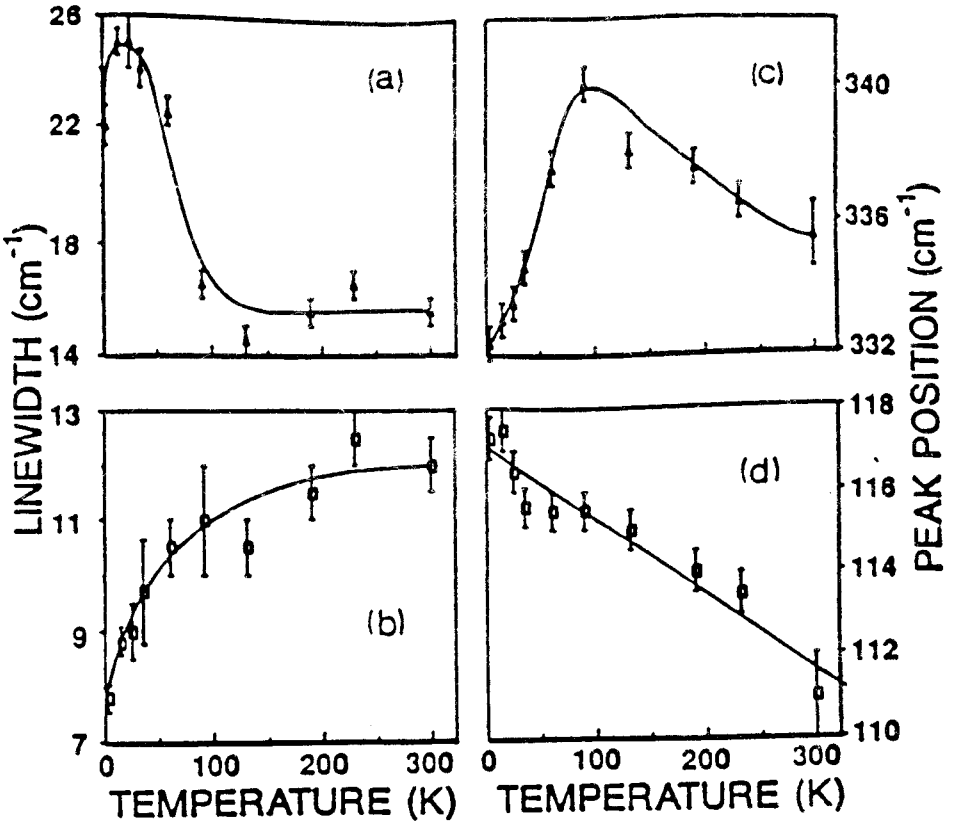

Fig. 10. (a) and (b) Full width at half maximum linewidths of 340cm^{-1} (filled triangles) and 116cm^{-1} (open squares) phonons respectively. (c) 340cm^{-1} phonon frequencies (d) Observed (open squares) phonon frequencies for the 116cm^{-1} phonon. The data represents averages over many spectra and error bars are standard deviations. Solid lines are guides to the eye. (After ref. 78.)

The linewidths of two Raman active phonons have been determined,[78,89] and the results are very interesting. First, consider the temperature dependence[89] of the linewidth of the phonon at 340 cm^{-1}, shown in Fig. 10. The linewidth indeed rises as T is reduced below T_c, but it then falls to a value *larger* than that of the normal state. This might be interpreted as evidence that there is no gap in the density of states. Alternatively, if there is a gap with $2\Delta_{min} < 340cm^{-1}$ then as the temperature is lowered, a local peak in the density of states initially below $340cm^{-1}$ might be pushed up past $340cm^{-1}$, giving rise to the observed behaviour.[104]

The situation is quite different for the linewidth of the A_{1g} phonon[78] at 116 cm^{-1}, shown in Fig. 10. Here, the linewidth continually *falls* as T decreases below T_c. This suggests that there is no peak at 2Δ in the single particle density of states at $\omega = 116cm^{-1}$ at *any* temperature.

We conclude that the Raman data do not provide evidence for a gap in the single particle density of states. On the other hand, it is not yet known whether the low energy excitations indicate the presence of gap function nodes.

C. Infra-red Reflectivity

Next we consider the infrared reflectivity (IR) experiments[105–118] which can, in principle, reveal an energy gap and show whether or not there is a significant density of states within that gap. Unfortunately the interpretation of these data is rather controversial at this time. There seem at present to be three conflicting interpretations of the data.

(1) The IR measurements reveal a small gap of $220cm^{-1}$.

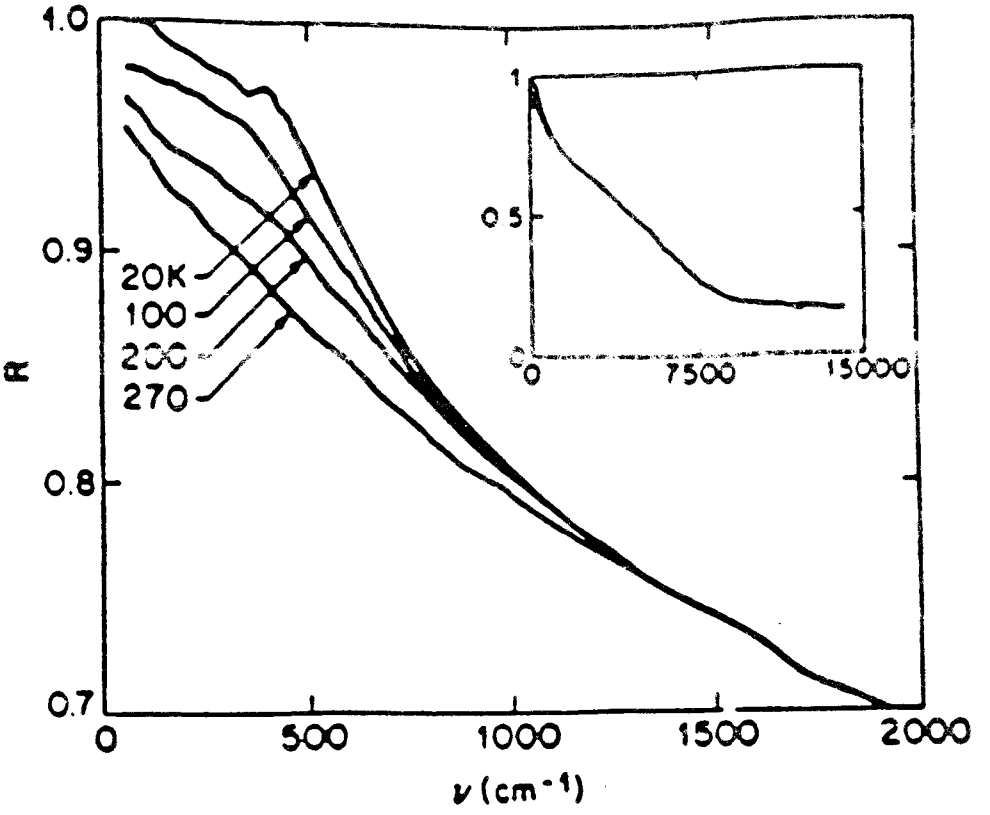

Fig. 11. Reflectivity, R, as a function of frequency, ν, for a sample of $YBa_2Cu_3O_{7-\delta}$ with $T_c = 50$K, at several temperatures as labeled in the main part of the figure. Inset: R over a wider range of ν at T=20K and 270K. (After Ref. 113.)

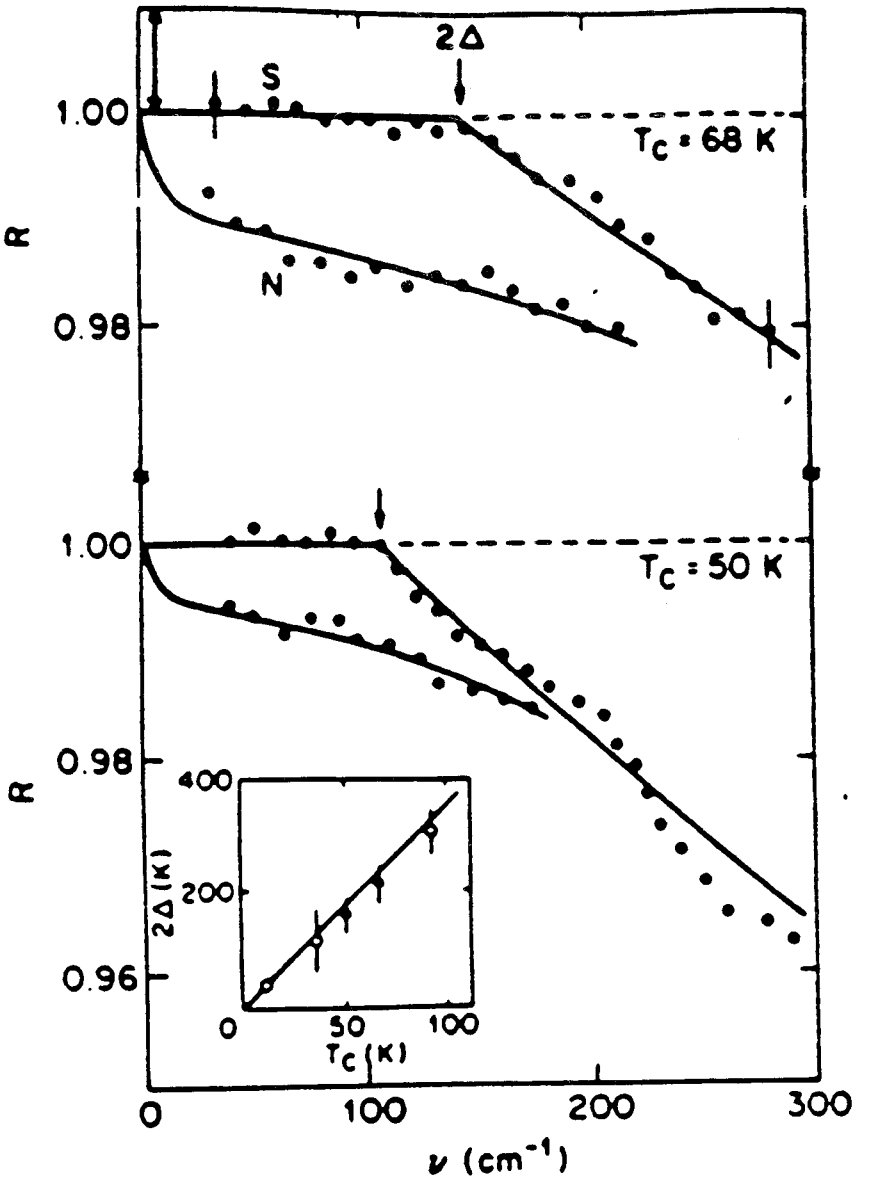

Fig. 12. Finer detail of the low frequency reflectivity for two samples of $YBa_2Cu_3O_{7-\delta}$ with depressed T_c's indicated. For each plot the lower points are taken just above T_c and the upper points are taken at T=20K. The solid lines are guides to the eye. The arrow in the upper left indicates the absolute uncertainty in R; the reflectivity is constant to within the much smaller relative errors below the frequency marked 2Δ Inset: 2Δ as a function of T_c for *different* materials as explained in the text. (After Ref. 113.)

(2) The IR measurements are incapable of observing a gap due to the small scattering rate.

(3) The IR measurements show a large gap of 480cm^{-1}.

We shall discuss each of these three interpretations in turn, and their implications for possible gap nodal structure.

The first of the interpretations of the IR reflectivity data is due to Thomas *et al.*[113] Consider the reflectivity data for a single crystal of oxygen depleted $YBa_2Cu_3O_{7-\delta}$ with $T_c \approx 50$K shown in Figs. 11, 12 and 13. A prominent feature in Figs. 11 and 12 is a region where the reflectivity is unity to within calibration errors ($< 2\%$). In this region the reflectivity remains constant for ω less than about 100cm^{-1} (for the T_c=50K sample). Above this frequency the reflectivity gradually decreases. By examining different materials ($La_{0.85}Sr_{0.15}CuO_4$[119] and $BaPb_{(1-x)}Bi_xO_3$[120,121]), Thomas *et al.* argue that the frequency of the second feature is consistent with the weak coupling BCS prediction of $2\Delta = 3.5k_BT_c$. This energy corresponds to about 220cm^{-1} in $YBa_2Cu_3O_{7-\delta}$ with $T_c = 90$K. If this unit reflectance feature is indeed the gap, then the absence of low frequency absorption provides evidence against a pairing state with nodes (or any other form of gapless superconductor).

However, as discussed by Timusk *et al.*,[107] the interpretation of this feature as a gap is consistent only if the scattering rate $1/\tau$ is not too much smaller than the gap $2\Delta_{\rm min}$. Values of $1/\tau$ can be estimated from the data of Thomas *et al.* above 270K, giving $1/\tau \sim 1.9k_BT$. Extrapolating to below T_c, this would correspond to 130cm^{-1}. Therefore the gap-like feature could not be a true gap. The interpretation of Thomas *et al.* would be valid only provided $1/\tau$ is constant below T_c rather than continuing to decrease as $2k_BT$. If the interpretation of

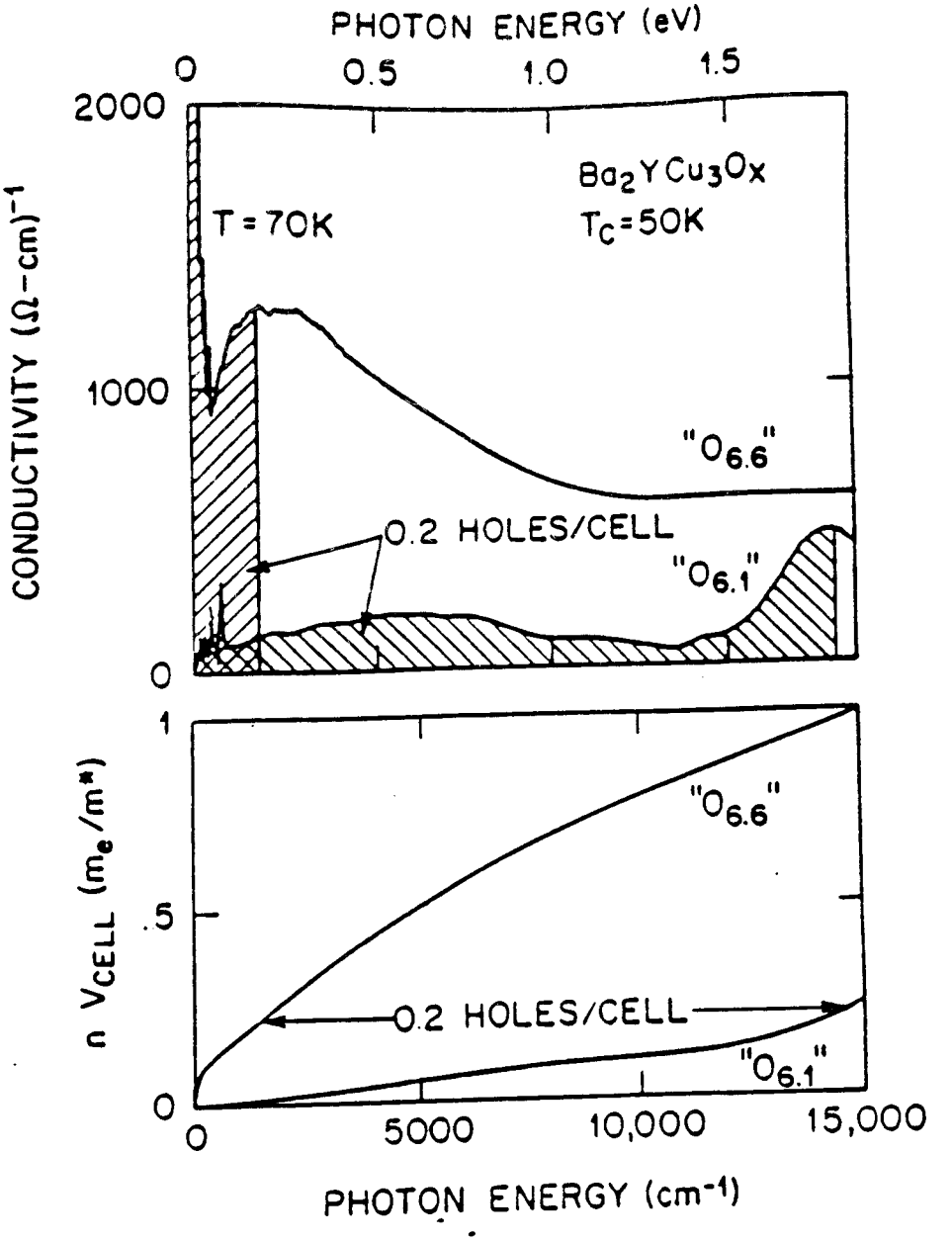

Fig. 13. Conductivity as a function of frequency for two different samples with different O concentrations. The shaded area indicates the spectral weight from 0.2 holes/cell (with mass ratio 1) derived from the integrated area under the curves plotted in the lower part of the figure. (After Ref. 118.)

Timusk *et al.* is correct, then, since the unit reflectance feature is not a true gap, nothing can be inferred about the gap nodal structure from this data.

We now come to the second interpretation of the IR data, that of the Florida-McMaster collaboration. This group has analysed the conductivity, obtained by a Kramers-Kronig analysis of the reflectivity data, and concludes that in addition to the far-infrared Drude absorption, there is a broad absorption band in the mid-infrared. Fig. 13 shows data from a typical optical conductivity measurement, with the mid-infrared band extending from 1000-5000cm^{-1}. This analysis has been carried out for mosaics of 10-20 small (300-1500 μm) crystals,[107] textured ceramics[107,109,110,111] and, most recently, thin films of $YBa_2Cu_3O_{7-\delta}$.[112] For both single crystals and ceramics, the normal state conductivity can be written as a sum of a Drude term, a temperature independent part associated with some unknown mid-infrared direct absorption process, and contributions from 6 infrared-active phonons, with frequencies w_j and widths γ_j, $j = 1, 2, \ldots 6$. They use,

$$\sigma = \frac{\omega}{4\pi} \mathrm{Im}\, \epsilon(\omega) \tag{5.4}$$

where the dielectric constant is

$$\epsilon(\omega) = -\frac{\omega_{pD}^2}{\omega^2 + i\omega/\tau} + \frac{\omega_{pe}^2}{\omega_e^2 - \omega^2 - i\omega\gamma_e} + \sum_{j=1,6} \frac{S_j \omega_j^2}{\omega_j^2 - \omega^2 - i\omega\gamma_j} + \epsilon_\infty \tag{5.5}$$

According to Timusk *et al*,[107] ω_{pD}=1.2eV is a temperature independent plasma frequency, ω_{pe} is the temperature independent strength of the midinfrared feature centered at ω_e = 0.25ev (2000cm^{-1}) with width γ_e = 0.6ev (5000cm^{-1}) and $1/\tau$=250cm^{-1} at 100K. These values are taken from data obtained from a crystal mosaic of $YBa_2Cu_3O_{7-\delta}$ with T_c = 85K (determined by the Meissner effect). For

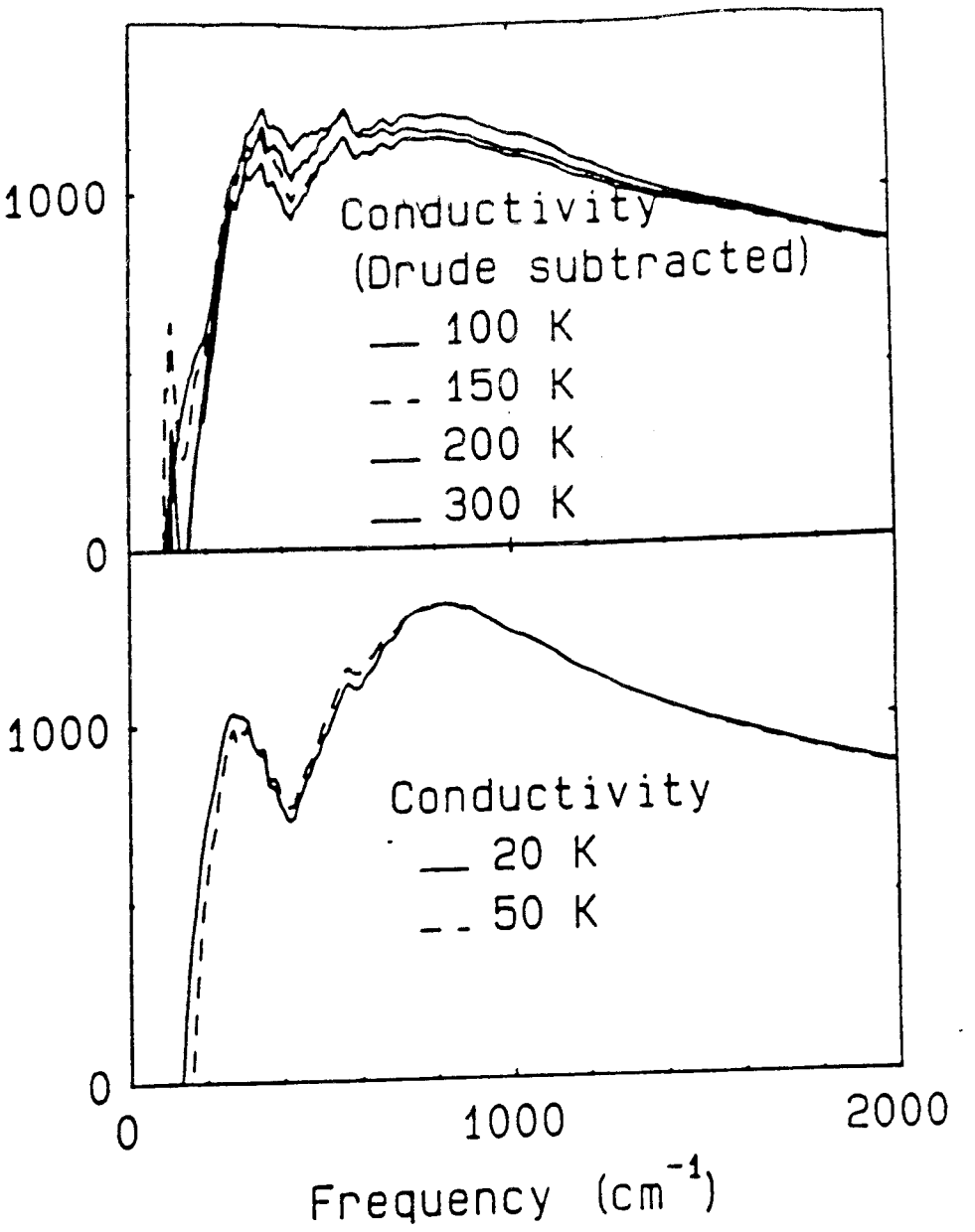

Fig. 14. Upper panel: frequency-dependent conductivity above T_c with the Drude contribution subtracted, for a laser deposited thin film. Lower panel: actual conductivity below T_c. After Ref. 112.

a superconducting ceramic, Timusk *et al.*[107] and Tanner *et al.*[108] find that the normal state Drude absorption is replaced by the London dielectric function

$$\epsilon = -\frac{\omega_{pD}^2}{\omega^2} + i\frac{\pi\omega_{ps}^2}{2\omega}\delta(\omega) + \frac{\omega_{pe}^2}{\omega_e^2 - \omega^2 - i\omega\gamma_e} + \sum_{j=1,6}\frac{S_j\omega_j^2}{\omega_j^2 - \omega^2 - i\omega\gamma_j} + \epsilon_\infty \quad (5.6)$$

where the parameters in this equation are found to be essentially identical to those in the corresponding normal state dielectric function. This is illustrated in Fig. 14. As expected for a clean superconductor, all the Drude oscillator strength below 2Δ appears in a delta function at zero frequency, leaving little oscillator strength for transitions above the gap. According to this analysis, one should interpret the onset of the absorption at 220cm^{-1} in Fig. 14 as the combined effect of both the onset of midinfrared absorption and the strong contributions from phonons at 277cm^{-1} and 311cm^{-1}. Thus, this onset cannot be identified with a superconducting gap. Most recently this group has obtained similar results for highly oriented laser-deposited thin films.[112] If this interpretation is correct then the IR data would be of little use in determining whether states occur within the gap.

We now consider the third possible interpretation of the infrared data, that of the IBM group.[114,115,116,117] They performed measurments on single crystals of $YBa_2Cu_3O_{7-\delta}$ with T_c=92K. The conductivity data were analysed in terms of a Drude function with a frequency dependent scattering time $\tau^*(\omega) = \tau(\omega)[1 + \lambda(\omega)]$ and a renormalized mass $m^*(\omega) = m_b[1 + \lambda(\omega)]$:

$$\sigma(\omega) = \frac{ne^2\tau^*(\omega)}{m^*(\omega)[1 - i\omega\tau^*(\omega)]} \quad (5.7)$$

According to this treatment, intraband absorption is responsible for both the far and midinfrared features. Both this group and Thomas *et al.*[122] have analysed

the damping rate, assuming that the frequency dependence of τ occurred through the emission of Bose excitations (Holstein processes). The coupling between the carriers and the bosons, $\alpha^2_{tr}F(\omega)$, was obtained from the data for $\tau(\omega)$ by using[123]

$$\frac{1}{\tau(\omega)} = \frac{2\pi}{\omega}\int_0^\omega \alpha^2_{tr}F(\Omega)(\omega - \Omega)d\Omega. \tag{5.8}$$

Here $\alpha^2_{tr}F$ is the Eliashberg function proportional to a density of excitations modified by the inclusion of a factor $(1 - \cos\theta)$ to weight large scattering angles. It was concluded that the absorption in the midinfrared region is associated with the carriers emitting a Bose excitation with a characteristic energy of about 500cm^{-1}. According to this picture, the 480cm^{-1} feature is associated with the superconducting gap, and corresponds to $2\Delta = 8k_BT_c$. Schlesinger *et al.*[115] were able to fit the reflectivity data in terms of the Bardeen-Mattiss formula using $2\Delta = 480\text{cm}^{-1}$. If this interpretation is correct, then the data imply a large gap, but with many low-energy excitations, since the reflectivity is less than unity well below 500cm^{-1}.

This interpretation of the data remains controversial at present. For example Timusk *et al.* argued that: (1) when the system goes superconducting, the mid-infrared band should shift up by 2Δ, whereas no such shift has been observed. (2) the slope of the temperature dependent dc resistivity should exhibit a bend at temperatures large enough to begin thermally exciting the Holstein excitations, which should be at about 300K;[106] this is not observed to occur until about 700K.

In conclusion, the infrared data does not yet, in our opinion, provide conclusive evidence either for a non-zero gap or for a gap with nodes.

D. Tunneling Conductance

Another class of experiments that can show the presence or absence of an excitation gap is the tunneling conductance. These experiments provide a direct observation of the superconducting density of states. In particular, the standard theory gives

$$dI/dV \sim |t|^2 N_{1s}(eV) N_2 \tag{5.9}$$

where $N_{1s}(E)$ and N_2 are the single particle densities of states on the superconducting and normal sides of the SIN junction respectively, and t is the tunneling matrix element. Measurement of dI/dV can, in principle, show whether or not there is a well defined gap without low energy quasiparticles and, if so, what is the magnitude of $\Delta_{\min}$.

Unfortunately widely different tunneling characteristics have been found in various types of junctions. Furthermore the reproducibility for any particular type of junction is often poor. Both of these problems are usually attributed to the presence of a surface dead layer, which is insulating because of oxygen depletion. The shortness of the coherence length (ξ_c=2-4Å, and ξ_{ab}=12-25Å in $YBa_2Cu_3O_{7-\delta}$) makes surface conditions more critical than in classic superconductors. Various methods have been used to mitigate surface quality problems including the use of: break junctions,[124] tunneling into films,[125–127] freshly cleaved surfaces,[128] point contact tunneling with tips driven into the surface[21,129] and, most recently, chemically etched single crystals with evaporated metal films.[130] Nevertheless, most of these studies do not reveal tunneling conductances that ressemble the classic density of states of a s-wave superconductor.

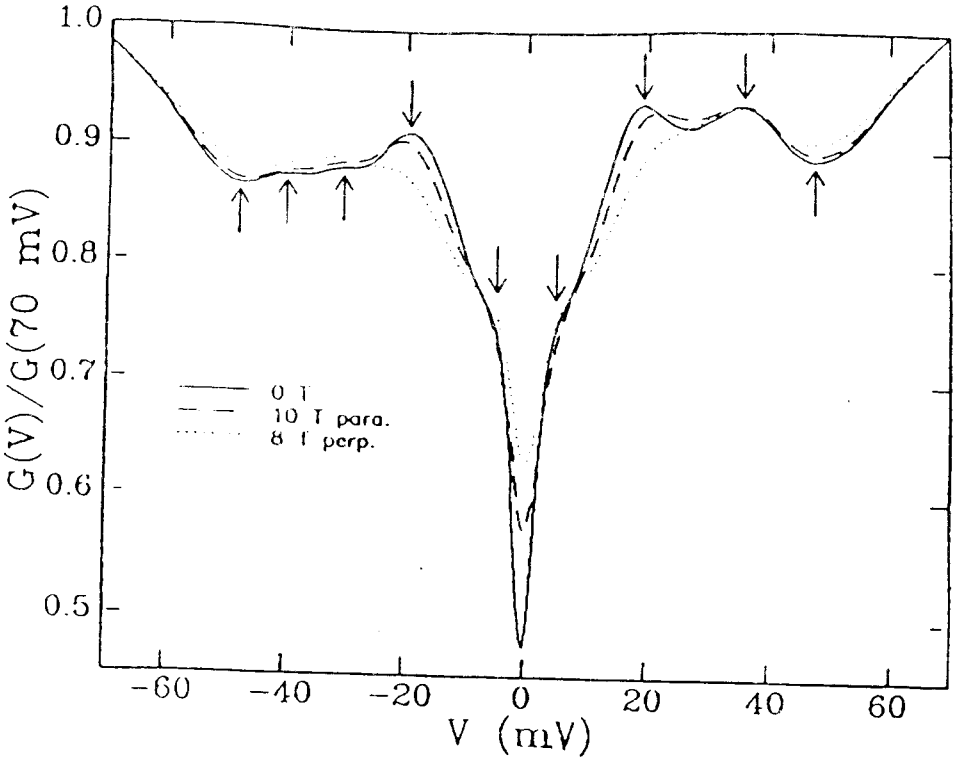

Fig. 15. Voltage dependence of dI/dV, normalized at 100meV at the fields indicated for a planar $YBa_2Cu_3O_{7-\delta}$/Pb junction. (After Ref. 130.)

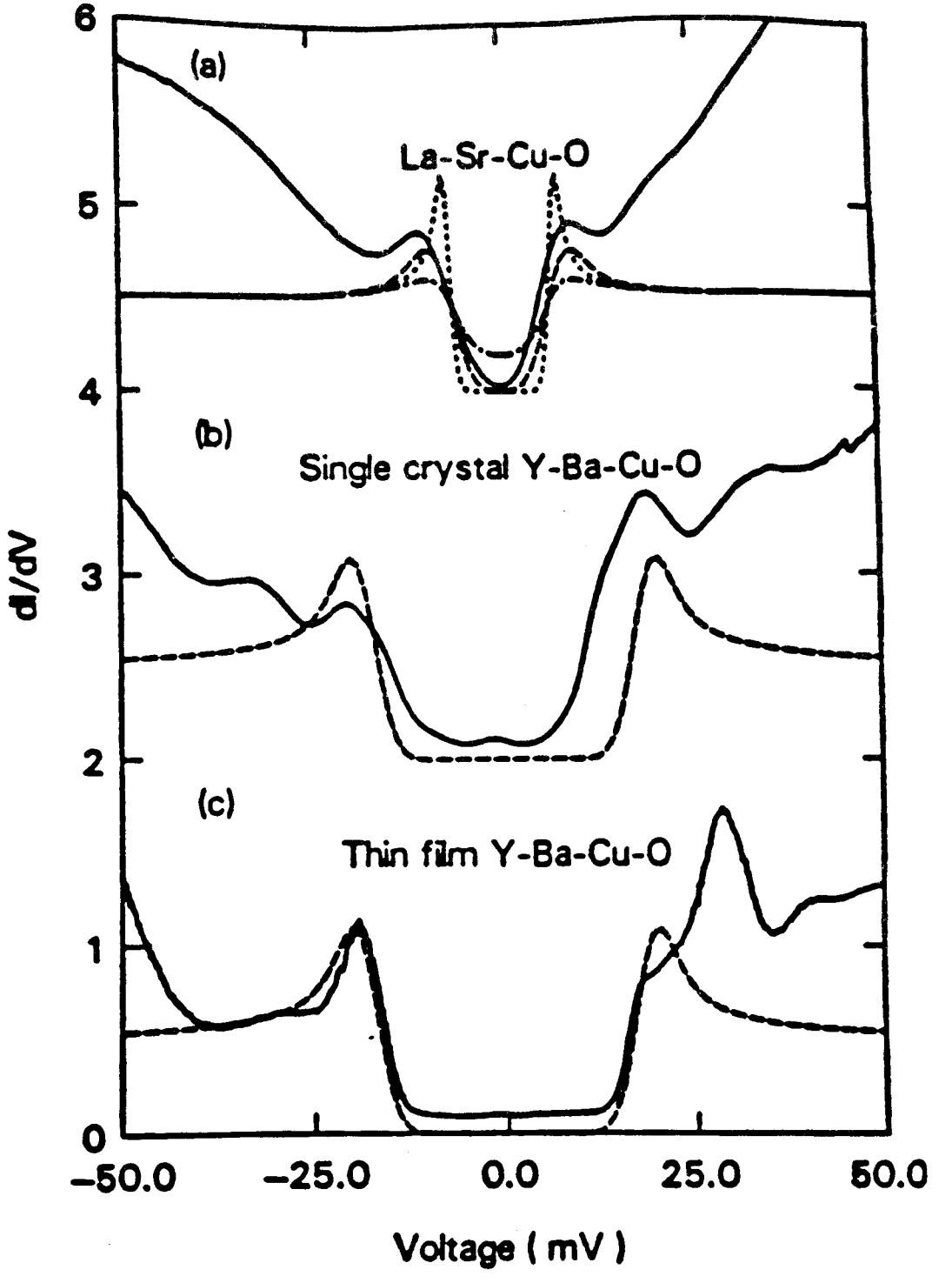

Fig. 16. Point contact tunneling conductance of $La_{2-z}Sr_zCuO_4$ and $YBa_2Cu_3O_{7-\delta}$. In (b) a PtIr tip approaches a single crystal of $YBa_2Cu_3O_{7-\delta}$ perpendicular to the CuO planes whereas in (b) a thin film is used. (After Ref. 129.)

An example of a typical tunneling characteristic for a planar $YBa_2Cu_3O_{7-\delta}$/Pb junction at low temperatures is shown in Fig. 15. The junction was prepared by depositing metallic contacts on a chemically etched surface of a single crystal of $YBa_2Cu_3O_{7-\delta}$. This method seems to give reproducible results (for over 100 samples) even when one varies junction parameters, such as counterelectrode materials and etch times. Fig. 15 shows a maximum in the conductance at around 19 meV; furthermore, the low bias conductance drops as T is decreased below T_c. Although these data certainly suggest the depletion of states around the Fermi level, they do not provide overwhelming support for a superconducting state with a clean gap, Δ_{min}. In particular we see a weakly temperature dependent zero bias conductance that is about half the conductance at 70meV. The gap-like density of states peak at 19meV seems to correspond with what is perhaps the most commonly reported value of the gap from tunneling experiments.[125]

The tunneling characteristics obtained from point contact studies are dramatically different from those of the planar junctions of Fig. 15. For example the early data by Kirtley *et al.* on a single crystal of $YBa_2Cu_3O_{7-\delta}$ and $La_{2-z}Sr_zCuO_4$ shown in Fig. 16 exhibit a sharp, clean BCS-like gap. Several other point contact studies also find similar junction characteristics.[131,132]

Unfortunately, the point contact data seem to be rather irreproducible. Different sets of point contact data exhibit gaps with size varying from sample to sample. As an example, a large spread of point contact gap values have been reported by Edgar *et al*,[133] who examined 30 point contact junctions with ceramic $YBa_2Cu_3O_{7-\delta}$ and found that the separation between conductance peaks (which, for lack of a better term, we will call 2Δ) was distributed from 28-65meV, with

Fig. 17. Temperature dependence of the gap like feature in the tunneling density of states. The gap closes at 70K, which is presumably the surface T_c. This $\Delta(T)$ curve was for a junction made with (001) film. After (Refs. 126 and 127.)

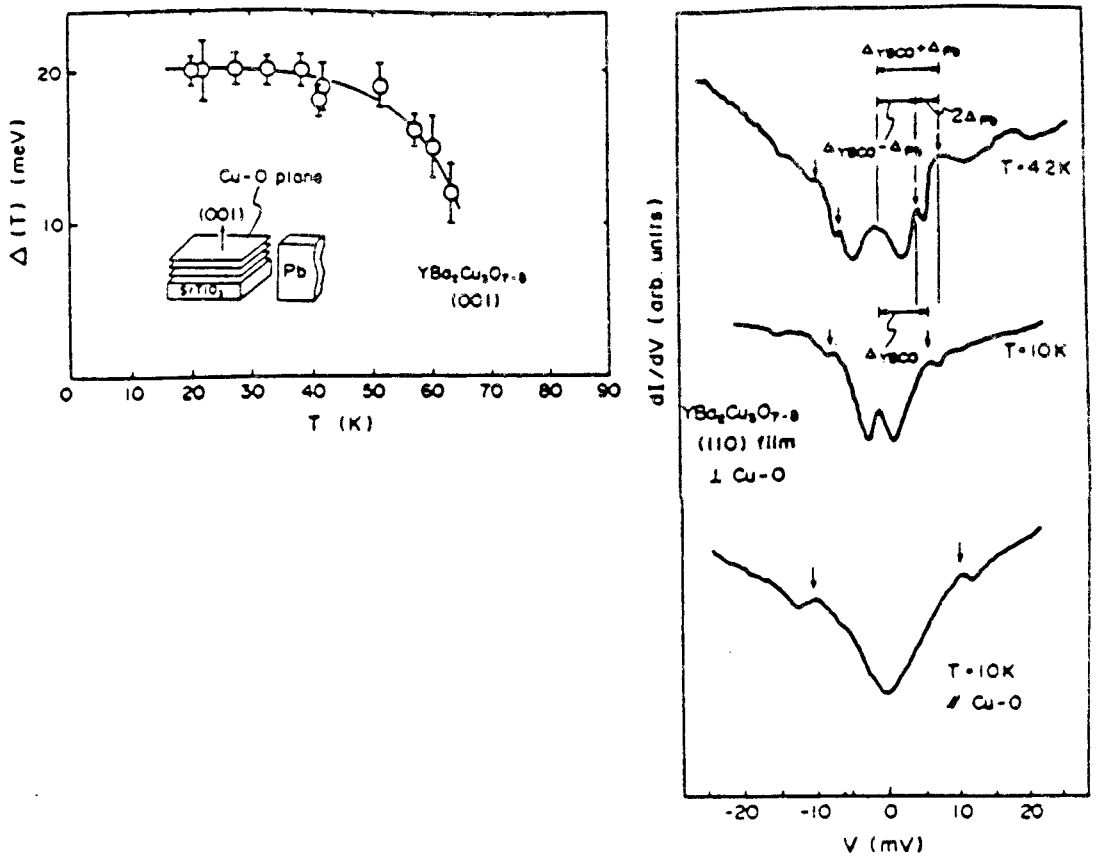

Fig. 18. dI/dV of junctions made with a (110) film broken parallel to the c-axis (a), (b); and broken along the c-axis (c). (a) and (b) are dI/dV curves taken below and above the superconducting transition in Pb. Curve (a) shows the gap difference and sum structures. (After Ref. 126.)

a marked peak in the distribution at 40meV.

One possible source of the variability in observed gaps is that, because of oxygen depletion, the T_c of the surface region is different from the bulk-T_c and depends upon the surface preparation. This is suggested by a number of studies[125,126,127,134] that find the gap often (but perhaps not always[135]) closing at much lower temperatures (between 60-70K) than the bulk transition temperature. It has been observed that[136] $2\Delta/k_BT_c$ is approximately constant (around 6-7).

A second possible problem[125] is that the gap may vary along the surface over a distance of a few coherence lengths, because of local variations in stoichiometry. This can explain why the point contact studies are less reproducible than the sandwich junction experiments, since successive tip insertions would be *expected* to reveal differing gap values, even for a single sample.[132] It may also explain why the high bias features present in the point contact studies (see Fig. 16) are smeared out or absent in the sandwich junction data.

A third possible source of the spread of gap values in point contact studies is that the different point contact junctions might be sensitive to different regions of the Fermi surface. Anisotropy in the gap, possibly arising from unconventional pairing, would then also give a spread in the measured gap values. Measurements of the gap anisotropy have been made in the broken film edge junction experiments of Tsai *et al.*[126,127] The junctions were fabricated by first epitaxially growing an oriented film on a $SrTiO_3$ substrate, and then breaking the substrate film (submerged in liquid He) at a pre-cut groove. The broken film was then joined with Pb electrodes to form the tunnel junction. (See inset in Fig. 17). The tunneling conductance shows gap-like features for junctions fabricated both

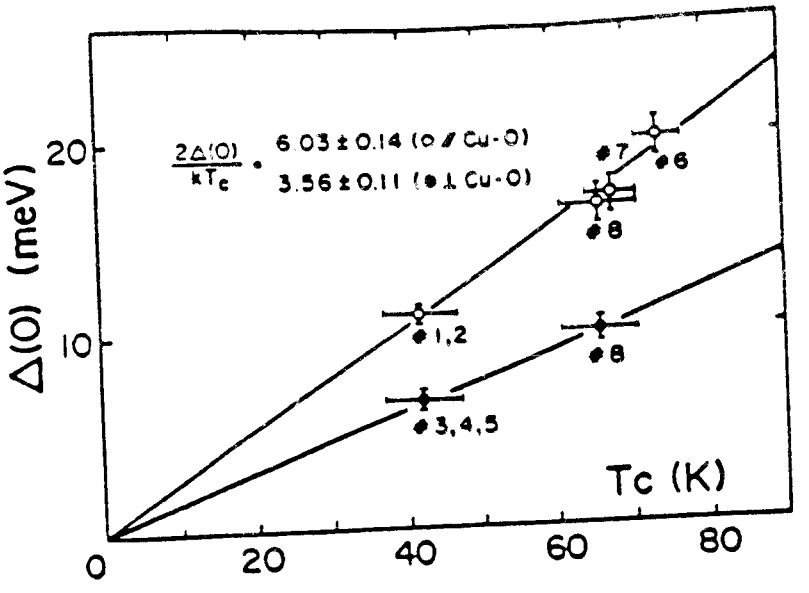

Fig. 19. Orientation dependence of the tunneling gap feature, for a given value of the surface T_c. (After Ref. 126.)

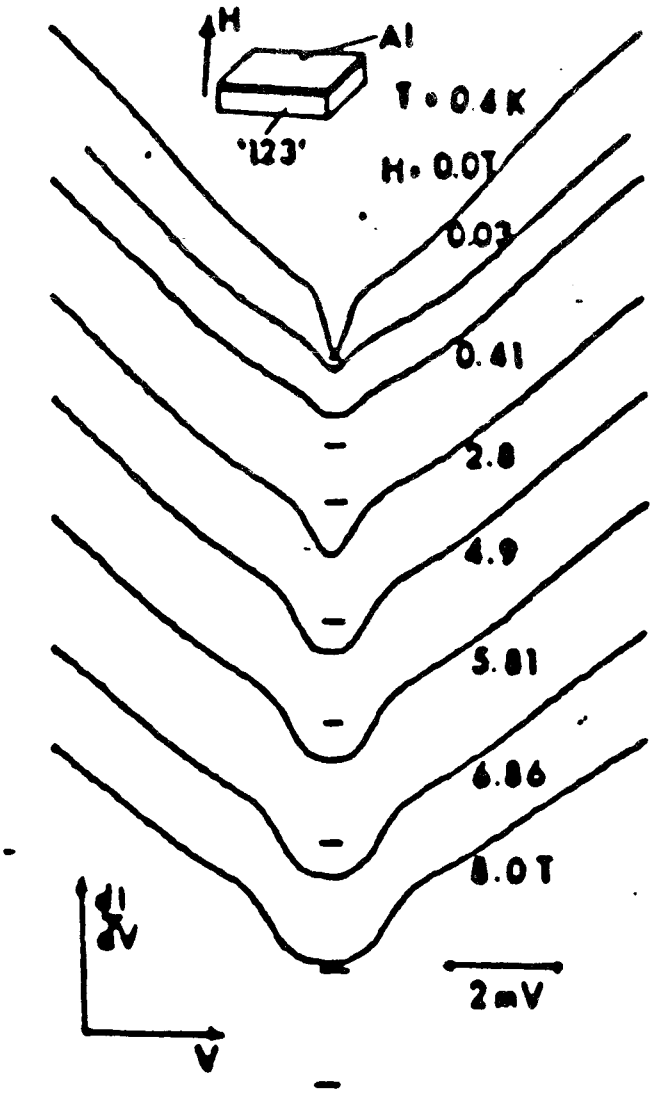

Fig. 20. Conductance curves for various applied fields in a high barrier Al-I-123 junction at 0.4K. At zero field the superconducting gap of Al is observed. The curve at 0.03T gives the conductance of normal Al into the oxygen depleted (i.e. non-superconducting) surface layer of $YBa_2Cu_3O_{7-\delta}$. At higher fields a Zeeman gap $\Delta_s = g\mu_B H$ opens up. Short horizontal ticks indicate the zero level of dI/dV for each curve. (After ref. 136.)

parallel and perpendicular to the c-axis; see Fig. 18. The identification of these tunneling conductance features with the superconducting energy gap is strongly supported by the temperature dependence as $T \rightarrow T_c^{\text{surface}}$, as shown in Fig. 17. The magnitude of the gap differs by a factor of two depending upon the orientation (for a given value of the surface T_c), being larger for tunneling along the a-b plane (see Fig. 19). The observed anisotropy could be caused by an anisotropic 's-wave' pairing state, or by an unconventional pairing state. The directions of the anisotropy might be used to rule out a particular pairing state; for example, some of the the singlet 'd-wave' states have a gap node in $\Delta(\boldsymbol{k})$ for $\boldsymbol{k}$ in the a-b plane, which would appear inconsistent with the large gap observed in this direction.

How is it possible to reconcile the point contact studies, which show evidence for a minimum excitation gap Δ_{min}, with the planar and break contact studies, which always show substantial zero bias conductance? This is, of course, a very important question, since the existence of a well defined gap rules out non-conventional singlet states. Perhaps a clue to the possible resolution of this problem has been provided by Ong and coworkers,[22] who studied the magnetic field behaviour of high resistance (more than 1 kΩ) barrier junctions, fabricated by evaporating Al film onto freshly grown crystals. The conductance curves for this system are shown in Fig. 20. Although the oxygen-depleted surface area was too thick to allow detection of the superconducting gap in $YBa_2Cu_3O_{7-\delta}$, they were able to show that a Zeeman-like gap of size $g\mu_B H$ with $g \sim 2.0$ opened up as the external magnetic field is increased. The interpretation suggested by Ong *et al.* is that the Zeeman gap is a sign that spin exchange scattering from local moments occurs in the insulating layer. The theory of this process[137–140]

$$\frac{T_1(T_c)}{T_1(T)} = \frac{2T}{T_c}\int_0^\infty dE\,(-\frac{\partial f}{\partial E})[N^2(E) + M^2(E)] \tag{5.10}$$

where

$$N(E) = \left\langle \mathrm{Re}\frac{\mathrm{E}}{\sqrt{\mathrm{E}^2 - |\Delta(\mathrm{k})|^2}} \right\rangle \tag{5.11}$$

is the anisotropic generalization of the BCS density of states and

$$M(E) = \left\langle \mathrm{Re}\frac{\Delta(\mathrm{k})}{\sqrt{\mathrm{E}^2 - |\Delta(\mathrm{k})|^2}} \right\rangle. \tag{5.12}$$

Here $< ... >$ denotes Fermi surface averaging, and $f(E)$ is the Fermi function. In the absence of anisotropy this becomes the usual result

$$\frac{T_1(T_c)}{T_1(T)} = \frac{2T}{T_c}\int_0^\infty dE\,(-\frac{\partial f}{\partial E})\frac{E^2 + \Delta^2}{E^2 - \Delta^2}. \tag{5.13}$$

For any unconventional singlet or unitary triplet superconductor (one for which $\vec{d}\,(k)^* \times \vec{d}\,(k) = 0$) the corresponding expression is:

$$\frac{T_1(T_c)}{T_1(T)} = \frac{2T}{T_c}\int_0^\infty dE\,(-\frac{\partial f}{\partial E})N^2(E). \tag{5.14}$$

In either case, provided that there is a minimum in the gap, Δ_{min}, then at low temperatures $1/T_1$ should show an activated behaviour $1/T_1 \sim \exp(-\Delta_{\mathrm{min}}/k_B T)$. On the other hand if the gap has nodes on the Fermi surface, then $1/T_1$ has the following power law behaviour at low temperatures: T^5, T^3, or T for point, line, or surface nodes, respectively.[142]

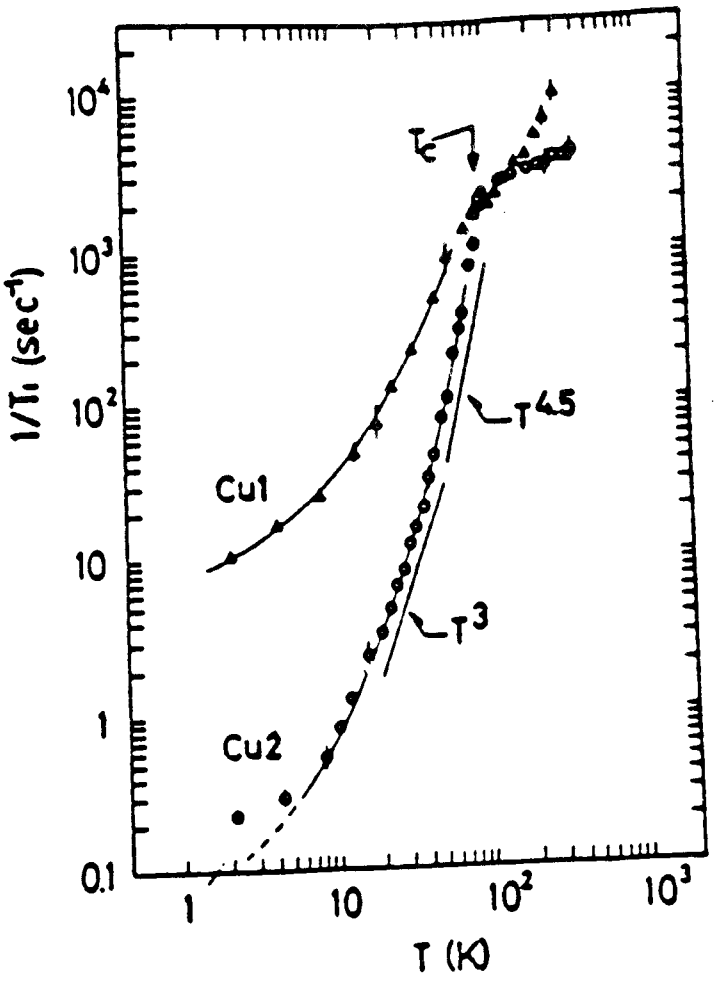

Fig. 21. Temperature dependence of $1/T_1$ for the plane (Cu2) and chain (Cu1) copper sites. The data are from Ref. 144.

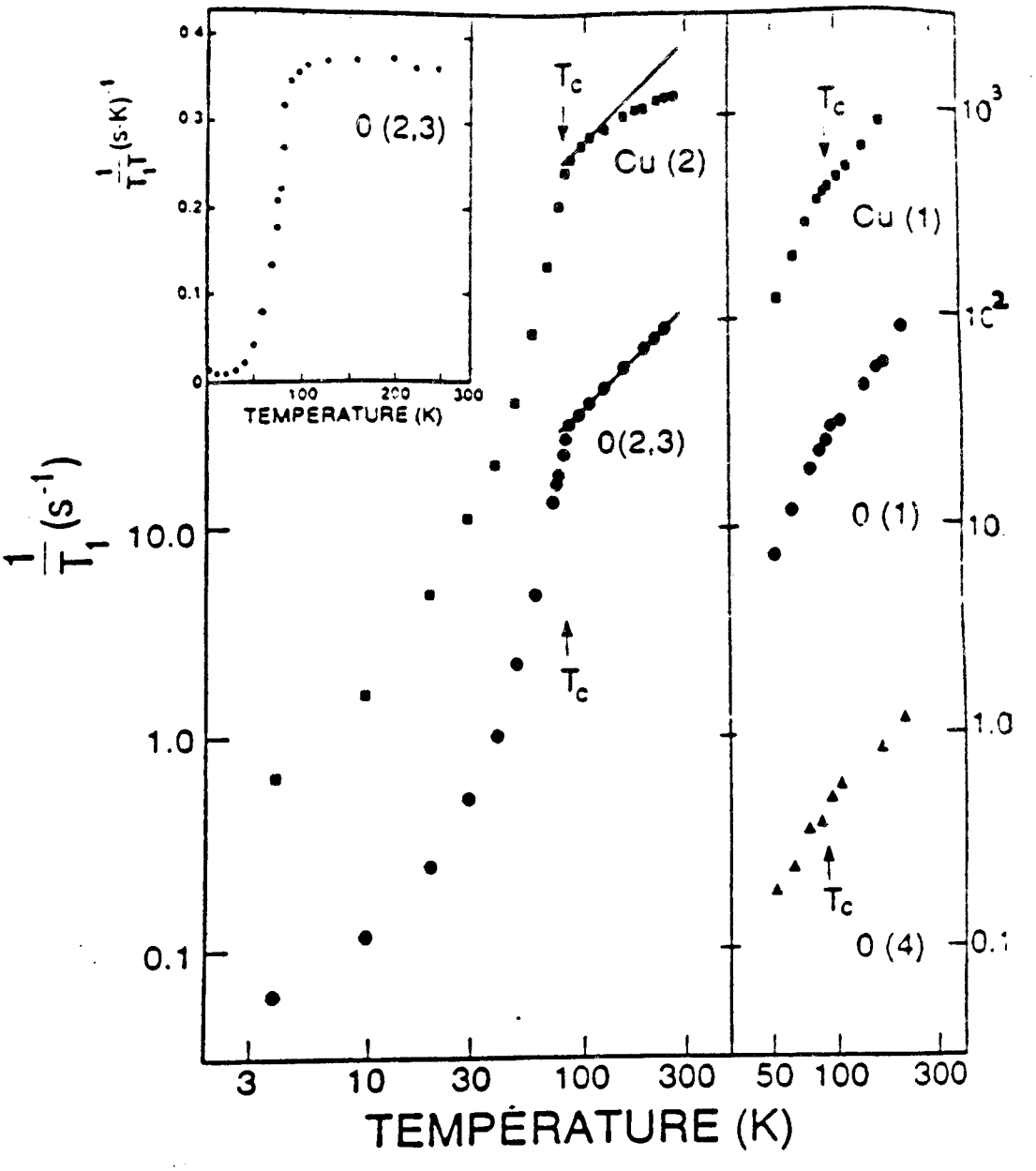

Fig. 22. $1/T_1$ for the oxygen and Cu sites in $YBa_2Cu_3O_{7-\delta}$. In particular, notice the absence of a coherence peak just below T_c for any of the sites. After Ref. 146.

The experimental data indeed show a power law behavior of $1/T_1$ below T_c of the planar Cu(2) site relaxation.[143,144] The data of Imai *et al.*[144] are shown in Fig. 21. The data are best fit by a T^3 power law at low temperatures, as expected for a superconducting state with line nodes in the clean limit.[142]

A second unusual feature of the NMR relaxation rate is the absence of a Hebel-Slichter coherence peak just below T_c,[145,146] as shown in Fig. 22. (Note that earlier reports[147,148] of a coherence peak in ^{17}O have not proved to be reproducible.)

The Hebel-Slichter coherence peak[149,150] occurs in s-wave superconductors because of the divergence of the integrand in Eq. (5.13) at $E = \Delta$. This leads to a rapid rise in $1/T_1$ as T drops below T_c. For an unconventional superconductor, one expects that the coherence peak will be substantially reduced or altogether absent. This is because the anisotropy in the gap implies that the integrand is much less singular than for an s-wave superconductor. The absence of the coherence peak may thus be an indication of unconventional pairing in $YBa_2Cu_3O_{7-\delta}$. However, it does not constitute conclusive proof, since the coherence peak may be absent even for a conventional pairing state when there is magnetic scattering.[151] Other effects that might reduce the coherence peak include substantial gap anisotropy or strong electron-phonon coupling, which can broaden the peak in the density of states.[146,152]

It is intriguing to compare the copper site relaxation rate data of Fig. 21 with comparable data for the heavy fermion compound UPt_3, which is now known to be an unconventional superconductor. The data of Kohori *et al.* for ^{195}Pt relaxation[153] are striking in their similarity to the copper NMR data in $YBa_2Cu_3O_{7-\delta}$, shown in Fig. 21, both in the low temperature power law and in the

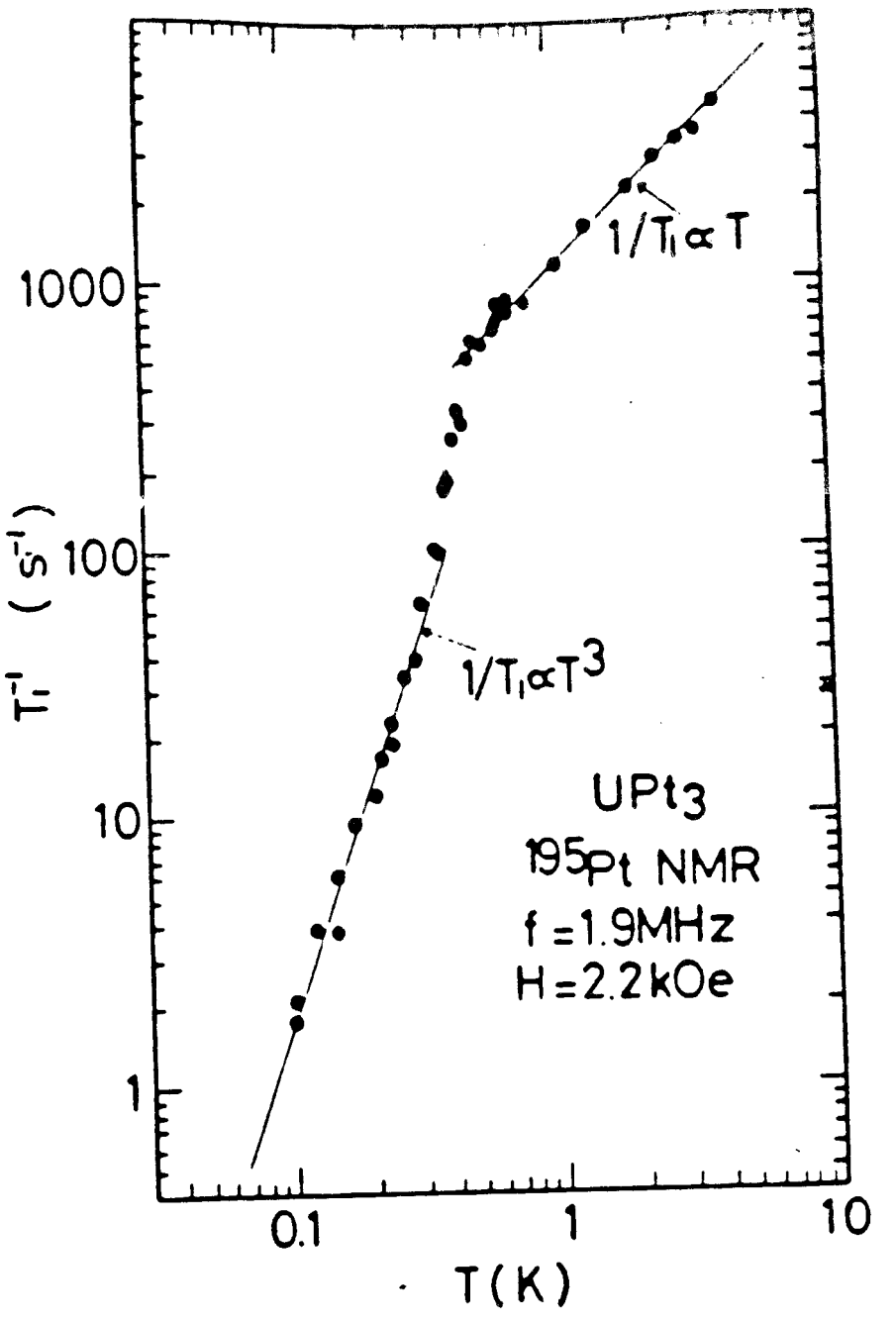

Fig. 23. Temperature dependence of ^{195}Pt NMR relaxation in UPt_3, showing both a T^3 low temperature power law and the absence of a coherence peak below T_c. (After Ref. 153.)

absence of the coherence peak. A T^3 relaxation of $1/T_1$ has also been observed in UBe_{13}.[142] This demonstrates that both the low T behaviour and the absence of the coherence peak can indeed arise from an unconventional pairing state.

Even the normal state Cu relaxation data[154,141] seem to be rather unusual. The plane sites do not exhibit the Korringa law expected of a normal metal (i.e. $T_1^{-1} \propto T$) above $1.35T_c$ (116K), although the chain sites do follow the expected behaviour. This has been observed in both fully oxygenated[144] and oxygen deficient[155] $YBa_2Cu_3O_{7-\delta}$. Furthermore the magnitude of T_1^{-1} is enhanced by more than an order of magnitude compared to the rate estimated from the density of states calculated with band theory.[156,157] Both of these effects seem to require that the antiferromagnetic correlations be taken into account in order to describe both normal and superconducting relaxation rates.

A consistent picture of unusual copper nuclear relaxation in both the superconducting and normal state has been provided recently by Monien and Pines.[158] These authors have analysed the Cu relaxation rates, using an RPA type expression for the spin-spin correlation function

$$\chi(q,\omega,T) = \frac{\chi_0(q,\omega,T)}{1 - N(0)J_{\rm eff}(q,T)\chi_0(q,\omega,T)}, \tag{5.15}$$

and assuming a cylindrical Fermi surface. Here $J_{\rm eff}(q,T)$ is an effective antiferromagnetic coupling constant, assumed to be peaked at the antiferromagnetic wavevector Q, $N(0)$ is the quasiparticle density of states at the Fermi level, and χ_0 is the bare susceptibility. According to this theory, the antiferromagnetic correlations enhance $1/T_1$ by a factor of $[1-\lambda Y(T)]^{-2}$ relative to the relaxation rate neglecting antiferromagnetic correlations. Here $\lambda \equiv \langle N(0)J_{\rm eff}(q,T)\chi_0(q,T)\rangle$ and $Y(T)$ is the Yosida function.[159,160] Using the zero temperature gap $\Delta(0)$ obtained

from an analysis of Cu Knight shift data (see below), Monien and Pines varied λ to achieve the best fits to the temperature dependent T_1^{-1} data of Imai *et al.*[144] Fits were attempted with a variety of pairing states, including a s-wave state, an anisotropic s-wave state, a d-wave state, and a d-wave state with higher orbital angular momentum harmonics, ℓ. The fits to s-wave or anisotropic s-wave pairing, were unsuccessful below $0.3T_c$ because of the exponential temperature dependence of the theoretical rate, which is not present in the data. Above $0.3T_c$, a reasonable fit was obtained, provided a large ($\lambda = 0.7$) antiferromagnetic enhancement was used. The fit to the pure d-wave state was better, but still deviated at low temperatures (using an antiferromagnetic enhancement of $\lambda = 0.65$). A good fit over the whole temperature range was obtained by using a d-wave state with an admixture of higher harmonics.

2. KNIGHT SHIFT

Experimental constraints on the pairing state in $YBa_2Cu_3O_{7-\delta}$ are also provided by NMR Knight shift data. These data are particularly important, since they appear to eliminate the possibility of triplet pairing.

The measured shifts in NMR resonance frequencies are related to the static magnetic susceptibility at the site of the nucleus. There are two distinct contributions to the shift, a spin susceptibility part (Knight shift), and an orbital contribution (chemical shift). Thus

$$K_{\alpha\beta}(T) = K^S_{\alpha\beta}(T) + K^L_{\alpha\beta} \tag{5.16}$$

where K is the total shift, K^L is the temperature independent chemical (or Van Vleck) shift and $K^S(T)$ is the temperature dependent Knight shift; each of these quantities is a tensor. For the plane copper sites, if one assumes that only the Cu

$d_{x^2-y^2}$ orbitals have significant hyperfine coupling or weight at the Fermi surface, then $K^S_{\alpha\beta}$ is proportional to the $d_{x^2-y^2}$ spin susceptibility:

$$K^S_{\alpha\alpha} = A_{\alpha\alpha}\chi_{\alpha\alpha}(T), \qquad \alpha = a, b, c \tag{5.17}$$

where a, b, c are the crystallographic axes and $A_{\alpha\alpha}$ are the hyperfine coupling constants. A more general form, introduced by Monien *et al.*[161] is discussed below.

In Eq. (5.17), the temperature dependence of the Knight shifts is related directly to the Pauli spin susceptibility in the superconducting state. We now summarise some key facts about the spin susceptibility of conventional and unconventional superconductors. For a singlet superconductor (neglecting Fermi liquid effects) this susceptibility is isotropic, and is given by[160]

$$\chi = \frac{1}{4}\mu_B^2 N_F Y(T) \tag{5.18}$$

where the Yosida function $Y(T)$ is the Fermi surface average of

$$Y(\hat{k}, T) = \int_0^\infty d\epsilon_k \, \frac{1}{2k_B T}\mathrm{sech}^2(E_k/2K_B T). \tag{5.19}$$

and where E_k is defined in Eq. (5.1). From this we see that for singlet states $\chi = 0$ for $T = 0$.[162]

For a triplet state, rotational invariance in spin space is broken, and the spin susceptibility is a tensor. For a unitary triplet state [one with $\vec{d}\,(k)^* \times \vec{d}\,(k) = 0$] it is given by:

$$\chi_{\alpha\beta} = \chi_n \left(\delta_{\alpha\beta} - \left\langle \left[1 - Y(\hat{k}, T)\right] \mathrm{Re}\left[\frac{d^*_\alpha(k) d_\beta(k)}{|\,\vec{d}\,(k)|^2} \right] \right\rangle \right), \tag{5.20}$$

where $< \ldots >$ denotes the Fermi surface average and χ_n is the normal state

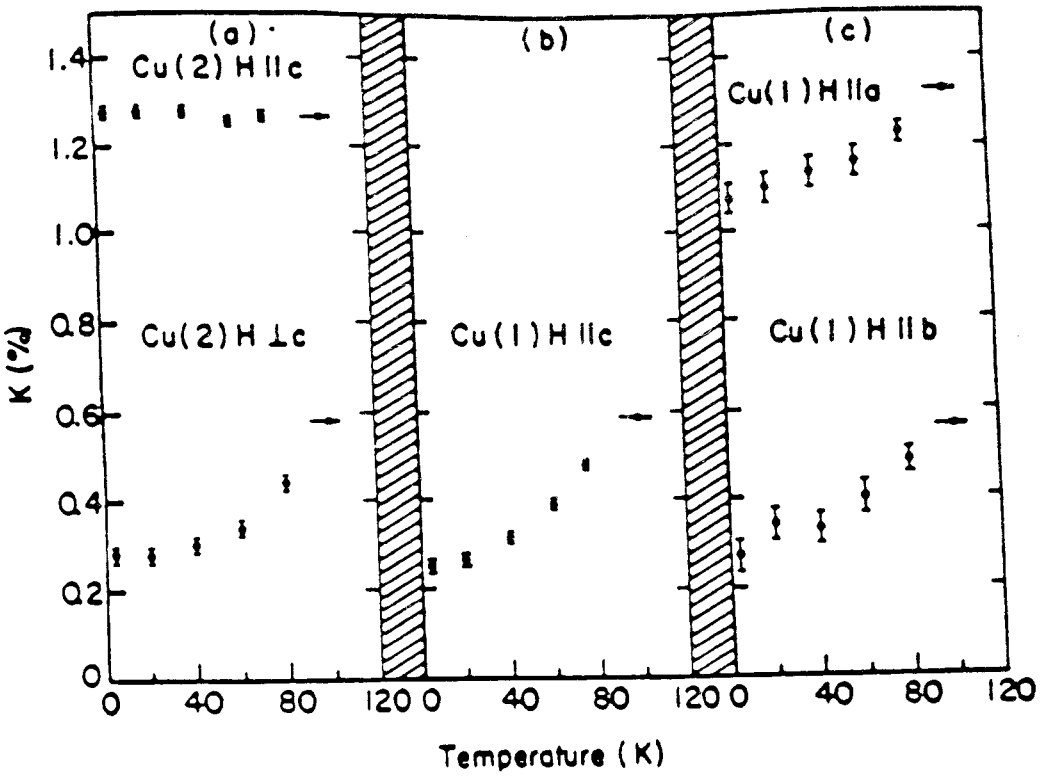

Fig. 24. Temperature dependence of the total magnetic shift as a function of temperature for (a) Cu(2) (plane site) with (upper) $H \| c$ and with (lower) $H \perp c$, (b) Cu(1) (chain site) with $H \| c$, (c) Cu(1) with (upper) $H \| a$ and with (lower) $H \| b$. (After Ref. 165.)

susceptibility. From this one can readily show that $\mathrm{Tr}(\chi) = \chi_n[2 + Y(T)] \rightarrow 2\chi_n$ as $T \rightarrow 0$. This result can also be shown to hold for non-unitary triplet phases as well.[160, 163] An important implication of this is that, for states with $\chi_{aa} = \chi_{bb}$, it is not possible for χ_{aa} to become less than $\chi_n/2$ at zero temperature. We shall soon use this result to show that the data are inconsistent with triplet pairing.

Temperature dependent Knight shifts have been measured for the copper sites in $YBa_2Cu_3O_{7-\delta}$ by Takigawa *et al.*[164], and have been repeated with an improved method by Barrett *et al.*[165] The data of Barrett *et al.* are shown in Fig. 24. The data show that the *c* component of the Cu(2) shift is temperature independent whereas the *ab* components are equal and drop sharply below T_c. The only states listed in the group theoretic classification of states in Section III that show this behaviour are the four triplet states ${}^3E_u$ (g), (h), (i), and (j) of Table 6. For each of these four states the temperature dependent susceptibility is given by

$$\chi_{\alpha\beta} = \chi_n \mathrm{diag}(1 + Y(T), 1 + Y(T), 2)/2. \tag{5.21}$$

Although these four triplet states seemingly provide a natural explanation for the temperature independence of the Cu(2) site *c* component of the Knight shift, they do not provide a consistent interpretation of all the shift data. In particular, in any of these phases the Knight shift K^S_{aa} falls to half of its normal state value as $T \rightarrow 0$. This implies that the total shift $K_{aa}(T)$ falls from $K^L_{aa} + K^S_{aa}(T_c)$ at T_c to $K^L_{aa} + K^S_{aa}(0) = K^L_{aa} + K^S_{aa}(T_c)/2$ at $T = 0$. Experimentally the total shift K_{aa} falls from 0.6% at T_c to 0.3% at T=0. Since $K_{aa}(0) \approx K_{aa}(T_c)/2$ this implies that the chemical shift $K^L_{aa} \approx 0$, and hence that the chemical shift anisotropy K^L_{cc}/K^L_{aa} should be very large. This is physically unreasonable; for a cubic crystal

the anisotropy ratio is rigorously equal to 4. Furthermore, a detailed calculation for La_2CuO_4 gives a possible range for the anisotropy from 4.1 to 4.3 which was insensitive to the precise energy levels assumed for the copper and oxygen sites.[165,166] The similarity of the local environment in the two crystals suggests that this result would not change much for $YBa_2Cu_3O_{7-\delta}$. In summary, the data are not consistent with triplet pairing.

Are the data consistent with singlet pairing? If $YBa_2Cu_3O_{7-\delta}$ is a singlet superconductor, then the chemical shifts should be given by the zero temperature total shifts (since $\chi(0) = 0$). According to Ref. 165 this means $K^L_{cc}/K^L_{aa} = 4.54$ which is in approximate agreement with the theoretical estimate, given above. The zero temperature values of the shift tensor are also consistent with calculated values of the chemical shift[166] implying that $K^S_{\alpha\alpha} \approx 0$. This implies a singlet state, since $\chi(0) = 0$. We thus make the extremely important conclusion that *the Knight shift data not only rule out triplet pairing, but seem to be consistent with singlet pairing.*

If one accepts these arguments that the pairing is singlet, then the temperature independence of the K_{cc} shift for the planar Cu(2) site is mysterious. In a singlet state, $\chi_{\alpha\beta}(T) = \chi(T)\delta_{\alpha\beta}$; thus since K^S_{aa} changes with temperature below T_c, it would be expected that K^S_{cc} would also be temperature dependent below T_c. A resolution of this problem has been proposed by Monien *et al.*[161] and Barrett *et al.*[165] These authors, as well as Mila and Rice,[167] found that the assumption that the Cu(2) nucleus couples only to the Cu $d_{x^2-y^2}$ orbital of the same atom cannot simultaneously explain the anisotropy in the Knight shifts and the anisotropy in the relaxation rates. Consequently, they considered additional couplings between the copper nuclei and electronic spins on the neighboring atoms, known

as the transferred hyperfine coupling. In this picture one achieves a large transferred hyperfine interaction by allowing the oxygen $p\sigma$ orbitals to hybridize with the Cu 4s state, which has a substantial contact hyperfine interaction with the Cu nucleus. Simple quantum chemical estimates have shown that this gives a substantial coupling between neighboring Cu(2) atoms[167] and presumably also between neighboring Cu(2) and O(4) bridging oxygen sites. In this model the Knight shift is related to the Cu(2) electron spin susceptibility, $\chi^{\ell}_{\alpha\beta}$, and the spin susceptibility of the oxygen band, χ^{h}, by

$$K^{S}_{\alpha\beta} = (\gamma_e \gamma_n \hbar^2)^{-1}[(A_{\alpha\beta} + 4B^{1}_{\alpha\beta})\chi^{S}_{\alpha\beta} + B^{h}_{\alpha\beta}\chi^{h}_{\alpha\beta}] \tag{5.22}$$

where γ_e and γ_n are the electron and nuclear gyromagnetic ratios, and $B^{1}_{\alpha\beta}$ and $B^{h}_{\alpha\beta}$ are the transferred hyperfine couplings. Then the mysterious temperature independence of K_{cc} can occur if it is assumed that $A_{cc}+4B^{1}_{cc} \approx 0$ and $B^{h}_{cc}\chi^{h}_{cc} \approx 0$.

Using this idea of the transferred hyperfine interaction, Barrett *et al.*[165] develop a consistent picture of all components of the shifts, that is consistent with singlet pairing. Barrett *et al.*[165] subtracted the $K_{cc}(T)$ data from the $K_{aa}(T)$ data, eliminating the contribution from the hole susceptibility, χ^{h}, and Monien *et al.*[158] fitted the result to the Yosida functions of various conventional and unconventional singlet states. The data were fitted variously to: an s-wave state with $2\Delta(T = 0)/k_B T_c$=3.8, an anisotropic s-wave state with $2\Delta_{\mathrm{max}}(T = 0)/k_B T_c$=4.3, a d-wave state with $2\Delta_{\mathrm{max}}(T = 0)/k_B T_c$=29.34, and a d-wave state with higher ℓ components, $2\Delta_{\mathrm{max}}(T = 0)/k_B T_c$=6.26. The pure d-wave state could also be reasonably well fit with a smaller Δ_{max} because of possible scatter in the data points. This was done by using Eq. (5.19) together

with the interpolation formula

$$\Delta(T) = \Delta(0)\tanh\left[\frac{\left\{(T_c - T)\frac{T_c}{T}\frac{\partial\Delta^2}{\partial T}\Big|_{T=T_c}\right\}^{1/2}}{\Delta(0)}\right]. \qquad (5.23)$$

Monien *et al.*[158] found that all of these states fit the data; however for the 'd-wave' case, Δ is unphysically large unless higher ℓ harmonics are included. The higher ℓ harmonics are important, since they reduce the area of the Fermi surface, close to the nodes, where the gap is small.

3. Summary

The low temperature nuclear relaxation is not exponential in temperature; this implies the existence of low energy excitations. The Hebel-Slichter coherence peak is absent, which might indicate unconventional pairing. The Knight shift anisotropies appear to rule out triplet pairing states. The Knight shift data can be fit by assuming either conventional or unconventional (with line nodes) singlet pairing.

F. Low Temperature Specific Heat

The low temperature specific heat is potentially a straightforward probe of the excitation spectrum in the superconducting state. At temperatures small compared to the Debye temperature, which has an average value[168] of 402K $\pm$ 32K, the phonon contribution to the specific heat is proportional to T^3. This would be expected to dominate the electronic contribution in a superconductor

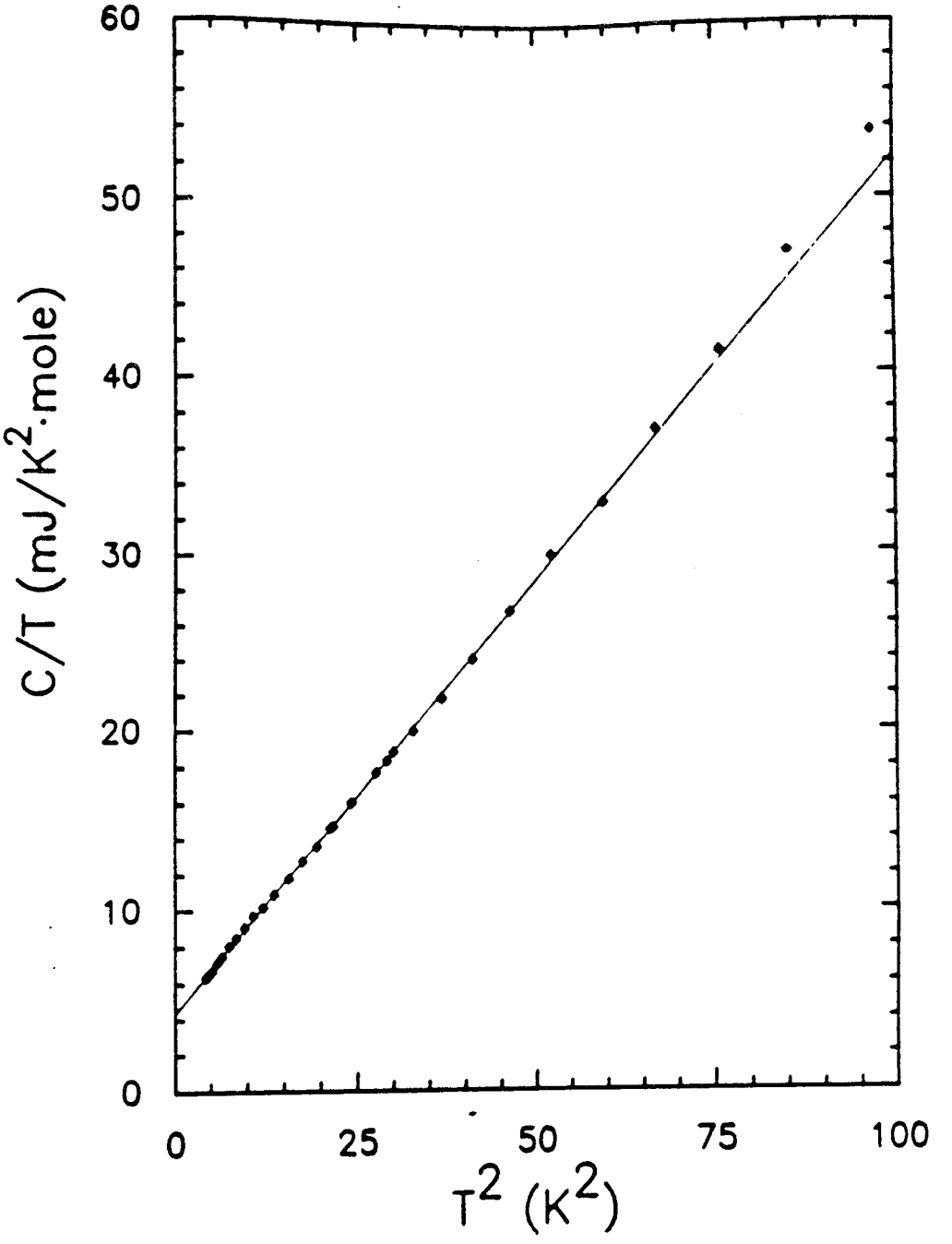

Fig. 25. Low temperature, zero field specific heat of $YBa_2Cu_3O_{7-\delta}$, plotted as $C(T)/T$ vs T^2. (After Ref. 172.)

with a non-zero minimum energy gap at zero temperature, Δ_0:

$$C(T) \sim \exp(-\Delta_0/k_B T). \tag{5.24}$$

Considerable interest was therefore aroused by the reports[169–171] that in polycrystalline $YBa_2Cu_3O_{7-\delta}$, for temperatures between 2K to about 6K, the specific heat could be fitted by the form

$$C \approx \alpha T + \beta T^3 \tag{5.25}$$

as shown[172] in Fig. 25. These measurements, on polycrystalline samples, have been reproduced with the conclusion[168] that the average value of α is 4.66 $\pm$0.69 mJ/mol K^2. Single crystals are too small to enable reliable absolute measurements of the specific heat to be made; instead, some groups have attempted to measure the specific heat of mosaics, but no consensus has emerged at the time of writing.[168] A detailed discussion of this topic may be found in the chapter by Junod in this volume.

Assuming that the linear term is indeed present, there are a number of possible explanations, of which unconventional pairing is the most exotic. The first of these is that the non-zero value of α is associated with the presence of impurity phases (chiefly $BaCuO_{2+x}$, which, at large concentrations, has been demonstrated to give a linear term in the specific heat[173,174]), but this is contradicted by two observations: (a) some of the best quality data do not exhibit Schottky anomalies at low temperatures, and (b) in the data shown in Fig. 25, the sample was characterised by Raman spectroscopy, and the inferred concentration of $BaCuO_{2+x}$ was too small to account for the observed value of α. A second explanation of

the linear behavior is that it is generated by the presence of two-level systems.[175] However, the value of α, estimated on the basis of oxygen tunneling, is only about 1.4 mJ/mol K^2.[175]

Unconventional pairing can lead to a linear term in the specific heat in two ways. First, if $YBa_2Cu_3O_{7-\delta}$ is in the clean limit at low temperatures, as the point contact tunneling measurements suggest, then, assuming that the relevant excitations are fermions, there would need to be surface nodes on the Fermi surface. On the other hand, if $YBa_2Cu_3O_{7-\delta}$ is in the weakly dirty limit, then line nodes could lead to a linear term in the specific heat (in fact, an infinitesimal amount of impurity would lead to a linear term, with a coefficient dependent upon the concentration of impurity).[176]

Finally, we comment briefly on the situation in $Bi_2Sr_2CuO_6$ and $Bi_2Sr_2CaCu_2O_8$. In these superconductors, it seems that the linear term has a very small coefficient at low temperatures and it may indeed be absent.[177,178] Chakraborty *et al.*[178] specifically tested their data for a T^2 contribution to C, and concluded that it was not present, thus ruling out an unconventional state with line nodes in these materials. There is another interesting difference between powdered samples of superconducting $YBa_2Cu_3O_{7-\delta}$ and $Bi_2Sr_2CaCu_2O_8$. For $0.02K < T < 3K$, the thermal conductivity is roughly proportional to T^2 in $Bi_2Sr_2CaCu_2O_8$, whereas in $YBa_2Cu_3O_{7-\delta}$, below about 300 mK, the thermal conductivity is proportional to T.[10] This behaviour is absent in insulating samples of $YBa_2Cu_3O_{7-\delta}$. It seems that the presence of a linear temperature dependence in the thermal conductivity at low temperatures may be correlated with the presence of a linear term in the specific heat at low temperatures,[10] a possible indication that resonant impurity scattering[179] may be present in powdered

$YBa_2Cu_3O_{7-\delta}$.

VI. ELECTROMAGNETIC PENETRATION DEPTH

No single set of measurements is more widely cited as evidence in favour of conventional pairing than that on the temperature dependence of the electromagnetic penetration depth, $\lambda(T)$.

A close examination, however, reveals that the interpretation of the data is not completely clear cut. Furthermore, the data are not without their puzzling discrepancies. In this section, we shall summarise the experimental findings and consider what constraints these observations place on the identification of the pairing state. We begin with a summary of the theory for the electromagnetic penetration depth.

First, let us define the penetration depth for a general superconductor. The starting point is the London equation

$$j_\mu = -\frac{e^2}{mc} K_{\mu\nu} A_\nu \tag{6.1}$$

where $\vec{j}$ is the supercurrent, $K_{\mu\nu}$ is the electromagnetic kernel, $\vec{A}$ is the vector potential, m is the mass of the electron and c is the speed of light in vacuum. The penetration depth tensor[180–183] λ is defined by

$$\frac{1}{\lambda^2} = \frac{4\pi^2}{mc^2}\mathbf{K}. \tag{6.2}$$

For example in an isotropic 's-wave' superconductor, λ is isotropic and given in

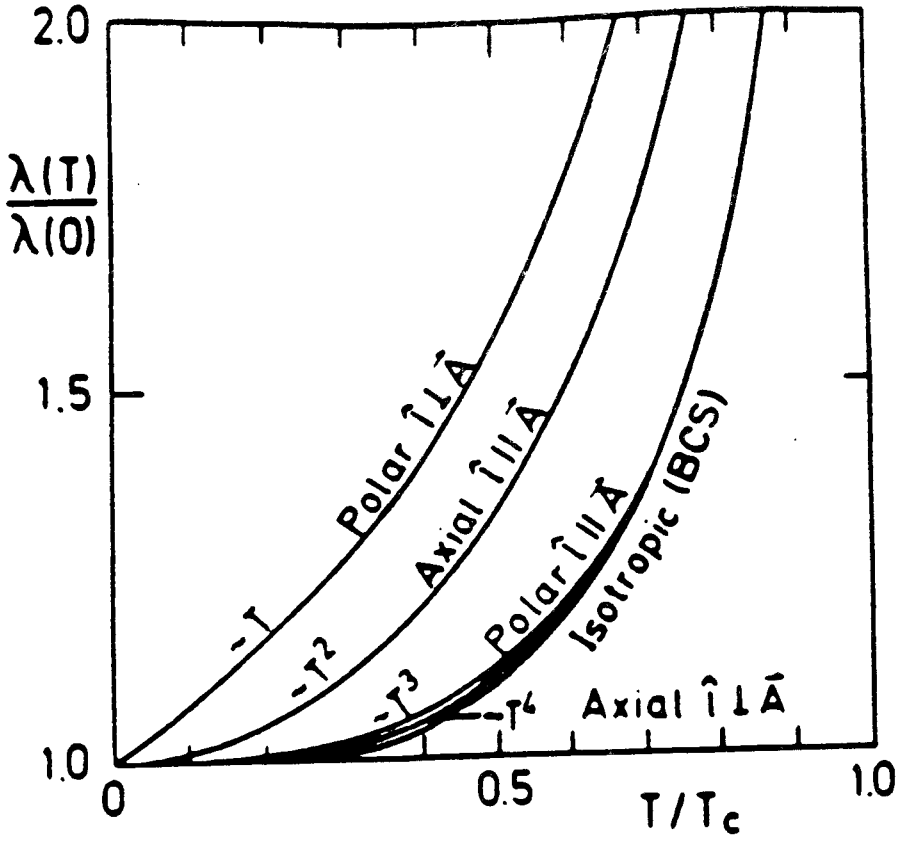

Fig. 26. Temperature dependence of penetration depth as a function of reduced temperature T/T_c, for polar, axial, and isotropic s-wave pairing on a spherical Fermi surface. These graphs assume that the component of the superfluid anisotropy axis along the direction of the surface normal, ℓ_z, equals zero or one for the polar or axial states. The temperature dependence of the gap was based on the interpolation formula Eq. (5.23). (After Ref. 181.)

where Δ_{max} is the maximum value of the gap function over the Fermi surface, and n is an exponent which depends on the type of node and the orientation of the node relative to the magnetic field, $\vec{B}$. As an example, consider triplet states on a spherical Fermi surface with uniaxial anisotropy. The possible values of n are: $n = 2$ (axial state, $\vec{\ell}$ perpendicular to $\vec{B}$), $n = 4$ (axial state, $\vec{\ell}$ parallel to $\vec{B}$), $n = 1$ (polar state, $\vec{\ell}$ parallel to $\vec{B}$ and the polar state with $\vec{\ell}$ perpendicular to $\vec{B}$ assuming $\ell_z = 1$, where z is the direction of the surface normal), and $n = 3$ (polar state, $\vec{\ell}$ perpendicular to $\vec{B}$ and $\ell_z = 0$).

In $YBa_2Cu_3O_{7-\delta}$, the Fermi surface has the topology of a cylinder, and the corresponding results for triplet states may be read off Tables 2, 3, 5, 6, 7, and 8. Power laws with $n = 1, 2, 3, 4$ are possible for various field directions and pairing states. For singlet states of relevance to $YBa_2Cu_3O_{7-\delta}$, the only possibilities are states with line nodes intersecting at 90°, which have $n = 1$ in all directions, and the state ^1E_g(c), which has nodes around the equator, and which has $n = 1$ unless both the direction of penetration and $\vec{B}$ lie in the a-b plane, in which case $n = 3$. Observation of these power laws as $T \rightarrow 0$ could, in principle, discriminate between possible pairing states.

Despite these asymptotic power laws, it is possible that certain unconventional states with nodes could generate a $\lambda(T)$ which is indistinguishable from the isotropic BCS prediction over much of the temperature range between 0K and T_c. An example is shown in Fig. 26, for p-wave and s-wave superconductors and a spherical Fermi surface. There are plotted curves of $\lambda(T)$ vs. T for a variety of p-wave states, characterised by the local axis of gap symmetry $\vec{\ell}$. In particular, the axial state (which has point nodes on a spherical Fermi surface, see discussion in Section III) with $\vec{\ell}$ parallel to the magnetic field $\vec{B}$ has almost

precisely the temperature dependence of the isotropic BCS form.

It is not only the nodal structure of the gap function that determines the power law behaviour of the penetration depth at low temperatures. Two additional factors may be important: Fermi liquid corrections[181,184] and impurity effects.[181,185] In the first case, renormalisation of the electron mass leads to a value of $n = 2$. In the second case, when the concentration of impurities exceeds a critical value, the value $n = 2$ is obtained, regardless of the pairing state predicted in the clean limit.

It has become customary to fit experimental data for $\lambda(T)$ to the Gorter-Casimir form

$$\lambda(T) = \lambda(0)\left[1 - \left(\frac{T}{T_c}\right)^4\right]^{-1/2}. \tag{6.6}$$

The Gorter-Casimir expression has no microscopic basis, but closely ressembles the BCS result for type I superconductors.[186] The Gorter-Casimir formula is purely empirical, and does not describe a gapped superconductor at asymptotically small temperatures, because it predicts that $\lambda(T) - \lambda(0)$ falls as T^4 rather than exponentially in temperature. Even throughout the range $0.25 < T/T_c < 1$, the Gorter-Casimir form for $\lambda(T)$ differs from that of a weak-coupling type II s-wave superconductor, and is, in fact, closer to the temperature dependence expected for a strong-coupling s-wave superconductor.[187] Thus, it seems that agreement with the Gorter-Casimir formula is indicative of one of two things: if the data are in the asymptotically small temperature range, then the pairing state cannot be conventional. Alternatively, if the data are not in the asymptotically small temperature regime, then strong-coupling effects are important. Most importantly, in the latter case, this does not necessarily mean that the supercon-

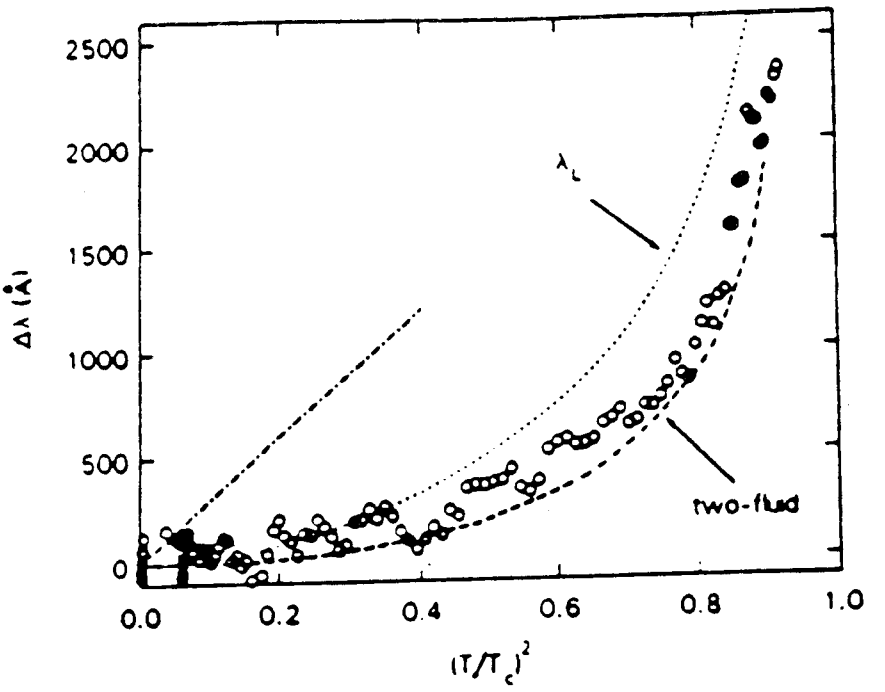

Fig. 27. The change of the in-plane magnetic penetration depth, $\lambda_{aa}(T) = \lambda_{bb}(T)$, of a single crystal as a function of reduced temperature, as determined by dc magnetisation. Dashed line is the Gorter-Casmir formula with $\lambda = 1400$Å. λ_L also fits data with $\lambda(0) = 900$Å. The dot-dashed line was behavior seen in some polycrystalline samples and films. (After Ref. 189.)

ductor is conventional, or even nodeless. One must check to see that there are no states with nodes which could also enable $\lambda(T)$ to resemble the Gorter-Casimir formula.

The use of the temperature dependence of $\lambda(T)$ as a diagnostic of the pairing state has been useful in the heavy fermion superconductors UBe_{13}, UPt_3, and $CeCu_2Si_2$. From a series of reversible magnetisation measurements on superconducting UBe_{13}, using a SQUID magnetometer, Gross *et al.*[181] were able to determine $\Delta\lambda(T) \equiv \lambda(T) - \lambda(0)$ in the temperature range $0.072 < T/T_c < 0.6$. They found a very good fit of the form $\Delta\lambda \propto (T/T_c)^2$, which they have interpreted as evidence for an axial p-wave state in this material. Their results contrasted strongly with those obtained on a Sn reference sample. Similar results have also been reported[188] for the heavy fermion superconductors UPt_3 and $CeCu_2Si_2$.

The situation for $YBa_2Cu_3O_{7-\delta}$ is not quite as unambiguous. The temperature dependent electromagnetic penetration depth has been measured in single crystals of $YBa_2Cu_3O_{7-\delta}$ by low field dc magnetisation[189] and by muon spin resonance.[190] In addition, using a variety of techniques, measurements have been made on polycrystalline samples[191–200] and on c-axis oriented films.[201,202]

With the exception of the results of Refs. 195, 196, 197, and 201, the data show a very weak temperature dependence at low temperatures, and throughout the temperature range are roughly consistent with the Gorter-Casimir formula. Some of the most recent data for single crystals are shown in Figs. 27 (dc magnetisation) and in 28 (muon spin resonance). Both of these measurements determine λ_{ab}, the penetration depth when the field is parallel to the ab plane; at $T = 0$, $\lambda_{ab}(0) \approx 1400$Å. In both cases, a fit to the Gorter-Casimir form is obtained, and is interpreted as being consistent with 's-wave' pairing.

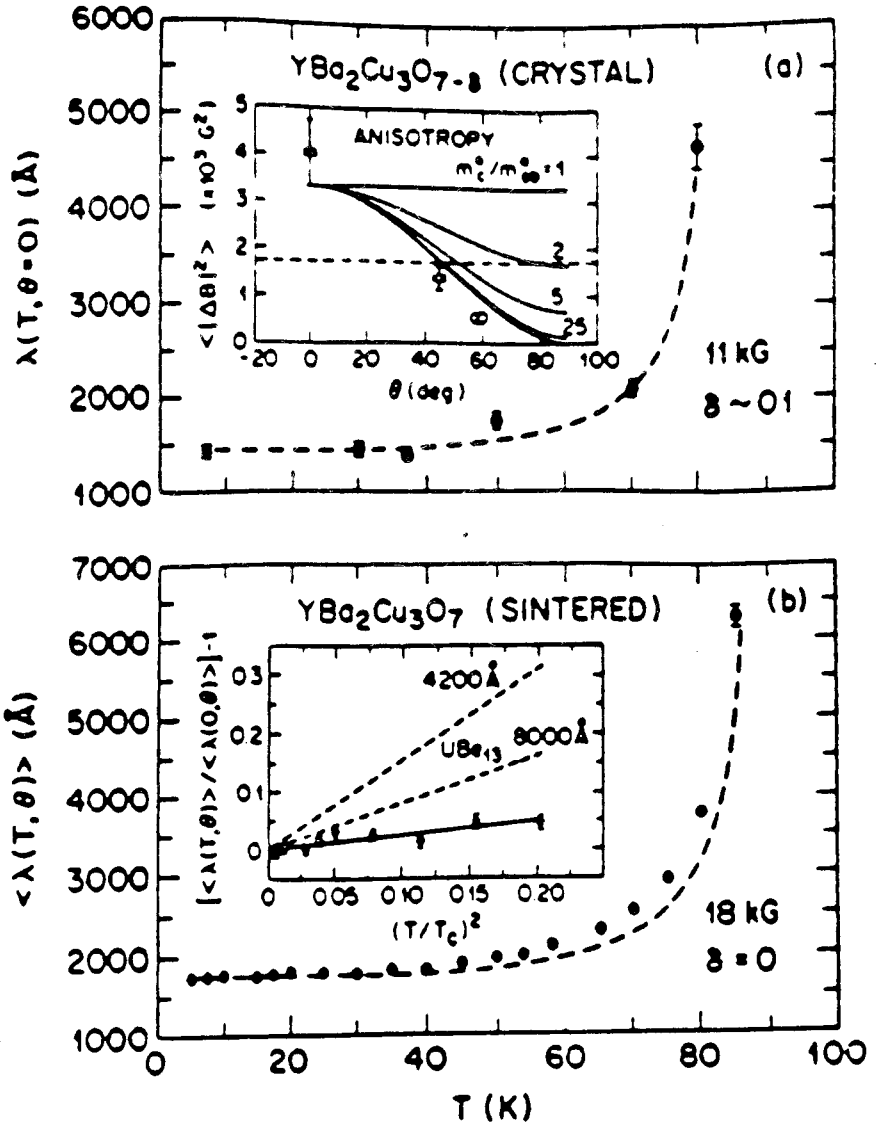

Fig. 28. The temperature dependence of (a) penetration depth of a single crystal of $YBa_2Cu_3O_{7-\delta}(\delta = 0.1)$ and (b) ceramic $YBa_2Cu_3O_{7-\delta}$. The dashed curves are fits to the Gorter-Casmir formula. The inset in frame (a) is $< |\Delta B|^2 >$ as a function of θ (open circles), along with the expected behavior, according to Ref. 190. The inset in (b) shows the relative change in penetration depth for $T < 40$K ploted against $(T/T_c)^2$. Results for UBe_{13} from Einzel *et al.*,[182] assuming $\lambda(0) = 4200$Åand $\lambda = 8000$Å, are shown (dashed lines). (After Ref. 190.)

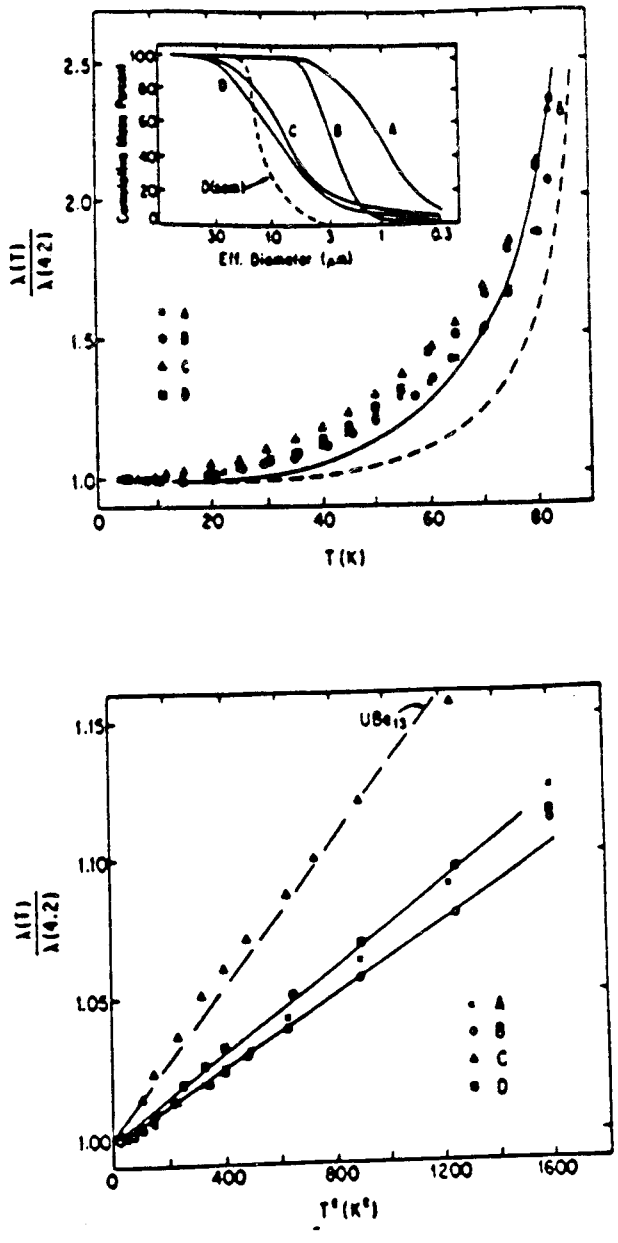

Fig. 29. Low temperature dependence of $\lambda(T)$ showing the T^2 behavior. The dashed line represents data for the heavy Fermion superconductor UBe_{13} scaled to T_c =91K. (After Ref. 196.)

Although the Gorter-Casimir formula provides a reasonable fit to the temperature dependent penetration depth over the range $0 < T < T_c$, the data[189,190,198,200] seem to be consistent with a low temperature behaviour of the form

$$\frac{\lambda_{ab}(T) - \lambda_{ab}(0)}{\lambda_{ab}(0)} = A\left(\frac{T}{T_c}\right)^2, \tag{6.7}$$

with $0 < A < 0.4$. These bounds on A were obtained from the data of Ref. 189. The other data are consistent with $A = 0.3 \pm 0.1$. In Ref. 189, two sets of data are displayed (reproduced in Fig. 27). Even the data with the smallest values of λ seem to show a deviation from the Gorter-Casimir form at low temperature (as can be clearly seen in Fig. 4 of Ref. 189), which may be consistent with the form of Eq. (6.7). The data in the dashed line are also from single crystalline samples, and are consistent with Eq. (6.7) with $A \approx 2.0$. Krusin-Elbaum *et al.* suggest that these data result from flux leakage into the sample, although it is not clear why leakage would result in a T^2 power law. In Ref. 190, the data on sintered powdered samples of $YBa_2Cu_3O_{7-\delta}$ also exhibit a T^2 dependence at low temperatures, but there are not enough data points for the single-crystal sample to attempt to ascertain reliably the low temperature dependence.

There are a few reports in the literature of measurements that could not be fitted to the Gorter-Casimir formula.[195,196,197,201] The results from Ref. 196 are shown in Fig.29. The authors used a low frequency mutual inductance method on fine powders, with controllable particle size. This technique gives 6100Å $< \lambda_c(0) <$ 6800Å. They also find that $\Delta\lambda \propto T^2$ giving a value of $A \approx 0.5$. This value of $\lambda_c(0)$ is comparable to a lower bound reported in Ref. 190 of 7000 Å, on the basis of muon spin resonance measurements on a single crystal. Finally,

there are two reports[195,197] that $\Delta\lambda \propto T$.

It is difficult to draw firm conclusions from the data because the theoretical situation is not very well understood. In particular, it is not known how strong coupling affects the theoretical predictions for many unconventional pairing states. Rammer[187] has studied strong coupling effects for s-wave states, and has exhibited the similarity between the temperature dependence of that case and the Gorter-Casimir formula. For triplet states without nodes, it is plausible that qualitatively similar results apply, and that the observation of a temperature dependence close to the Gorter-Casimir formula would be consistent with these states in the strong-coupling limit.

It is not possible, in our opinion, to rule out definitely a small T^2 contribution to $\Delta\lambda$. This effect, if confirmed, might arise from point nodes; in this case, possible dependence of the power law with orientation of the magnetic field should be sought. Alternatively, it is conceivable that resonant impurity scattering is responsible for this term,[203] as is thought to be the case in UPt_3.[179]

The observations[195,197] that $\Delta\lambda \propto T$ have not been confirmed in experiments on single crystals; this seems to rule out singlet states with line nodes. The only way in which the data could still be consistent with singlet states with line nodes is if the slope of the gap function at these nodes were sufficiently large that the temperature below which linear behaviour would occur would be unobservably small.[158] Alternatively, temperature dependent Fermi liquid effects and scattering processes could conceivably conspire to produce the observed temperature dependence.[179,203] Indeed, this is precisely what is believed to occur in UPt_3, which is thought to have line nodes, but which exhibits the low temperature behaviour[188] $\Delta\lambda \propto T^2$.

In conclusion, it seems probable that the data are consistent with a nodeless gap function, which can arise from both conventional and unconventional pairing states. There is some evidence for a small T^2 contribution to $\Delta\lambda$. Unless a number of *caveats* apply, singlet states with line nodes are ruled out by the data. The only other singlet state is the conventional 's-wave' state.

VII. CONCLUSIONS

In this final Section, we will try to present a coherent picture built from the many experiments which we have discussed. In our opinion, there are two principal scenarios for the pairing state: one is that the pairing state is of the 's-wave' variety, whilst the other is that the pairing state is 'd-wave', with line nodes. Neither scenario is compelling at present, and neither scenario can be firmly ruled out by the existing experiments. In fact, adopting either of these scenarios requires additional assumptions, which we shall discuss in detail below.

We start by considering the probes of order parameter structure. At present, these yield no firm evidence for or against unconventional pairing, but certain experiments are at the point where a decisive test of the symmetry of the order parameter could be attempted in the near future. Among the possible decisive tests are:

(1) High accuracy specific heat-fluctuation measurements on untwinned crystals.

(2) Confirmation of the existence or absence of a double peak in the specific heat.

(3) Confirmation of the presence or absence of Josephson effects between $YBa_2Cu_3O_{7-\delta}$ and an s-wave superconductor, in planar junctions along specific

crystallographic axes. This experiment is uniquely important, because a conclusion about the pairing state can be drawn from each of the possible outcomes.

(4) Angular dependence of H_{c2} in the basal plane of an untwinned crystal.

None of these tests requires any input from a microscopic theory of superconductivity, which is why these experiments should be more easily interpreted than probes of low energy excitations.

The remaining experiments all involve microscopic probes of the superconductivity. The strongest constraint comes from the inferred magnitudes and anisotropies of the copper plane site Knight shifts, which seem to rule out triplet pairing. An immediate consequence of this result is that the pairing state is singlet; i.e. either 's-wave' or unconventional with line nodes (presumably 'd-wave').

Can the remaining experiments eliminate either of these two possibilities? First, consider the scenario that the pairing state is 's-wave'. The temperature dependence of $\lambda(T)$ is consistent with this state, provided that strong coupling corrections are present. 'S-wave' pairing is also consistent with the point-contact tunneling measurements, which indicate that at low temperature, $YBa_2Cu_3O_{7-\delta}$ is a clean superconductor with a gap $2\Delta/k_BT_c \approx 6$. Fits to the temperature dependence of the Knight shift are also consistent with 's-wave' pairing. Other experiments can be made consistent with 's-wave' pairing only by invoking additional assumptions. The tunneling characteristics of broken film and planar junctions do not show a clean gap, perhaps because of paramagnetic impurities in the junction. The absence of a coherence peak in the NMR relaxation rate is difficult to explain by 's-wave' pairing, but may be caused by inelastic scattering processes important near T_c. The most difficult measurements to explain are the

low temperature T^3 power law of Cu site T_1 relaxation and the observed small frequency continuum in the Raman scattering intensity. These observations imply the existence of gapless excitations that cannot be electron-hole pairs because of the assumed non-zero gap.

The second scenario is that the pairing state is 'd-wave' with line nodes. A singlet state with line nodes is consistent with the absence of the coherence peak in the NMR relaxation rate at all sites, and with the T^3 power law behaviour of the low temperature Cu T_1^{-1}. Furthermore, the observations of the low energy Raman scattering intensity and the zero-bias conductance observed in broken film and planar tunnel junctions are consistent with nodes in the gap. However, the penetration depth measurements seem to rule out this scenario unless the gap function has a large slope near the nodes, or unless any temperature dependent effects intervene from Fermi liquid corrections or scattering processes. The near total infra-red reflectance below 100 cm^{-1} may also be evidence against a state with line nodes. Fits to the temperature dependent Knight shift data require a large slope of the gap function near the nodes. Finally, the well-defined gap seen in the point-contact tunneling data may result from sampling only a portion of the Fermi surface; moreover, the sharpness of this feature suggests that scattering processes should be weak.

At present, neither 's-wave' nor 'd-wave' can be conclusively ruled out. In the 's-wave' case, the major outstanding problems are the vanishing of the coherence peak and the identification of the low energy excitations seen in NMR relaxation and Raman scattering. On the other hand, for the 'd-wave' case, more detailed calculations of the penetration depth and the reflectivity are required, taking into account possible Fermi liquid corrections or scattering processes.

In summary, given the presently available data, it appears that triplet states are ruled out by the Knight shift anisotropy, and singlet states with line nodes seem to be ruled out by the temperature dependence of the penetration depth. If both of these tentative results stand up to further scrutiny, then the only remaining candidate state would be the conventional one.

ACKNOWLEDGEMENTS

We are grateful to the editor of this volume for giving us the opportunity to contribute a chapter. We have drawn upon the experience and wisdom of many of our colleagues at Illinois and elsewhere. We especially thank Don Ginsberg, Miles Klein, Charles Slichter, David Pines, Fred Zawadowski, Hartmut Monien, Peter Hirschfeld, Francis Slakey, Charles Pennington, Rob Kiefl, Laura Greene, Tom Timusk, Clare Yu, Sue Inderhees, Ken Lyons, and Dale Van Harlingen for their valuable insights and comments on this manuscript. One of us (JFA) thanks Prof. V. Heine for his hospitality at the Cavendish Laboratory, Cambridge, England, where some of this work was carried out.

This work was supported in part by NSF grant DMR-88-18713 and in part by NSF grant DMR-86-12860 through the Materials Research Laboratory at the University of Illinois and in part by NSF Grant STC-88-09854 through the Science and Technology Center for Superconductivity. One of us (NDG) gratefully acknowledges receipt of an Alfred P. Sloan Foundation Fellowship.

REFERENCES

1. V.L. Ginzburg, *J. Superconductivity* (to appear).
2. P. Hirschfeld, *Phys. Rev. B* **37**, 9331 (1988).
3. B. Arfi *et al.*, *Phys. Rev. Lett.* **60**, 2206 (1988); B. Arfi and C.J. Pethick, *Phys. Rev. B* **38**, 2312 (1988); B. Arfi, H. Bahlouli and C.J. Pethick, *Phys. Rev. B* **39**, 8959 (1989).
4. M. Doria, H. Brand, H. Pleiner, *Physica C* **159**, 46 (1989).
5. R. Joynt, *Upward Curvature of H_{c2} in High T_c Superconductors: Possible Evidence for s-d Pairing*, preprint.
6. P.M. Horn *et al.*, *Phys. Rev. Lett.* **59**, 2772 (1987).
7. J.J. Capponi *et al.*, *Europhys. Lett.* **3**, 1301 (1987).
8. P. Day *et al.*, *J. Phys. C* **20**, L429 (1987).
9. D. Zhu, A.C. Anderson, E.D. Bukowski, and D.M. Ginsberg, *Phys. Rev. B* **40**, 841 (1989).
10. J.L. Cohn, S.D. Peacor and C. Uher, *Phys. Rev. B* **38**, 2892 (1988); C. Uher and J.L. Cohn, *J. Phys. C* **21**, L957 (1988); S.D. Peacor and C. Uher, *Phys. Rev. B* **39**, 11559 (1989).
11. Although the momentum is a vector, for simplicity we have used the notation k throughout this chapter.
12. P.W. Anderson and W.F. Brinkman, *The Helium Liquids: Proceedings of the 15th Scottish Universities Summer School in Physics, 1974*, edited by J.G.M. Armitage and I.E. Farquhar, pp. 315 (Academic Press, New York, 1975). Reprinted in P.W. Anderson, *Basic Notions of Condensed Matter Physics*, (Benjamin-Cummings, Menlo Park, 1984).

13. C.E. Gough *et al.*, *Nature* **326**, 855 (1987).

14. R.H. Koch *et al.*, *Appl. Phys. Lett.* **51**, 200 (1987).

15. T. Yamashita *et al.*, *J. Appl. Phys.* **26**, L635 (1987).

16. T. Yamashita *et al.*, *ibid* **26**, L671 (1987).

17. T.J. Witt, *Phys. Rev. Lett.* **61**, 1423 (1988).

18. A.F. Andreev *Zh. Eksp. Teor. Fiz.* **46**, 1823 (1964)[*Sov. Physics JETP* **19**, 1228 (1964)].

19. G.E. Blonder, M. Tinkham, and T.M. Klapwijk, *Phys. Rev. B* **25**, 4515 (1982).

20. H. van Kempen, H.F.C. Hoevers, P.J.M. van Bentum, A.J.G. Schellingerhout, and D. van der Marel, *IBM. J. Res. Develop.* **33**, 389 (1989).

21. H.F.C. Hoevers, P.J.M. van Bentum, L.E.C. van der Leemput, H. van Kempen, A.J.G. Schellingerhout, and D. van der Marel, *Physica C* **152**, 105 (1988).

22. N.P. Ong *et al.*, to be published in the *Proceedings of the 1st Asia Pacific Conference on Condensed Matter Physics*, (World Scientific, Singapore, 1990).

23. G.E. Volovik and L.P. Gorkov, *Zh. Eksp. Teor. Fiz.* **88**, 1412 (1985)[*Sov. Phys. JETP* **61**, 843 (1985)]; K. Ueda and T.M. Rice, *Phys. Rev. B* **31**, 7114 (1985); M. Ozaki, K. Machida and T. Ohmi, *Prog. Theo. Phys.* **74**, 221 (1985) and *ibid.* **75**, 442 (1986); E.I. Blount, *Phys. Rev. B.* **32**, 2935 (1985); M. Sigrist and T.M. Rice, *Z. Phys. B* **68**, 9 (1987).

24. L.P. Gor'kov, *Sov. Sci. Rev. A. Phys* **9**, 1 (1987).

25. A detailed review may be found in a recent paper by J.F. Annett (submitted to *Advances in Physics*).

26. M. Tinkham, *Group Theory and Quantum Mechanics* (McGraw-Hill, New York 1964).

27. Actually $\Delta = \eta_0 XYF(k)$ where F(k) is some unknown temperature dependent function which is invariant under the full point group. Such a function should multiply all entries in the fourth column of Tables 1-5. However, for simplicity, we will omit all such factors.

28. W.E. Pickett, *Rev. Mod. Phys.* **61**, 433 (1989).

29. Our analysis is not affected if the Fermi surface has a cross-section other than circular, although we will require that the cross-section does not introduce any singularities into the Fermi velocity.

30. G.E. Volovik and L.P. Gorkov, *Zh. Eksp. Teor. Fiz.* **88**, 599 (1985)[*Sov Phys. JETP* **61**, 843 (1985)].

31. S.E. Inderhees, M.B. Salamon, N.D. Goldenfeld, J.P. Rice, B.G. Pazol, D.M. Ginsberg, J.Z. Liu, and G.W. Crabtree, *Phys. Rev. Lett.* **60**, 1178 (1988); *ibid.* **60**, 2445 (1988); *ibid.* **61**, 481 (1988).

32. M.B. Salamon, S.E. Inderhees, J.P. Rice, B.G. Pazol, D.M. Ginsberg, and N.D. Goldenfeld, *Phys. Rev. B* **38**, 885 (1988).

33. P.P. Freitas, C.C. Tsuei, and T.S. Plaskett, *Phys. Rev. B* **36**, 833 (1987).

34. N. Goldenfeld, P.D. Olmsted, T.A. Friedmann, and D.M. Ginsberg, *Solid State Comm.* **65**, 465 (1988).

35. M.A. Dubson, J.J. Calabrese, S.T. Herbert, D.C. Harris, B.R. Patton, and J.C. Garland, p. 981 in *Novel Superconductivity*, edited by S.A. Wolf and

V.Z. Kresin (Plenum, New York, 1987).

36. M. Ausloos and Ch. Laurent, *Phys. Rev. B* **37**, 611 (1988).

37. B. Oh, K. Char, A.D. Kent, M. Naito, M.R. Beasley, T.H. Geballe, R.H. Hammond, A. Kapitulnik, and J.M. Graybeal, *Phys. Rev. B* **37**, 7861 (1988).

38. S.J. Hagen, Z.Z. Wang, and N.P. Ong, *Phys. Rev. B* **37**, 7861 (1988).

39. T.A. Friedmann, J.P. Rice, and D.M. Ginsberg, *Phys. Rev. B* **39**, 4258 (1989).

40. K. Kanoda, T. Kawagoe, M. Hasumi, T. Takahashi, S. Kagoshima and T. Mizoguchi, *J. Phys. Soc. Jpn* **57**, 1554 (1988); *Physica C* **153-155**, 749 (1988).

41. W.C. Lee, R.A. Klemm, and D.C. Johnston, *Phys. Rev. Lett.* **63**, 1012 (1989).

42. J.F. Annett, N.D. Goldenfeld, and S.R. Renn, unpublished.

43. M.A. Howson, M.B. Salamon, T.A. Friedmann, S.E. Inderhees, J.P. Rice, D.M. Ginsberg, and K.M. Ghiron, *J. Phys.: Condensed Matter* **1**, 465 (1989).

44. K. Fossheim, O.M. Nes, T. Lægreid, C.N.W. Darlington, D.A. O'Connor, and C.E. Gough, *Int. J. Mod. Phys. B* **1**, 1171 (1988).

45. M.B. Salamon in *Physical Properties of High Temperature Superconductors, I*, D.M. Ginsberg (ed.), (World Scientific, Singapore, 1989).

46. J. Annett, M. Randeria, and S. Renn, *Phys. Rev. B* **38**, 4660 (1988).

47. N. Goldenfeld and C.J. Pethick, *Phys. Rev. B* **39**, 9601 (1989).

48. F. Sharifi, J. Giapintzakis, D.M. Ginsberg, and D.J. Van Harlingen, *Physica C* (in press).

49. S. Inderhees, private communication.

50. N.D. Goldenfeld, unpublished.

51. R. Joynt, *Physica Scripta* **36**, 175 (1987).

52. G.E. Volovik, *JETP Lett.* **48**, 41 (1988).

53. D.W. Hess, T.A. Tokuyasu, and J.A. Sauls, *Broken Symmetry in an Unconventional Superconductor: A Model for the Double Transition in* UPt_3, preprint.

54. R.A. Ficher *et al.*, *Phys. Rev. Lett.* **62**, 1411 (1989).

55. K. Hasselbach, L. Taillefer, and J. Floquet, *Phys. Rev. Lett.* **63**, 93 (1989).

56. R.A. Butera, *Phys. Rev. B* **37**, 5909 (1988).

57. M. Ishikawa, Y. Nakazawa, T. Takabatake, A. Kishi, R. Kato, and A. Maesono, *Solid State Comm.* **66**, 201 (1988).

58. M. Ishikawa, private communication.

59. R. Joynt, *Supercond. Sci. Technol.* **1**, 210 (1988).

60. J. Niemeyer, M.R. Dietrich, and Z. Politis, *Z. Phys B* **67**, 155 (1987).

61. A. Barone, *Physica C* **153-155**, 1072 (1988).

62. M.N. Keene, T.J. Jackson, and C.G. Gough, *Nature* **340**, 210 (1989).

63. W.A. Little, *Proc. M^2S-HTSC Conference, Stanford, July 23-28 (1989)*,* to appear in Physica C.

64. J.A. Pals, W. van Haeringen, and M.H. van Maaren, *Phys. Rev. B* **15**, 2592 (1977).

65. E.W. Fenton, *Solid State Comm.* **54**, 709 (1985); *ibid.* **60**, 347 (1986); J.A. Sauls, Z. Zou and P.W. Anderson, unpublished.

66. O.S. Akhytyamov, *ZhETF Pis'ma*, **3**, 284 (1966)[*Sov. Phys. JETP Lett.* **3**, 183 (1966)].

67. A.J. Millis, *Physica B*, **135**, 69 (1985).

68. V.B. Geshenbein and A.I. Larkin, *Pis'ma Zh. Eskp. Theor. Fiz.* **43**, 306 (1986)[*JETP Lett.* **43**, 396 (1986)].

69. L.H. Greene, *et al.*, *Proc. M^2S-HTSC Conference, Stanford, July 23-28, (1989)*, to appear in Physica C.

70. L.P. Gorkov, *Pis'ma Zh. Eksp. Teor. Fiz.*, **40**, 351 (1984)[*JETP Lett.*, **40**, 1155 (1984)].

71. L.I. Burlachkov, *Zh. Eksp. Teor. Fiz.*, **89**, 1382 (1985)[*Sov. Phys. JETP* **62**, 800 (1985)].

72. See, for example, A.P. Malozemoff in *Physical Properties of High Temperature Superconductors, I*, D.M. Ginsberg (ed.), (World Scientific, Singapore, 1989).

73. J. Bardeen, L.N. Cooper, and J.R. Schrieffer, *Phys. Rev.* **106**, 162 (1957); *ibid.* **108**, 1175 (1957).

74. A.A. Abrikosov and L.P. Gorkov, *Zh. Eksp. Teor. Fiz*, **39**, 1781 (1960)[*Sov. Phys. JETP*, **12**, 1243 (1961)].

75. P.G. de Gennes, *Superconductivity of Metals and Alloys*, chap. 8, (W.A. Benjamin, New York, 1966).

76. dc resistive measurements and Drude fits to the far infra-red conductance indicate that $1/\tau \sim k_B T$ extrapolating from above T_c. See T. Timusk and

D.B. Tanner in *Physical Properties of High Temperature Superconductors I*, D.M. Ginsberg (ed.) (World Scientific, Singapore, 1989).

77. M. Lee, A. Kapitulnik, and M.R. Beasley in *Mechanisms of High Temperature Superconductivity*, H. Kamimura and A. Oshiyama (eds.),(Springer, New York, 1989).

78. S.L. Cooper *et al.*, *Phys. Rev. B* **37**, 5920 (1988).

79. R. Häckl *et al.*, *Phys. Rev. B* **38**, 7133 (1988).

80. K.B. Lyons, *Phys. Rev. B* **36**, 5592 (1987).

81. A.V. Bazhenov *et al.*, *Pisma Zh. Eksp. Teor. Fiz.* **46**, 35 (1987)[*JETP Lett.* **46**, 32 (1987)].

82. F. Slakey, M.V. Klein, J.P. Rice, and D.M. Ginsberg, *M^2S-HTSC conference, Stanford July 23-28*, To appear in *Physica C.*

83. A. Yamanaka *et al.*, *Jpn. J. Appl. Phys.* **27**, L1902 (1988).

84. M.C. Krantz *et al.*, unpublished.

85. C. Thomsen and M. Cardona in *Physical Properties of High Temperature Superconductors, I*, D.M. Ginsberg (ed.), (World Scientific, Singapore, 1989).

86. F. Slakey, S.L. Cooper, M.V. Klein, J.P. Rice, and D.M. Ginsberg, *Phys. Rev. B.* **39**, 2781 (1989).

87. F. Slakey, M.V. Klein,S.L. Cooper, E.D. Bukowski, J.P. Rice, and D.M. Ginsberg, *IEEE J. Quan. Electronics*; Special Issue on High Temp. Superconductors (in press).

88. S.L. Cooper, M.V. Klein, B.G. Pazol, J.P. Rice, and D.M. Ginsberg, *Phys. Rev. B* **37**, 5920 (1988).

89. S.L. Cooper, F. Slakey, M.V. Klein, J.P. Rice, E.D. Bukowski, and D.M. Ginsberg, *Phys. Rev. B* **38**, 11934 (1988).

90. S.L. Cooper, F. Slakey, M.V. Klein, J.P. Rice, E.D. Bukowski, and D.M. Ginsberg, *J. Opt. Soc. Am. B* **6**, 436 (1989).

91. R. Hackel, W. Glaser, P. Muller, D. Einzel, and K. Andres, *Phys. Rev. B.* **38**, 7133 (1988).

92. R.M. Macfarlane *et al.*, *Phys. Rev. B* **38**, 284 (1988).

93. C .Thomsen *et al.*, *Solid State Comm.* **65**, 55 (1988).

94. A. Yamanaka, T. Kimura , F. Minami, K. Inoue, and S. Takekawa, *Jap. J. Appl. Phys.* **27**, L1902 (1988).

95. M.C. Krantz,H.J. Rosen, J.Y. Wei, and D.E. Morris, *Phys. Rev. B*, to be published.

96. S. Sugai, Y. Enomoto, and T. Murakami, *Difference in the extent of the itinerant electron wave function in* $Ba_xK_{1-x}BiO_3$ *and* $BaPb_{1-x}Bi_xO_3$, preprint.

97. S. Sugai, and Y. Enomoto, and T. Murakami, NTT preprint 6/24/89.

98. K.F. McCarty, H.B. Radousky, D. G. Hinks, Y. Zheng, A.W. Mitchell, T.J. Folkerts, and R.N. Shelton, *Phys. Rev. B* **40**, 2662 (1989).

99. F. Slakey, private communication.

100. H. Monien and A. Zawadowski, *Phys. Rev. Lett.* **63**, 911 (1989).

101. M. Cardona *et al.*, *Phys. Rev. B* **32**, 924 (1985).

102. I.P. Ipatova *et al.*, *Sol. State Comm.* **37**, 893 (1981).

103. Jaejun Yu, S. Massida, A.J. Freeman, and D.D. Koeling, *Phys. Lett.* **122**, 198 (1987).

104. This explanation was suggested to us by K. Lyons.

105. T. Timusk and D.B. Tanner in *Physical Properties of High Temperature Superconductors, I*, D. M. Ginsberg (ed.), (World Scientific, Singapore, 1989).

106. D.B. Tanner and T. Timusk, *Mod. Phys. Lett. B* **3**, 189 (1989).

107. T. Timusk *et al.*, *Phys. Rev. B*, **38**, 6683 (1988).

108. D.B. Tanner *et al.*, *Synth. Met.* **29**, F715 (1989).

109. S.L. Herr *et al.*, *Phys. Rev. B.* **36**, 733 (1987).

110. K. Kamaras *et al.*, *Phys. Rev. Lett.* **59**, 919 (1987).

111. D.A. Bonn *et al.*, *Phys. Rev. B.* **37**, 1547 (1988).

112. K. Kamaras *et al.*, *In a Clean HTSC You Don't See the Gap*, U. Florida preprint 5/27/89.

113. G.A. Thomas *et al.*, *Phys. Rev. Lett.* **61**, 1313 (1988).

114. Z. Schlesinger *et al.*, *Phys. Rev. Lett.* **59**, 1958 (1987).

115. Z. Schlesinger *et al.*, *Physica C* **153-155**, 1734 (1988).

116. R.T. Collins *et al.*, *Phys. Rev. B* **39**, 6571 (1989).

117. R.T. Collins *et al.*, *IBM J. Res. Dev.* **33**, 238 (1989).

118. G.A. Thomas, *The Energy Gap and Two Component Absorption in a High T_c Superconductor*, preprint.

119. G.A. Thomas, A.Millis, R.N. Bhatt, R.J. Cava, and E.A. Rietman, *Phys. Rev. B* **36**, 736 (1987).

120. B. Batlogg, J.P. Remeika, R.C. Dynes, H. Barz, A.S. Cooper, and J.P. Garno, in *Superconductivity in d- and f- Band Metals*, W. Buckel and W. Weber (eds.) (Kernforschungszentrun Karlsruhe GmbH, Karlsruhe, 1982).

121. S. Tajima, S. Uchida, A. Masaki, H. Takagi, K. Kitazawa, S. Tanaka, and A. Katsue, *Phys. Rev B* **32**, 6302 (1985).

122. G.A. Thomas, M. Capizzi, J. Orenstein, D.H. Rapkine, A.J. Millis, P. Gammel, L.F. Schneemeyer, and J.V. Waszczak, to be published in *Proceedings of the International Symposium on the Electronic Structure of High T_c Superconductors*, Rome 10/88, A. Bianconi (ed.), (Pergamon Press, Oxford, 1988).

123. P.B. Allen, *Phys. Rev. B* **3**, 305 (1971).

124. J. Moreland *et al.*, *Phys. Rev. B* **35**, 8856 (1987).

125. M. Lee, A. Kapitulnik, and M.R. Beasley in *Mechanisms of High Temperature Superconductivity*, H. Kamimura and A. Oshiyama (eds.),(Springer, New York, 1989).

126. J.S. Tsai *et al.*, *ibid.* p. 229.

127. J.S. Tsai, I. Takeuchi, I. Fujita, S. Miura, T. Terashima, Y. Bando, K. Iijima, and K. Yamamoto, *Physica C* **157**, 537 (1989).

128. A. Fournel *et al.*, *Europhys. Lett.* **6**, 653 (1988).

129. J.R. Kirtley *et al.*, *Phys. Rev. B* **35**, 8846 (1987).

130. M. Gurvitch, J.M. Valles,Jr., A.M. Cucolo, R.C. Dynes, J.P. Garno, L.F. Schneemeyer, and J.V. Waszczak, *Phys. Rev. Lett.* **63**, 1008 (1989).

131. M.D. Kirk, D.P.E. Smith, D.B. Mitzi, J.Z. Sun, D.J. Webb, K. Char, M.R. Hahn, M. Naito, B. Oh, M.R. Beasley, T. H. Geballe, R. H. Hammond, A. Kapitulnik, and C.F. Quate, *Phys. Rev. B* **35**, 8850 (1987).

132. M.A. Ramos and S. Vieira, *Proc. M^2S-HTSC Conference*, Stanford July 23-28 (1989), Physica C to be published.

133. A. Edgar, C.J. Adkins, and S.J. Chandler, *J. Phys. C:Solid State Phys.* **20**, L1009 (1987).

134. I. Iguchi, S. Narumi, Y. Kasai, and A. Sugishita, *Physica B* **148**, 322 (1987).

135. The zero bias conductance in the data of Gurvitch *et al.*[130] has a shoulder precisely at the bulk T_c=89K even though the gap value, if compared with the plots of Tsai *et al.* (see Fig. 17), would correspond to a surface transition temperature of 70K.

136. J.C. Phillips, *The Physics of High T_c Superconductors*, (Academic Press, Boston, 1989).

137. J.A. Appelbaum, *Phys. Rev. Lett.* **17**, 91 (1966); *Phys. Rev.* **154**, 633 (1967); P.W. Anderson, *Phys. Rev. Lett.* **17**, 95 (1966).

138. L.Y.L. Shen and J.M. Rowell, *Phys. Rev.* **165**, 566 (1968).

139. S. Bermon, D.E. Paraskevopoulos, and P.M. Tedrow, *Phys. Rev. B* **17**, 2110 (1978).

140. E.L. Wolf and D.L. Losee, *Phys. Rev. B* **2**, 2360 (1970).

141. For a more detailed review of this field see the chapter by C.H. Pennington and C.P. Slichter in this volume.

142. D.E. MacLaughlin *et al.*, *Phŷs. Rev. Lett.* **53**, 1833 (1984); Y. Kitaoka, *et al.*, *J. Magn. Mater.* **52**, 341 (1985).

143. T. Imai *et al.*, *Int. J. Mod. Phys. B* **3**, 93 (1989).

144. T. Imai *et al.*, *J. Phys. Soc. Jpn.* **57**, 2280 (1988).

145. W.W. Warren *et al.*, *Phys. Rev. Lett.* **59**, 1860 (1987).

146. P.C. Hammel, M. Takigawa, R.H. Heffner, Z. Fisk, and K.C. Ott, *Spin Dynamics at Oxygen Sites in* $YBa_2Cu_3O_{7-\delta}$, unpublished.

147. K. Ishida *et al.*, *J. Phys. Soc. Jpn* **57**, 2897 (1988).

148. P. Wzietek *et al.*, *Europhys. Lett.* **8**, 363 (1989).

149. L.C. Hebel and C.P. Slichter, *Phys. Rev.* **113**, 1504 (1959); L.C. Hebel, *Phys. Rev.* **116**, 79 (1959).

150. J. R. Schrieffer, *Theory of Superconductivity*, (Benjamin, New York, 1964).

151. A. Griffin and V. Ambegaokar, *Proc. Int. Low Temp. Phys.*, Ohio (1964), J.G. Daunt *et al.* (eds.), p. 524.

152. Phonon broadening of the coherence peak would give a $1/T_1$ which decreases with temperature much more slowly than than is in fact observed. (H. Monien, private communication.)

153. Y. Kohori, T. Kohara, H. Shibai, Y. Oda Y. Kitaoka, and K. Asayama, *J. Phys. Soc. Japan* **57**, 395 (1988); For a review of NMR in heavy fermion systems, see K. Asayama, Y. Kitaoka and Y. Kohori, *J. Magn. Mag. Mater.* **76-77**, 449 (1988).

154. T. Imai, T. Shimizu, and H. Yasuoka, *Nuclear relaxation Studies on Copper Spin Dynamics in High* T_c *and Related Metallic Oxides*, preprint 5/89.

155. W.W. Warren, Jr. *et al.*, *Phys. Rev. Lett.* **62**, 1193 (1989).

156. S. Massida, J. Yu, and A.J. Freeman, *Physics Lett. A* **122**, 138 (1987).

157. P. Monthoux, to be published.

158. H. Monien and D. Pines, *Do the Planar Excitations in* $YBa_2Cu_3O_{7-\delta}$ *Form an Antiferromagnetically Coupled Fermi Liquid?*, Univ. of Illinois preprint 7/89.

159. K. Yosida, *Phys. Rev.* **110**, 769 (1958).

160. A.J. Leggett, *Rev. Mod. Phys.* **47**, 331 (1975).

161. H. Monien, D. Pines, C.P. Slichter (to be published).

162. In fact spin-orbit corrections may make $\chi(0) \neq 0$. See: F. Reif, *Phys. Rev.* **106**, 208 (1957), and P.W. Anderson, *Phys. Rev.* **96**, 266 (1954).

163. S. Takagi, Ph.D thesis, University of Tokyo (unpublished).

164. M. Takigawa, P.C. Hammel, R.H. Heffner, and Z. Fisk, *Phys. Rev. B* **39**, 7371 (1989)

165. S. E. Barrett, D.J. Durand, C.H. Pennington, C.P. Slichter, T.A. Friedmann, J.P. Rice, and D.M. Ginsberg, *^{63}Cu Knight shifts in the superconducting state of $YBa_2Cu_3O_{7-\delta}(T_c=90K)$*, Univ. of Illinois preprint.

166. J.F. Annett, R.M. Martin, A.K. McMahan, and S. Satpathy, *Phys. Rev. B.* **40**, 2620 (1989).

167. F. Mila and T.M. Rice, *Physica C* **157**, 561 (1989).

168. For a recent review of the low temperature specific heat of $YBa_2Cu_3O_{7-\delta}$ see S.E. Stupp and D.M. Ginsberg, *Physica C* **158**, 299 (1989).

169. M.E. Reeves, T.A. Friedmann, and D.M. Ginsberg, *Phys. Rev. B* **35**, 7207 (1987).

170. B.D. Dunlap *et al.*, *Phys. Rev. B* **35**, 7210 (1987).

171. L.E. Wenger *et al.*, *Phys. Rev. B* **35**, 7213 (1987).

172. M.E. Reeves, S.E. Stupp, T.A. Friedmann, F. Slakey, and D.M. Ginsberg, and M.V. Klein, *Field Dependent Specific Heat of Polycrystalline $YBa_2Cu_3O_{7-\delta}$*, Univ. of Illinois preprint 4/89.

173. R. Kuentzler *et al.*, *Solid State Comm.* **65**, 1529 (1988).

174. A.P. Ramirez *et al.*, *Mat. Res. Soc. Symp. Proc.* **99**, 459 (1987).

175. B. Golding *et al.*, *Phys. Rev B* **36**, 5606 (1987).

176. K. Ueda and T.M. Rice, in *Theory of Heavy Fermions and Valence Fluctuations*, T. Kasuya, and T. Saso (eds.), (Springer-Verlag, Berlin, 1985), p. 263. See especially Fig. 1 and Fig. 3.

177. R.A. Fisher *et al.*, *Phys. Rev. B* **38**, 11942 (1988).

178. A. Chakraborty *et al.*, *Phys. Rev. B* **39**, 12267 (1989).

179. P. Hirschfeld, D. Vollhardt and P. Wölfle, *Solid State Comm.* **59**, 111 (1986); P. Hirschfeld, P. Wölfle, and D. Einzel, *Phys. Rev. B* **37**, 83 (1988); S. Schmitt-Rink, K. Miyake and C.M. Varma, *Phys. Rev. Lett.* **57**, 2575 (1986); H. Monien *et al.*, *Solid State Comm.* **61**, 581 (1987); C.J. Pethick and D. Pines, *Phys. Rev. Lett.* **57**, 118 (1986).

180. W. Barford, and J.M.F Gunn, *Physica C*, **156**, 512 (1988).

181. F.Gross, B.S. Chandrasekhar, D. Einzel, K. Andres, P.J. Hirschfeld, H.R. Ott, J. Beuers, Z. Fisk, and J.L. Smith, *Z. Phys. B* **64**, 175 (1986).

182. D. Einzel, P.J. Hirschfeld, F. Gross, B.S. Chandrasekhar, K. Andres, H.R. Ott, J. Beuers, Z. Fisk, and J.L. Smith, *Phys. Rev. Lett.* **56**, 2513 (1986).

183. A. J. Millis, *Phys. Rev. B* **35**, 151 (1987).

184. C.M. Varma, K. Miyake, and S. Schmitt-Rink, *Phys. Rev. Lett.* **57**, 626 (1986).

185. J.Takada *et al.*, *Appl. Phys. Lett* **53**, 332 (1988).

186. A.L. Fetter and J.D. Walecka, *Quantum Theory of Many Particle Systems*, (McGraw-Hill, New York, 1971).

187. J. Rammer, *Europhys. Lett.* **5**, 77 (1988).

188. F, Gross, B.S. Chandrasekhar, K. Andres, U. Rauchschwalbe, E. Buecher, and B. Luthi, *Physica C* **153-155**, 439 (1988).

189. L. Krusin-Elbaum *et al.*, *Phys. Rev. Lett.* **62**, 217 (1989).

190. D.R. Harshman *et al.*, *Phys. Rev. B* **39**, 851 (1989).

191. D.R. Harshman *et al.*, *Phys. Rev. B* **36**, 2386 (1987).

192. D.W. Cooke *et al.*, *Phys. Rev. B* **37**, 9401 (1988); *Phys. Rev. B* **39**, 2748 (1989).

193. A. Schenck, *Physica C* **153-155**, 1127 (1988).

194. Y.J. Uemura *et al.*, *Phys. Rev. B* **38**, 909 (1988).

195. T. Ishida and H. Mazaki, *Jpn. Jnl. Appl. Phys.* **26**, L2003 (1987).

196. J.R. Cooper *et al.*, *Phys. Rev. B* **37**, 638 (1988).

197. P. Monod *et al.*, *Physica C* **153-155**, 1489 (1988).

198. S. Mitra *et al.*, *Phys. Rev. B* **40**, 2674 (1989).

199. A. Porch, J.R. Waldram, and L. Cohen, *J. Phys. F* **18**, 1547 (1988).

200. T. Riseman *et al.*, *Magnetic Penetration Depths in High T_c CuO_2 Superconductors Measured by Muon Spin Rotation*, preprint.

201. J.P. Carinei *et al.*, *Phys. Rev. B* **37**, 9726 (1988).

202. A.T. Fiory, A.F. Hebard, P.M. Mankiewich, and R.E. Howard, *Phys. Rev. Lett.* **61**, 1419 (1988).

203. K. Scharnberg *et al.*, *Physica C* **153-155**, 715 (1988).